MICROCOPY RESOLUTION TEST CHART

NATIONAL BUREAU OF STANDARDS-1963-A

MECHANICAL PROPERTIES OF MISERS BLUFF SAND

by

Bruce R. Phillips

Structures Laboratory

DEPARTMENT OF THE ARMY
Waterways Experiment Station, Corps of Engineers
PO Box 631, Vicksburg, Mississippi 39180-0631

September 1986
Final Report

Approved For Public Release; Distribution Unlimited

US Army Corps
of Engineers

AD-A171 499

DTIC FILE COPY

DTIC
SELECTE
SEP 2 1986
D
A

86 9 2 046

STRUCTURES
LABORATORY

ADA 171499

REPORT DOCUMENTATION PAGE

Form Approved
OMB No 0704-0188
Exp Date Jun 30 1986

1a REPORT SECURITY CLASSIFICATION Unclassified	1b RESTRICTIVE MARKINGS		
2a SECURITY CLASSIFICATION AUTHORITY	3 DISTRIBUTION/AVAILABILITY OF REPORT Approved for public release; distribution unlimited.		
2b DECLASSIFICATION/DOWNGRADING SCHEDULE			

4 PERFORMING ORGANIZATION REPORT NUMBER(S) Technical Report SL-86-28	5. MONITORING ORGANIZATION REPORT NUMBER(S)

6a. NAME OF PERFORMING ORGANIZATION USAEWES Structures Laboratory	6b. OFFICE SYMBOL (If applicable) WESSD	7a. NAME OF MONITORING ORGANIZATION

6c. ADDRESS (City, State, and ZIP Code) PO Box 631 Vicksburg, MS 39180-0631	7b. ADDRESS (City, State, and ZIP Code)

8a. NAME OF FUNDING/SPONSORING ORGANIZATION Air Force Office of Scientific Research	8b. OFFICE SYMBOL (If applicable)	9. PROCUREMENT INSTRUMENT IDENTIFICATION NUMBER

8c. ADDRESS (City, State, and ZIP Code) Bolling Air Force Base Washington, DC 20332	10. SOURCE OF FUNDING NUMBERS See reverse.			
	PROGRAM ELEMENT NO.	PROJECT NO.	TASK NO.	WORK UNIT ACCESSION NO

11. TITLE (Include Security Classification)

Mechanical Properties of MISERS BLUFF Sand

12. PERSONAL AUTHOR(S)

Phillips, Bruce R.

13a. TYPE OF REPORT Final report	13b. TIME COVERED FROM _____ TO _____	14. DATE OF REPORT (Year, Month, Day) September 1986	15. PAGE COUNT 85

16. SUPPLEMENTARY NOTATION

This report was originally published as a draft report to the sponsor in September 1982.

17.	COSATI CODES		18. SUBJECT TERMS (Continue on reverse if necessary and identify by block number)
FIELD	GROUP	SUB-GROUP	See reverse.

19. ABSTRACT (Continue on reverse if necessary and identify by block number)

This report documents (a) the results of laboratory tests performed to supplement laboratory data previously reported on MISERS BLUFF (MB) sand and (b) the results of an analysis of all the MB laboratory data to develop representative laboratory material properties. The laboratory tests and analysis were conducted for use in evaluating the ability of mathematical constitutive models to simulate the behavior of soils to complex dynamic loadings produced by both explosive- and earthquake-induced ground shock.

MB sand is a medium- to coarse-grained, silty sand obtained at Planet Ranch, Arizona. The laboratory tests reported are unconsolidated-undrained tests on the sand in an air-dried condition. The analysis considered the response of the sand under three different test conditions, i.e., unconsolidated-undrained tests on dry sand, consolidated-drained tests on saturated sand, and consolidated-undrained tests on saturated sand. Representative responses of MB sand in terms of uniaxial strain (UX) compressibility; UX stress path; triaxial

(Continued)

20 DISTRIBUTION/AVAILABILITY OF ABSTRACT ☒ UNCLASSIFIED/UNLIMITED ☐ SAME AS RPT ☐ DTIC USERS	21 ABSTRACT SECURITY CLASSIFICATION Unclassified	
22a. NAME OF RESPONSIBLE INDIVIDUAL	22b TELEPHONE (Include Area Code)	22c OFFICE SYMBOL

10. SOURCE OF FUNDING NUMBERS (Continued).

AFOSR-MIPR-82-00003, Project 2307/C1 FY 82

18. SUBJECT TERMS (Continued).

Consolidated-drained	Triaxial compression
Consolidated-undrained	Triaxial extension
Laboratory tests	Unconsolidated-undrained
MISERS BLUFF sand	Uniaxial strain compression

19. ABSTRACT (Continued).

compression stress-strain, stress path, and failure; and triaxial extension
failure (where available) are presented for each of the test conditions.

PREFACE

The U.S. Army Engineer Waterways Experiment Station (WES) was requested by the Air Force Office of Scientific Research (AFOSR) to provide a complete and consistent set of laboratory mechanical properties for two soils for use in support of AFOSR contract number F49620-80-C-008, "Fundamental Properties of Soils for Complex Dynamic Loading," with Applied Research Associates, Inc., Albuquerque, New Mexico. The work reported herein was funded under AFOSR-MIPR-82-00003, Project 2307/C1 FY 82; the technical contact was LTC John J. Allen, AFOSR/NA.

The WES project engineer for this study was Mr. B. R. Phillips of the Geomechanics Division (GD), Structures Laboratory (SL), working under the general direction of Mr. J. Q. Ehrgott, Chief, Operations Group, GD, and Dr. J. G. Jackson, Jr., Chief, GD. The laboratory composition and mechanical property tests were conducted by personnel of GD and the Instrumentation Services Division. The laboratory classification and index tests were conducted by personnel of the Soils Testing Facility, Soil Mechanics Division, Geotechnical Laboratory. This report was prepared by Mr. Phillips and was transmitted to the sponsor in September 1982.

COL Tilford C. Creel, CE, and COL Robert C. Lee, CE, were the Commanders and Directors of WES during this investigation. COL Allen F. Grum, USA, was the previous Director and COL Dwayne G. Lee, CE, is the present Commander and Director. Mr. F. R. Brown and Dr. Robert W. Whalin were the WES Technical Directors. Mr. Bryant Mather was Chief, SL.

1

CONTENTS

CONVERSION FACTORS, NON-SI TO SI (METRIC)
UNITS OF MEASUREMENT

Non-SI units of measurement used in this report can be converted to SI (metric) units as follows:

Multiply	By	To Obtain
degrees (angle)	0.01745329	radians
feet	0.3048	metres
gallons (US liquid)	3.785412	cubic decimetres (litres)
inches	2.54	centimetres
kips (force)	4.448222	kilonewtons
kips (force) per square inch	6.894757	megapascals
megatons (nuclear equivalent of TNT)	4.184	petajoules
pounds (force) per square inch	6.894757	kilopascals
pounds (mass)	0.4535924	kilograms
pounds (mass) per cubic foot	16.01846	kilograms per cubic metre

MECHANICAL PROPERTIES OF MISERS BLUFF SAND

CHAPTER 1

INTRODUCTION

1.1 BACKGROUND

Applied Research Associates, Inc. (ARA), was funded by the Air Force Office of Scientific Research (AFOSR) to evaluate the ability of different mathematical constitutive models to simulate the behavior of soils subjected to complex dynamic loadings produced by both explosive- and earthquake-induced ground shock. To accomplish this study, ARA required a complete set of laboratory data for two sands. A complete set of properties included static and dynamic uniaxial strain and triaxial shear data on both dry and fully-saturated specimens. The U. S. Army Engineer Waterways Experiment Station (WES) was requested by AFOSR to assemble data from WES files on two sands and to supplement this information with additional laboratory tests as required. In January 1982, the available laboratory data on dry Reid-Bedford Model (RB) sand and back-pressure saturated Misers Bluff (MB) sand were reported in convenient formats for constitutive property analyses (Reference 1). Additional laboratory tests were then conducted on dry MB sand to complete the MB sand set of properties.

1.2 PURPOSE AND SCOPE

The purposes of this report are to present the results of the additional laboratory tests conducted on dry MB sand remolded to a density of about 1.72 g/cc and to document an analysis of all the MB sand laboratory data. Results of laboratory classification, index, and composition property tests and the additional mechanical property data on dry MB sand are presented in Chapter 2. Chapter 3 documents the analysis of all the laboratory data on MB sand and presents representative responses. A comparison of the representative relations for this material under three different test conditions are contained in Chapter 4.

CHAPTER 2

LABORATORY TESTS

2.1 CONVENTIONAL SOIL TESTS

Samples of MB sand were split from the available supply of material and tested to determine grain size distribution, Atterberg limits, and specific gravity (Reference 2). Results of these tests indicated that the MB sand used in this study was nonplastic and had a specific gravity of 2.67. The results of grain size distribution tests are shown in Figure 2.1. Using these data, the MB sand was classified according to the Unified Soil Classification System (Reference 3) as an SW-SM silty sand.

The grain size distribution and specific gravity reported above differ from those reported in Reference 1. Figure 2.2 shows a plot of the grain size distribution data reported earlier compared with that in Figure 2.1. The new data contain more fine-grained material than that reported earlier. This is believed to be a result of the procedure that was used to obtain the specimens. To obtain the data reported herein, the specimens were separated from the sand supply by a splitting technique, which insures a more uniform gradation for each specimen, while the earlier data were obtained by "scooping" the specimen from the top of the supply. During transportation, the finer particles probably settled to the bottom of a supply, leaving the coarser particles on top. This assumption is substantiated by the close agreement in the material gradations coarser than the 1-mm size and the gradually increasing difference in the material gradations finer than 1 mm.

2.2 COMPOSITION PROPERTY TESTS

Prior to performing each mechanical property test, the height, diameter, and weight of the remolded specimen were obtained. These measurements, along with the sand's specific gravity of 2.67 and air-dried moisture content of 0.4 percent, were used to calculate wet density γ , dry density γ_d , degree of saturation S (percent of void volume filled with water), percent volume of air V_a , and void ratio e (the ratio of void volume to solid volume). These composition data are listed in Table 2.1 for each test.

2.3 MECHANICAL PROPERTY TESTS

A total of 20 unconsolidated-undrained mechanical property tests were performed on remolded specimens of air-dried MB sand in order to complete the laboratory data base for this material.

2.3.1 Description of Tests and Test Program

A brief description of each type of test conducted to augment the MB sand data reported in Reference 1 follows:

    a.   The isotropic compression (IC) test subjects a cylindrically shaped specimen to an equal all-around confining pressure while measurements of the specimen's height and diameter changes are made. The data are normally plotted as pressure versus volumetric strain, the slope of which is the bulk modulus K .

    b.   The triaxial compression (TXC) test is conducted after a desired confining pressure is applied during the IC test. While the confining pressure is held constant, axial load is increased and measurements of the specimen's height and diameter changes are made. The data can be plotted as principal stress difference versus axial strain, the slope of which is Young's modulus E , or as principal stress difference versus principal strain difference, the slope of which is twice the shear modulus G . The maximum principal stress difference the specimen can support or the principal stress difference at 15 percent axial strain during shear loading (whichever occurs first) is defined as failure and describes one point on a failure surface under positive principal stress difference states of stress. The failure surface is depicted as a plot of principal stress difference versus mean normal stress.

    c.   The triaxial extension (TXE) test is also conducted after a desired confining pressure is applied during the IC test. While lateral pressure is held constant, vertical pressure is decreased and measurements of the specimen's height and diameter changes are made. As with the TXC test, the data are plotted as principal stress difference versus axial strain or as principal stress difference versus principal strain difference. The maximum negative principal stress difference or the point at which the material separates (whichever occurs first) is defined as failure and describes one point on a failure surface under a negative principal stress difference state of stress.

    d.   Two types of uniaxial strain (UX) tests were conducted:

    (1) The first (designated UX) is conducted by applying an axial (vertical) pressure to a wafer-shaped specimen that is physically constrained from deflecting radially. Measurements are made of the applied axial stress and the specimen's height change. The data are plotted as axial (vertical) stress versus axial (vertical) strain, the slope of which is the constrained modulus M .

6

(2) The second type of UX test (designated UX/K_0) is conducted by applying radial pressure to a specimen until a slight inward movement of the diameter is detected. Axial load is then applied until the specimen returns to its original radial position (zero radial strain). This process is repeated throughout the test. As in the UX test, the data are plotted as axial stress versus axial strain, the slope of which is the constrained modulus M. When the data are plotted as principal stress difference versus mean normal stress, the slope, assuming elastic theory, is 2G/K, or in terms of Poisson's ratio ν, $3(1-2\nu)/(1+\nu)$.

The test program consisted of four static UX (S-UX) tests, three dynamic UX (D-UX) tests, four static UX/K_0 tests, six static IC-TXC tests, and three static IC-TXE tests. These tests were all performed unconsolidated-undrained; results are summarized in Table 2.1. The confining pressure- (IC test), load- (TXC and TXE tests), and vertical stress- (UX and UX/K_0 tests) time histories can be characterized by two types of curves, shown in Figure 2.3. All static tests are characterized by curve type 1; dynamic tests are characterized by an unload-reload cycle as shown in curve type 2. A summary of the applied time histories for each test is in Table 2.2.

2.3.2 Test Procedures

2.3.2.1 UX Tests. Procedures to prepare specimens for static and dynamic UX tests were identical. The weight of air-dried material required to obtain a density of 1.714 g/cc was split from the supply of MB sand to insure a representative specimen. The material was placed into a chamber 9.1 centimeters in diameter and 2.3 centimeters high and compacted until the target density was obtained. The device was assembled by placing a rubber membrane containing a footing over the specimen and securing the top of the chamber. The footing rode directly on the center of the specimen and was connected to a linear variable differential transducer (LVDT) which measured the specimen's deflection during the test. The vertical stress applied to the specimen was measured by a pressure transducer mounted in a fluid chamber above the rubber membrane. Stress and deflection measurements were stored on both magnetic tape and light beam oscillograph for later processing. These data were processed and plotted as vertical stress versus vertical strain.

2.3.2.2 IC-TXC, IC-TXE, and UX/K_0 Tests. Specimens for all three of the remaining types of tests on the dry MB sand were prepared in the same way and tested in the same test device. The required amount of air-dried

7

material was split from the supply and placed into a steel remolding jacket containing a 0.06-centimeter-thick rubber membrane. A vacuum was applied through the jacket to pull the membrane against the jacket's sides while the material was spooned into the device until a density of approximately 1.714 g/cc was obtained. Each specimen was remolded to 5.1 centimeters in diameter and 11.4 centimeters tall. After the specimen was prepared, the membrane was attached to a top cap and base with rubber bands. A second 0.06-centimeter-thick membrane was then placed over the first and also secured to the top cap and base. The outside membrane was coated with a layer of liquid synthetic rubber to inhibit breakdown of the membrane due to the hydraulic oil confining fluid.

The vertical measurement system consisted of two vertically-mounted LVDT's positioned 180 degrees apart on top of the specimen. The radial measurement system for the IC-TXC and IC-TXE tests was a lateral deformeter consisting of four strain-gaged steel arms positioned equidistant around the specimen's periphery at the midheight of the specimen. The radial measurement system for the UX/K_o tests was a midheight lateral deformeter consisting of four horizontally mounted LVDT's positioned at quarter points around the specimen. During the conduct of the UX/K_o test, the lateral deformeter was continuously monitored to maintain the lateral deflection at zero. All data were recorded by a digital data acquisition system which sampled the data channels at designated intervals and recorded them on a minicassette tape for later processing and plotting.

2.3.3   Test Data

The recorded data were related to the pretest calibration steps of the particular unit to calculate pressure, load, or deformation. Using these raw data along with the specimen's height and diameter, calculations of appropriate stresses and strains were made. Once the stresses and strains were calculated, computer plots were generated. Results of the mechanical property tests conducted on dry MB sand are presented in Plates 1 through 20 and are summarized in Table 2.1.

The results of the static and dynamic UX tests are shown as plots of vertical (axial) stress versus vertical (axial) strain in Plates 1 through 7. The UX/K_o tests are shown in Plates 8 through 11. Each UX/K_o plate includes

8

a plot of (a) principal stress difference versus mean normal stress, (b) principal stress versus principal strain difference, and (c) vertical (axial) stress versus vertical (axial) strain.

Plates 12 through 17 show the results of the IC-TXC tests. These plates consist of four plots: (a) principal stress difference versus mean normal stress, (b) principal stress difference versus both principal strain difference and axial strain, (c) mean normal stress versus volumetric strain (calculated by assuming the specimen deformed as a right circular cylinder; see Reference 4), and (d) volumetric strain versus both principal strain difference and axial strain. The same plots are also shown for the IC-TXE tests in Plates 18 through 20. For the IC-TXE tests plots (a) and (b) are shown with negative values of principal stress difference. The IC tests conducted with the TXE tests are not considered to be strictly an isotropic compression loading because vertical stress was applied by a piston which is thought to impose a small amount of shear loading.

Table 2.1 Summary of mechanical property tests on remolded Misers Bluff sand.

Plate No.	Test Number	Wet Density ρ, g/cc	Water Content w, %	Dry Density γd, g/cc	Specific Gravity Gs	Air Voids Content Va, %	Degree of Saturation Sr, %	Void Ratio	Test Type	UX & UX/Ko Tests		IC Tests		TXC and TXE Tests			
										Peak Vertical Stress MPa	Vertical Strain at Peak Vertical Stress %	Peak Mean Normal Stress MPa	Volumetric Strain at Peak Mean Normal Stress ΔV/V	Confining Pressure σ_r, MPa	Vertical Strain at Failure ε_z, %	Vertical Principal Stress Difference at Failure $\sigma_z-\sigma_r$, MPa	Mean Normal Stress at Failure MPa
1	MBDUX.1	1.714	0.4	1.707	2.67	35.9	1.9	0.58	S*-UX	9.5	4.0	---	---	---	---	---	---
2	MBDUX.1A	1.714	0.4	1.707	2.67	35.9	1.9	0.58	S-UX	13.8	9.3	---	---	---	---	---	---
3	MBDUX.2	1.714	0.4	1.707	2.67	35.9	1.9	0.58	S-UX	34.5	12.0	---	---	---	---	---	---
4	MBDUX.2A	1.714	0.4	1.707	2.67	35.9	1.9	0.58	S-UX	20.9	7.8	---	---	---	---	---	---
5	MBDUX.3	1.714	0.4	1.707	2.67	35.9	1.9	0.58	D**-UX	14.1	5.5	---	---	---	---	---	---
6	MBDUX.4	1.714	0.4	1.707	2.67	35.9	1.9	0.58	D-UX	33.5	9.6	---	---	---	---	---	---
7	MBDUX.5	1.714	0.4	1.707	2.67	35.9	1.9	0.58	D-UX	31.8	11.1	---	---	---	---	---	---
8	MBDK.1	1.732	0.4	1.725	2.67	34.7	2.0	0.55	UX/Ko	19.8	9.8	---	---	---	---	---	---
9	MBDK.2	1.714	0.4	1.707	2.67	35.4	1.9	0.56	UX/Ko	28.0	11.0	---	---	---	---	---	---
10	MBDK.3	1.743	0.4	1.736	2.67	34.3	2.0	0.54	UX/Ko	36.5	13.0	---	---	---	---	---	---
11	MBDK.4	1.732	0.4	1.725	2.67	34.7	2.0	0.55	UX/Ko	19.6	9.4	---	---	---	---	---	---
12	MBDTX.1	1.743	0.4	1.736	2.67	34.8	2.0	0.55	IC-TXC	---	---	1.8	2.5	1.8	12.0	5.0	3.2
13	MBDTX.2	1.708	0.4	1.701	2.67	36.1	1.9	0.58	IC-TXC	---	---	3.5	5.7	3.5	15.0	8.9	6.4
14	MBDTX.3	1.704	0.4	1.698	2.67	36.2	1.8	0.59	IC-TXC	---	---	2.8	4.6	3.5	14.7	9.0	6.5
15	MBDTX.5	1.701	0.4	1.694	2.67	36.3	1.8	0.59	IC-TXC	---	---	0.1	1.5	0.1	3.9	0.5	0.3
16	MBDTX.6A	1.728	0.4	1.721	2.67	35.3	1.9	0.56	IC-TXC	---	---	0.1	1.1	0.1	5.1	0.5	0.3
17	MBDTX.7	1.721	0.4	1.714	2.67	35.6	1.9	0.57	IC-TXC	---	---	6.9	6.2	6.9	15.0	16.6	12.4
18	MBDE.1	1.701	0.4	1.696	2.67	36.0	1.4	0.57	IC-TXE	---	---	3.6	4.7	3.6	-6.1	-2.9	2.6
19	MBDE.5	1.704	0.4	1.697	2.67	35.8	1.9	0.57	IC-TXE	---	---	7.0	6.0	7.0	-2.3	-4.6	5.5
20	MBDE.6	1.723	0.4	1.716	2.67	35.0	1.9	0.56	IC-TXE	---	---	7.2	6.4	7.0	-5.5	-4.8	5.4

* Static.
** Dynamic.

10

Table 2.2 Summary of load/stress-time histories from tests on dry Misers Bluff sand.

Test No.	Test Type	Curve Type	Vertical Stress, σ_z, Time History (UX and UX/K_o Tests)				Confining Pressure σ_r, Time History (IC Tests)		Load/Vertical Stress-Time History (TXC and TXE Tests)	
			Time at Point 1 sec	Vertical Stress at Point 1 MPa	Time at Point 2 sec	Vertical Stress at Point 2 MPa	Time at Point 1 sec	Mean Normal Stress at Point 1 MPa	Time at Point 1 sec	Principal Stress Difference at Point 1 MPa
MBDUX.1	S-UX	1	25.2	9.0	--	--	--	--	--	--
MBDUX.1A	S-UX	1	36.2	13.8	--	--	--	--	--	--
MBDUX.2	S-UX	1	69.4	34.5	--	--	--	--	--	--
MBDUX.2A	D-UX	1	40.0	20.9	--	--	--	--	--	--
MBDUX.3	D-UX	2	0.006	11.2	0.080	14.5	--	--	--	--
MBDUX.4	D-UX	2	0.006	17.2	0.088	33.6	--	--	--	--
MBDUX.5	D-UX	2	0.006	18.0	0.084	32.2	--	--	--	--
MBDK.1	UX/K_o	1	1834	15.6	--	--	--	--	--	--
MBDK.2	UX/K_o	1	1445	22.3	--	--	--	--	--	--
MBDK.3	UX/K_o	1	2662	36.5	--	--	--	--	--	--
MBDK.4	UX/K_o	1	1914	19.0	--	--	--	--	--	--
MBDTX.1	IC-TXC	--	--	--	--	--	320	1.8	765	4.9
MBDTX.2	IC-TXC	--	--	--	--	--	241	3.5	850	8.9
MBDTX.3	IC-TXC	--	--	--	--	--	265	3.5	820	8.9
MBDTX.5	IC-TXC	--	--	--	--	--	95	0.1	350	0.5
MBDTX.6A	IC-TXC	--	--	--	--	--	64	0.1	337	0.5
MBDTX.7	IC-TXC	--	--	--	--	--	250	6.9	865	17.0
MBDE.1	IC-TXE	--	--	--	--	--	167	3.7	816	-2.6
MBDE.5	IC-TXE	--	--	--	--	--	305	7.1	275	-4.1
MBDE.6	IC-TXE	--	--	--	--	--	416	7.1	655	-4.8

11
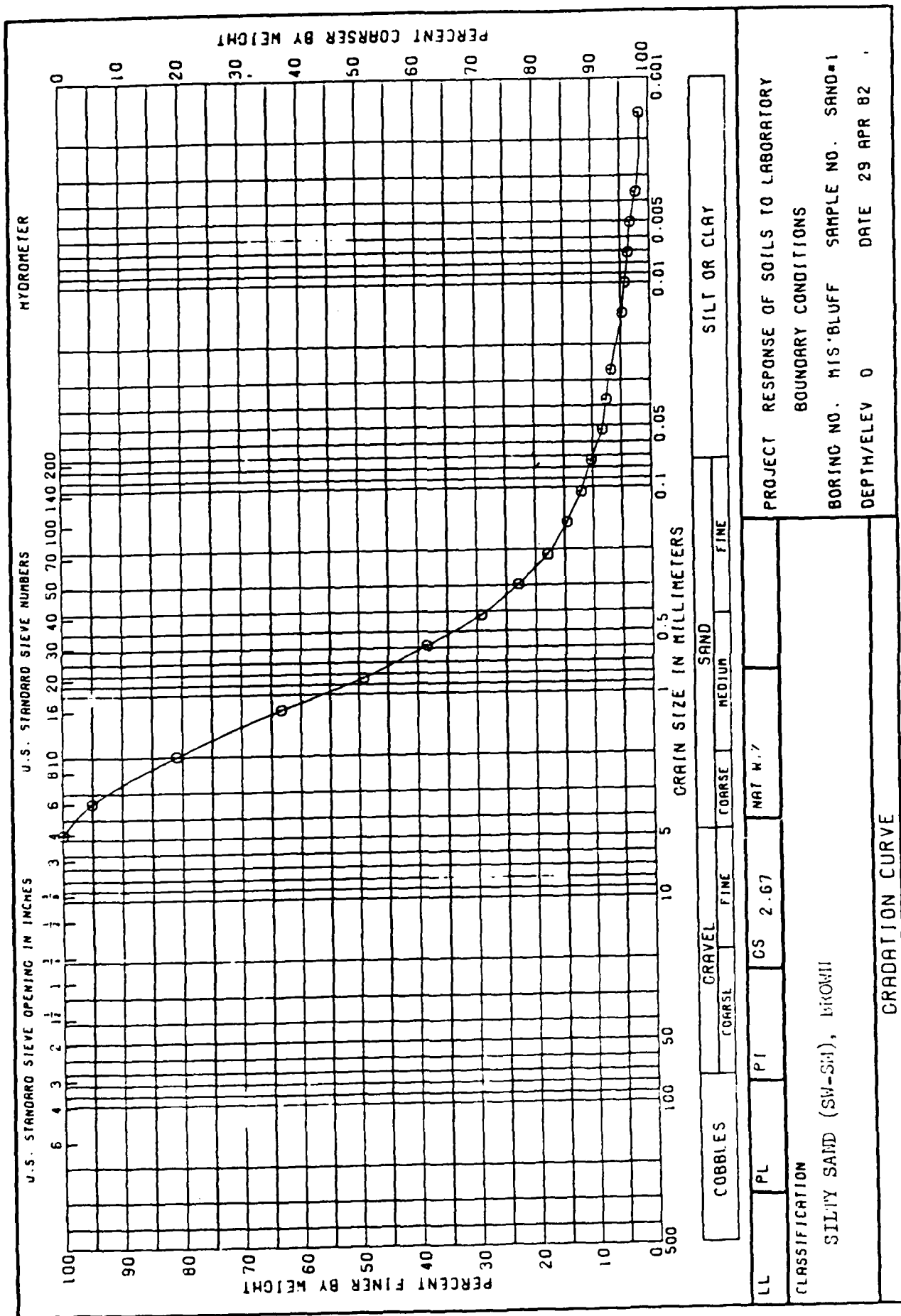
Figure 2.1 Gradation of Misers Bluff sand.
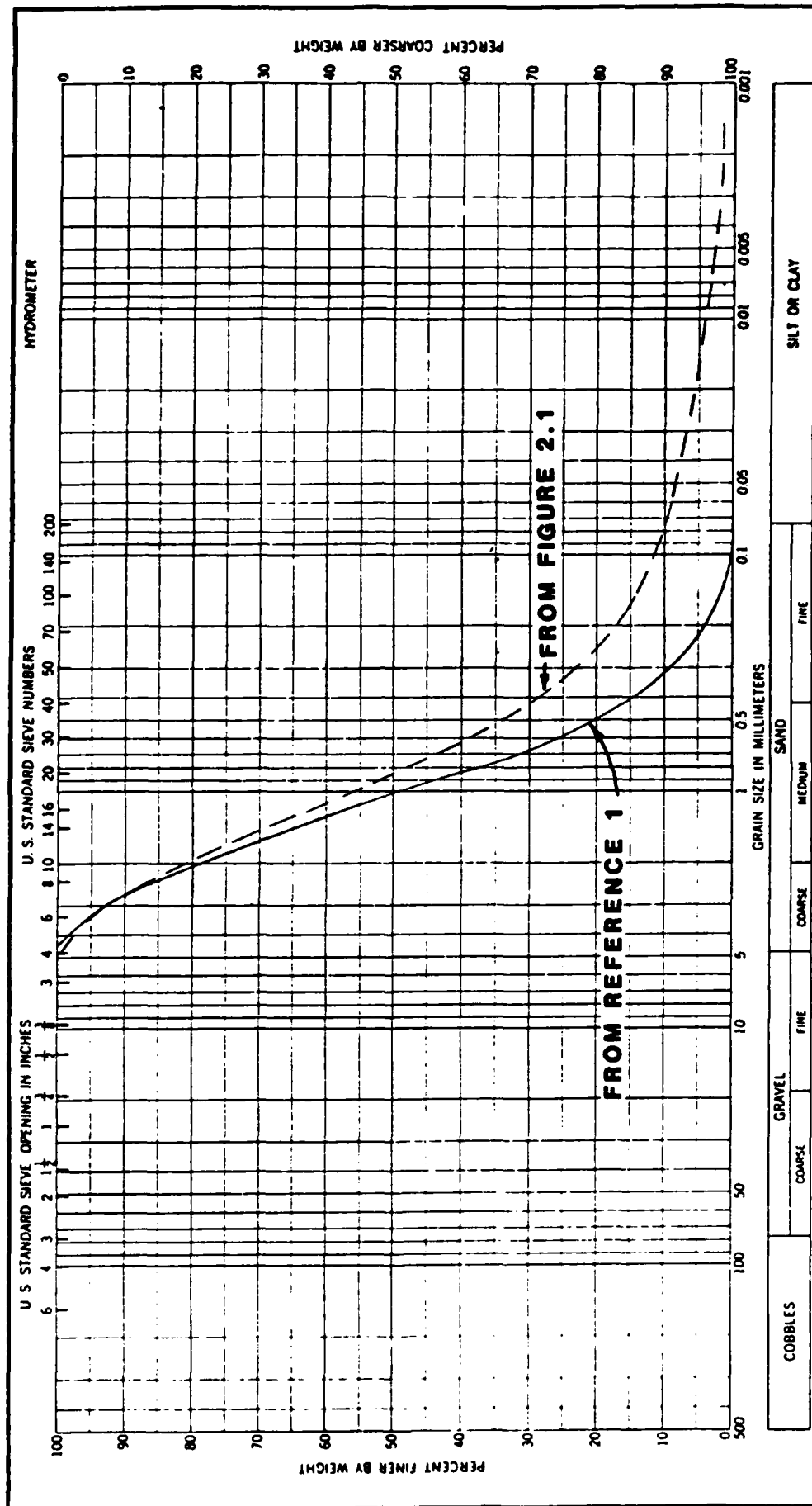
Figure 2.2 Comparison of gradation data for two test programs on MB sand.

13
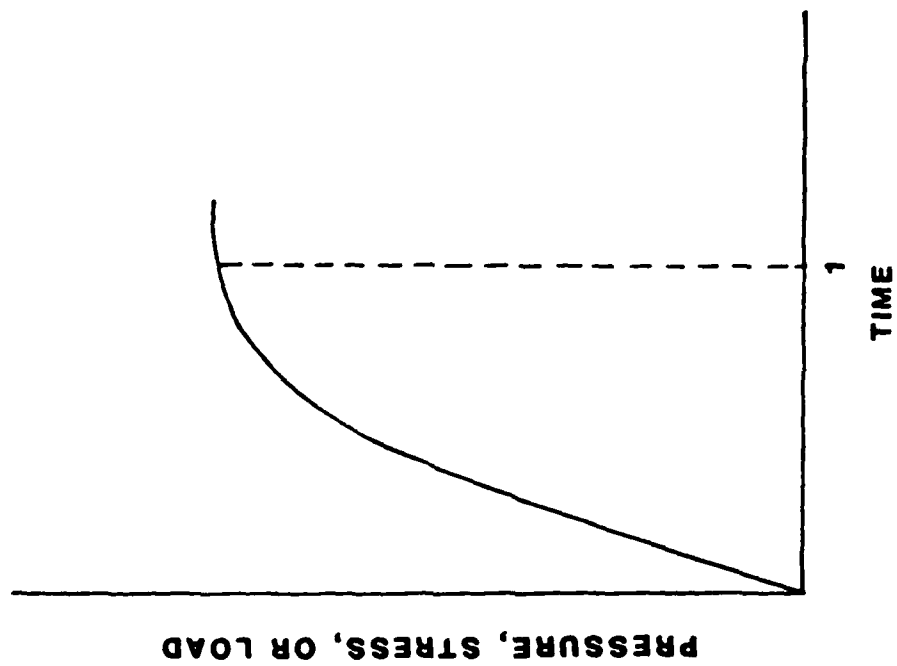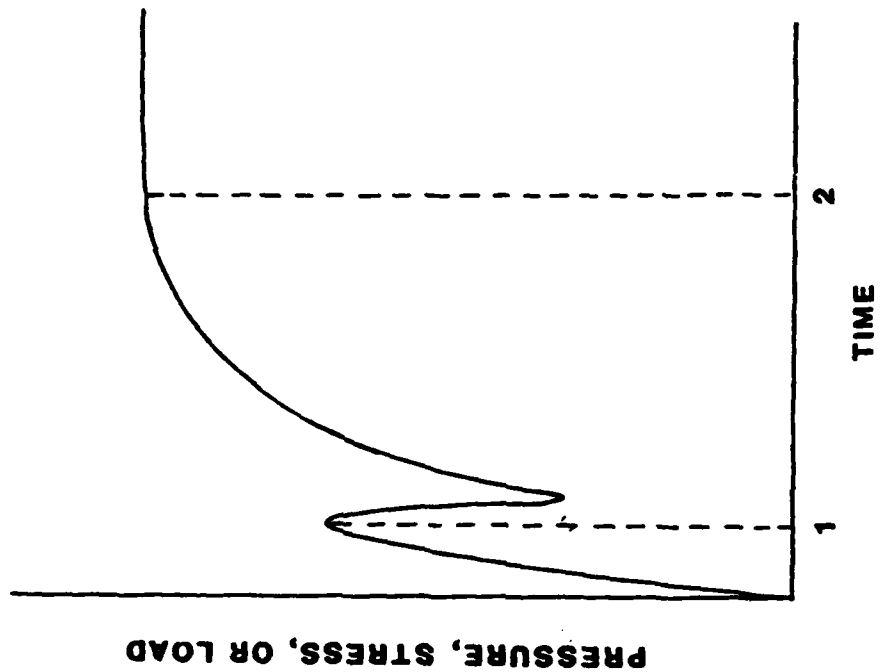
Figure 2.3 Typical pressure, stress, and/or load versus time curves.

CHAPTER 3

DATA ANALYSIS AND REPRESENTATIVE PROPERTY RECOMMENDATIONS

The laboratory test results on MB sand, reported in Reference 1 and in Chapter 2 of this report, were used to develop a consistent set of representative laboratory properties that could be used in assessing mathematical calculation techniques. Representative property recommendations include a UX compressibility relation, a UX stress path, a total-stress TXC failure relation, and a total-stress TXC stress path for MB sand under three different conditions, i.e., unconsolidated-undrained (UU) tests on dry material, consolidated-drained (CD) tests on saturated material, and consolidated-undrained (CU) tests on saturated material. In addition, a TXE failure relation is presented for the UU response of dry material, and an effective TXC stress path relation and pore pressure versus axial strain relation are given to represent the CU response of the saturated sand. All representative curves for saturated MB sand are shown referenced to the end of back-pressure saturation or the end of application of the effective stress.

To develop these representative responses, all valid test data of a given type were plotted on a single page and a representative curve (with respect to an initial dry density of 1.714 g/cc) was selected. When all representative curves were available for each test type and condition, the curves were reexamined and adjusted so that the complete set of representative properties was internally consistent. The analysis results presented in this chapter constitute only one approach to the development of representative calculational properties; other approaches and analysis results are possible.

3.1 COMPRESSIBILITY RELATION

3.1.1 UU Tests on Dry Sand

The results from the static and dynamic UX tests on dry MB sand are shown in Figure 3.1. Results from the four UX/K_o tests are represented in the figure by one curve (labeled UX/K_o) because their results overlay. The dynamic tests are shown as dashed lines and appear to be slightly less compressible than the static test results; however, this is not considered to be an indication of rate effects. Because of the characteristics of the

15

loading device, a large portion of the vertical stress was applied to the specimens in 6 msec (see Figure 3.2) and the remaining portion at a slower rate. No appreciable difference is noticed in the dynamic UX stress-strain curves due to this loading rate change, indicating that no appreciable loading rate effect is present in the 6-msec or longer rise time region.

Although the UX/K_o tests agree within themselves, the method used to conduct the tests leads one to believe that the results may not be under as strict a uniaxial strain loading condition as the UX tests. During the conduct of a UX/K_o test, only the center point of the specimen is monitored and maintained at zero radial deflection; the remainder of the specimen is assumed to respond identically. For MB sand the results of the static UX/K_o tests appear slightly more compressible than responses from UX tests. For this analysis, the UX tests were weighted heavier than the UX/K_o tests because a uniaxial strain loading condition is assured in the UX tests. One representative curve was developed to define both static and dynamic behavior. The curve was developed using a loading relation through the center of the data; the unloading relation was drawn parallel to that of test MBDUX.2 since all of the unloading curves were essentially the same.

3.1.2 CD Tests on Saturated Sand

Figure 3.3 shows the results of the uniaxial strain portions of the static CD UX tests and the static CD UX/K_o tests. The UX tests were rezeroed at the end of the back-pressure saturation phase; UX/K_o tests were rezeroed at the end of the application of effective stress. Examination of the UX/K_o tests indicated a less compressible loading curve for the specimens with higher effective stresses (tests DNA 17 and DNA 18). This is because the isotropic effective stress is applied prior to uniaxial strain loading and therefore densifies the specimen. The UX tests do not show this effect because application of vertical stress during drained uniaxial strain loading begins immediately after the specimen is back-pressure saturated. Results of Test DNA.UX.5SA are unusually soft and, therefore, were not considered in the development of the representative curve. Because results of the UX/K_o tests were not weighted as heavily as the UX test results, as discussed earlier, the loading portion of the representative curve was established so that the initial portion (up to a vertical stress of about 10 MPa) exhibited the same

16

behavior as the drained UX tests. The remainder of the curve was drawn
parallel to the dry UX relation; this matches the data in Figure 3.3 quite
well. Since the unloading curves were all similar, the representative
unloading relation was developed from the unloading curve for test DNA.UX.9S.

3.1.3 CU Tests on Saturated Sand

Linear approximations of the static and dynamic CU UX and static UX/K_o
test data are shown in Figure 3.4. These test results form three groups.
The UX/K_o tests are slightly more compressible than the UX tests as was
observed in the results of UU tests on dry material and CD tests on saturated
material. The dynamic and two static UX tests appear much less compressible
than the remaining static UX data in Figure 3.4. Mixture theory (Reference
5) assumes that the compressibility of individual minerals and water can be
mathematically combined to calculate the compressibility of the mixture. If
it is assumed that the only mineral in MB sand is quartz, a quartz/water
mixture with a back-pressure saturated density of 2.086 g/cc would yield a
bulk modulus of 8450 MPa. Since a saturated specimen should have a con-
strained modulus approximately equal to the bulk modulus (based on elastic
theory), the calculated modulus agrees with the more compressible static
data. The dynamic test results were much less compressible, i.e., their
average constrained modulus equals 25,970 MPa. This value was thought to be
unrealistically stiff, so these dynamic test results were disregarded.
Hence, the representative loading relation was drawn through the static UX
and UX/K_o data. At the pressure levels of interest in this study, the
representative relation can be approximated by a linear elastic relation;
however, at higher pressure ranges, the relation is expected to become
nonlinear.

3.2 UX STRESS PATH RELATION

3.2.1 UU Tests on Dry Sand

The results of four static UX/K_o tests are plotted as principal stress
difference versus mean normal stress in Figure 3.5. All curves have the same
characteristic shape and exhibit similar unload-reload responses. A compari-
son of the specimens' densities indicated that test MBDK.2 was closest to the
target density of 1.714 g/cc; therefore, the representative curve was based
on this test. Loading Poisson's ratio implied by the representative curve is
0.38.

17

3.2.2 CD Tests on Saturated Sand

A summary of the consolidated-drained UX/K_o tests on saturated sand is shown in Figure 3.6. These curves were rezeroed to the point after back-pressure saturation or after application of the isotropic effective stress occurred. The high effective-stress tests (DNA 17 and DNA 18) exhibited different responses than those at the lower effective stress (tests DNA 25 and DNA 26) because of density differences discussed earlier. The representative curve was based on tests DNA 25 and DNA 26 because the specimens for these tests had densities closer to the target density. It should be noted that the representative curve depicts the response of the material at a dry density of 1.714 g/cc at the beginning of uniaxial strain loading and is independent of back-pressure saturation pressures and isotropic effective stresses.

3.2.3 CU Tests on Saturated Sand

A summary of data from the CU UX/K_o tests on saturated sand is shown in Figure 3.7. The test data show an initially steep stress path followed by a flat portion that implies a Poisson's ratio of about 0.497. One explanation for this behavior is that the specimens were not fully saturated prior to uniaxial strain loading and, therefore, exhibited responses like the drained UX/K_o relation until full saturation occurred. The B-factors (a value used to determine the degree to which a specimen is saturated; Reference 6) calculated for tests DNA 15, DNA 16, and DNA 29 ranged from 0.95 to 0.98. The remaining tests had calculated B-factors greater than 0.99 but still exhibited the initially steep response. All of these B-factors are considered to be sufficiently high enough so that one may assume that the specimens were fully saturated. It is also interesting to note that the level of principal stress difference at which the stress path slope change occurs increases with increasing effective stress. This might lead one to assume that the response is a function of effective stress and is indeed a property of the material. However, at this point, there is insufficient data to make any definite conclusions about this behavior. Therefore, the representative relation (shown in Figure 3.7) was developed assuming that the test specimens were not fully saturated prior to UX loading and were constructed

parallel to the flat portion of the UX/K_o data. This corresponds to a Poisson's ratio of 0.497.

3.3 TXC STRESS-STRAIN

3.3.1 UU Tests on Dry Sand

Figure 3.8 shows the results of the TXC tests on dry sand at four different confining stresses, i.e., 0.14, 1.72, 3.45, and 6.90 MPa. Representative TXC principal stress difference versus axial strain and principal stress difference versus principal strain difference relations are shown for each level of confining stress based on the target density.

3.3.2 CD Tests on Saturated Sand

The CD triaxial tests on saturated MB sand are shown in Figure 3.9 for the three target effective stresses, i.e., 0.14, 1.72, and 3.45 MPa. The results indicate that tests labeled DNA have slightly higher values of maximum principal stress difference at a given level of effective stress than those tests labeled MXLD and MB; however, curve shapes are the same. A comparison of the available gradation data obtained from the supply materials for these tests indicates very little difference, as shown in Figure 3.10. The representative relation for each level of effective stress was based on the tests which most closely replicated the target density and effective stress. The maximum principal stress difference was based on the representative failure relation for the CD tests. The representative curves are shown in Figure 3.9 as plots of principal stress difference versus vertical strain and principal stress differences versus principal strain difference.

3.3.3 CU Tests on Saturated Sand

Figure 3.11 shows the results of the CU tests on saturated sand adjusted to zero axial strain at zero principal stress difference. As mentioned earlier, there appears to be a difference in the strengths of the MB tests and the DNA tests. In the low effective-stress tests, the differences in density and initial effective stresses (σ_c') show no consistent trend; therefore, a representative curve was established through the center of the data. At an initial effective stress of 1.72 MPa, tests MB 4A and MB 5A are closest to the target density and effective stress; therefore, the representative

19

curve for this effective stress was drawn through these test results. For the high initial effective stress (3.45 MPa), the representative curve was drawn through the center of the data. Representative curves are shown in Figure 3.11 for both the principal stress difference versus axial strain data and principal stress difference versus principal strain difference data.

3.4 TX FAILURE

3.4.1 UU Tests on Dry Sand

The failure points from the TXC and TXE tests on dry sand are shown plotted in Figure 3.12 as maximum principal stress difference versus mean normal stress. Failure in the TXC tests is defined as the maximum principal stress difference that the specimen can support or the principal stress difference at 15 percent vertical strain during application of the load, whichever occurs first. For these tests, failure occurred at or close to 15 percent in all tests at confining pressures greater than 0.14 MPa (see Figure 3.8). A linear approximation to the TXC failure data has a slope of 1.39, which implies a Coulomb friction angle of 34 degrees. The TXE failure points in Figure 3.12 are shown plotted as negative values of principal stress difference. For each of the TXE tests, the minimum stress difference or failure occurred at a vertical strain of 5 percent or less. A linear approximation to the data points indicate a slope of -0.85. Also included in Figure 3.12 is a $\sigma_z = 0$ line which indicates the failure limit in triaxial extension. The TXE failure points and representative relation do not reach the $\sigma_z = 0$ line and therefore both are valid. The representative failure relation is indicated by a heavy dark line in Figure 3.14.

3.4.2 CD Tests on Saturated Sand

Failure data from the CD triaxial compression tests are shown plotted as principal stress difference versus effective mean normal stress in Figure 3.13. Data at three levels of effective stress (0.14, 1.72, and 3.45 MPa) are presented. An examination of the principal stress difference versus vertical strain plots (Figure 3.9) indicates that failure occurred at about 6 percent vertical strain for the low effective stress and at 15 percent axial strain for the tests at the intermediate effective stress. Principal stress

differences in the high effective stress tests were still increasing at 15 percent axial strain. The failure points in Figure 3.13 indicate a non-linear, gradually softening, failure relation for these tests. However, a different failure relation would result if a different failure criterion was used. Also shown in Figure 3.13 is a representative TXC stress path for each level of effective stress.

3.4.3 CU Tests on Saturated Sand

The data from the CU tests on saturated MB sand are plotted as principal stress difference versus effective mean normal stress in Figure 3.14. To develop a set of representative curves, the representative failure relation was constructed to go through zero and to parallel the failure relation indicated by the CU tests at the three initial effective stress levels. Once the failure relation was obtained, the representative TXC effective-stress path for each level of effective stress was constructed by beginning at the target initial effective stress and selecting a curve parallel to the test data until the failure envelope was encountered. At that point the curve was drawn along the failure relation until the peak principal stress difference, as determined by the representative curves for each effective stress in Figure 3.11 was encountered. Unloading paths for each level of initial effective stress were very similar. In each case, the unloading relation for the test nearest the peak principal stress difference was used as the most representative curve.

The CU test failure data were also plotted as principal stress difference versus total mean normal stress in Figure 3.15. The failure points indicated that the CU tests on saturated MB sand reached maximum principal stress differences that did not increase with increasing confining stress, i.e., the von Mises limiting strength was achieved. However, the von Mises limit does increase with increasing effective stress. The representative von Mises limits for initial effective stresses of 0.14, 1.72, and 3.45 MPa are 1.30, 1.82, and 2.67 MPa, respectively. The Coulomb portion of the representative total stress failure relations in Figure 3.15 is the same as the drained TXC failure relation shown in Figure 3.13.

21

3.5 PORE PRESSURE RESPONSE DURING TXC LOADING

Figure 3.16 shows the results of the CU TXC tests plotted as pore pressure versus axial strain. The curves are initialized so that zero pore pressure occurs at the beginning of the TXC test. Since the curves for each effective stress were all very similar, the representative curves were drawn through the center of the data consistent with the representative principal stress difference versus axial strain plots shown in Figure 3.11.

3.6 SUMMARY

The analyses discussed in this chapter represent one technique used to develop representative relations for calculational properties. Each representative relation was compared with the others to insure internal consistency of all the properties. Individual plots of the representative relations for dry MB sand are shown in Figures 3.17-3.20. Plots of the representative drained and undrained curves on saturated sand are shown in Figures 3.21-3.24 and 3.25-3.30, respectively.
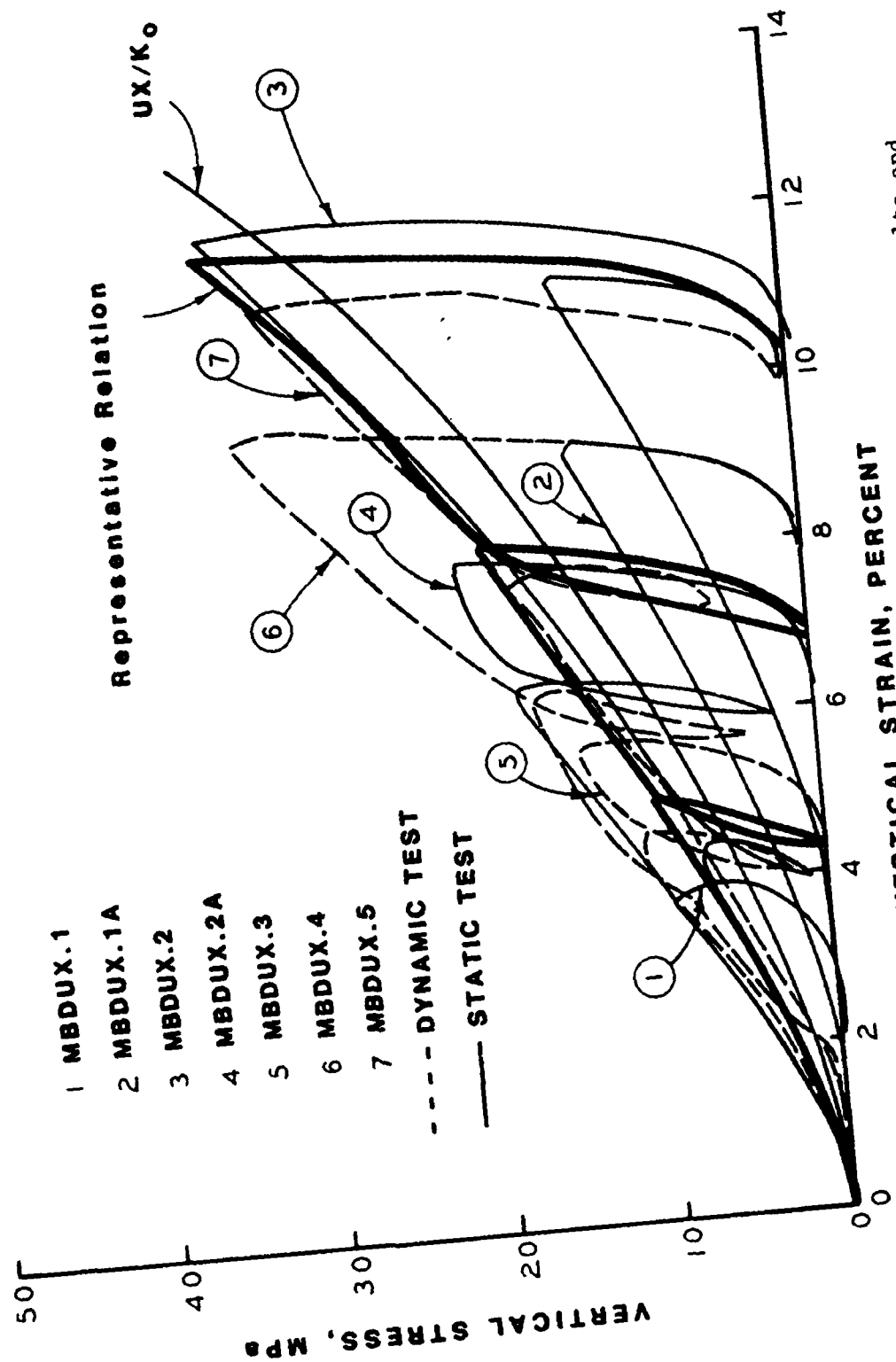
Figure 3.1 Static and dynamic UX and static UX/K_o test results and representative UX compressibility relation for dry MB sand.

23

UNIAXIAL STRAIN TEST RESULTS

Figure 3.2 Dynamic UX test results and stress-time histories.
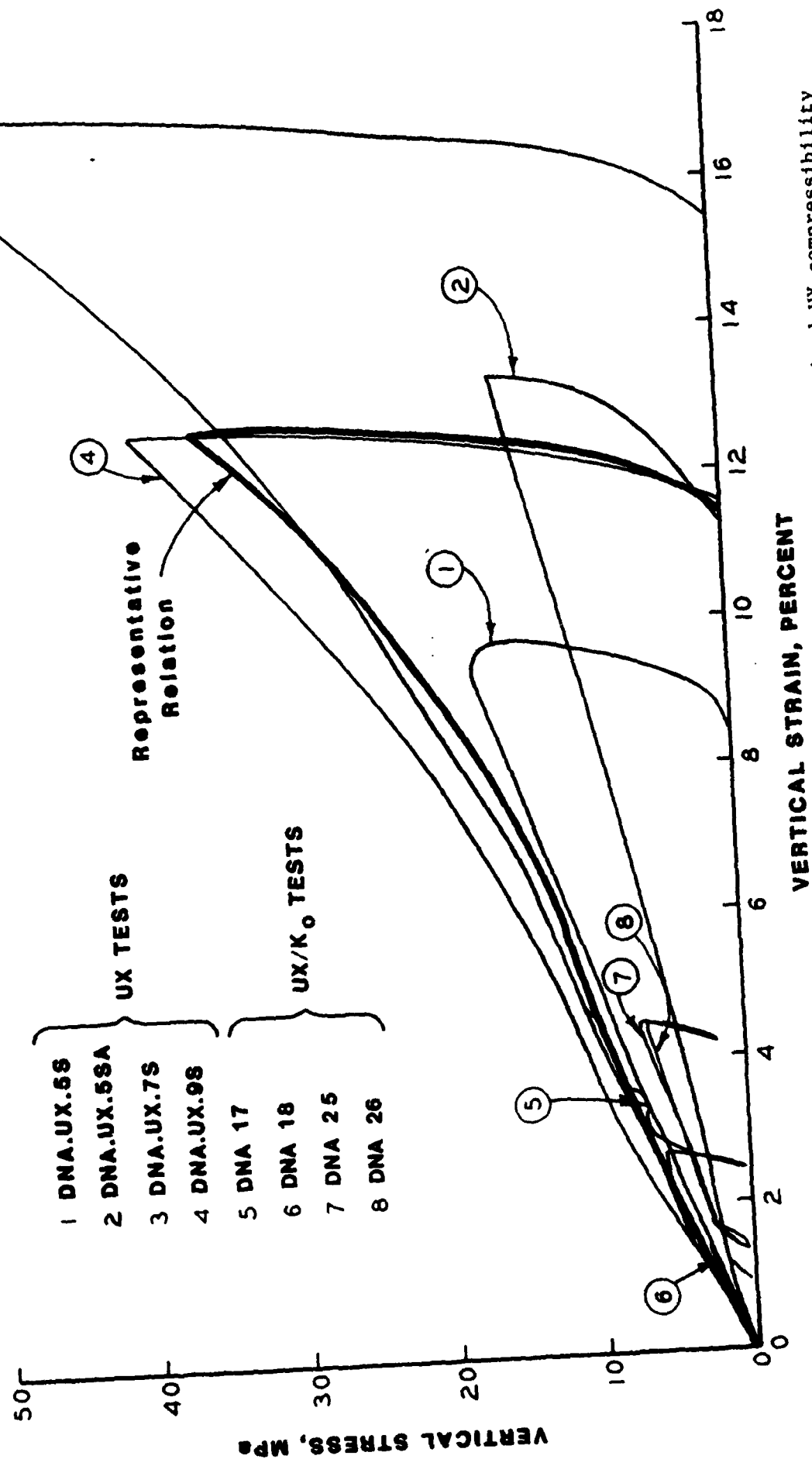
Figure 3.3 Static UX and static UX/K_o test results and representative drained UX compressibility relation for saturated MB sand.

Chart axis labels and legend:

VERTICAL STRESS, MPa (y-axis: 0, 10, 20, 30, 40, 50)

VERTICAL STRAIN, PERCENT (x-axis: 0, 2, 4, 6, 8, 10, 12, 14, 16, 18)

Representative Relation

UX TESTS
1 DNA.UX.5S
2 DNA.UX.5SA
3 DNA.UX.7S
4 DNA.UX.9S

UX/K_o TESTS
5 DNA 17
6 DNA 18
7 DNA 25
8 DNA 26

Figure 3.4   Static and dynamic UX and static UX/K_o test
results and representative undrained UX
compressibility relation for saturated MB
sand.

26

Figure 3.5 Static unconsolidated-undrained UX/K test results and representative UU-UX stress path relation for dry MB sand.
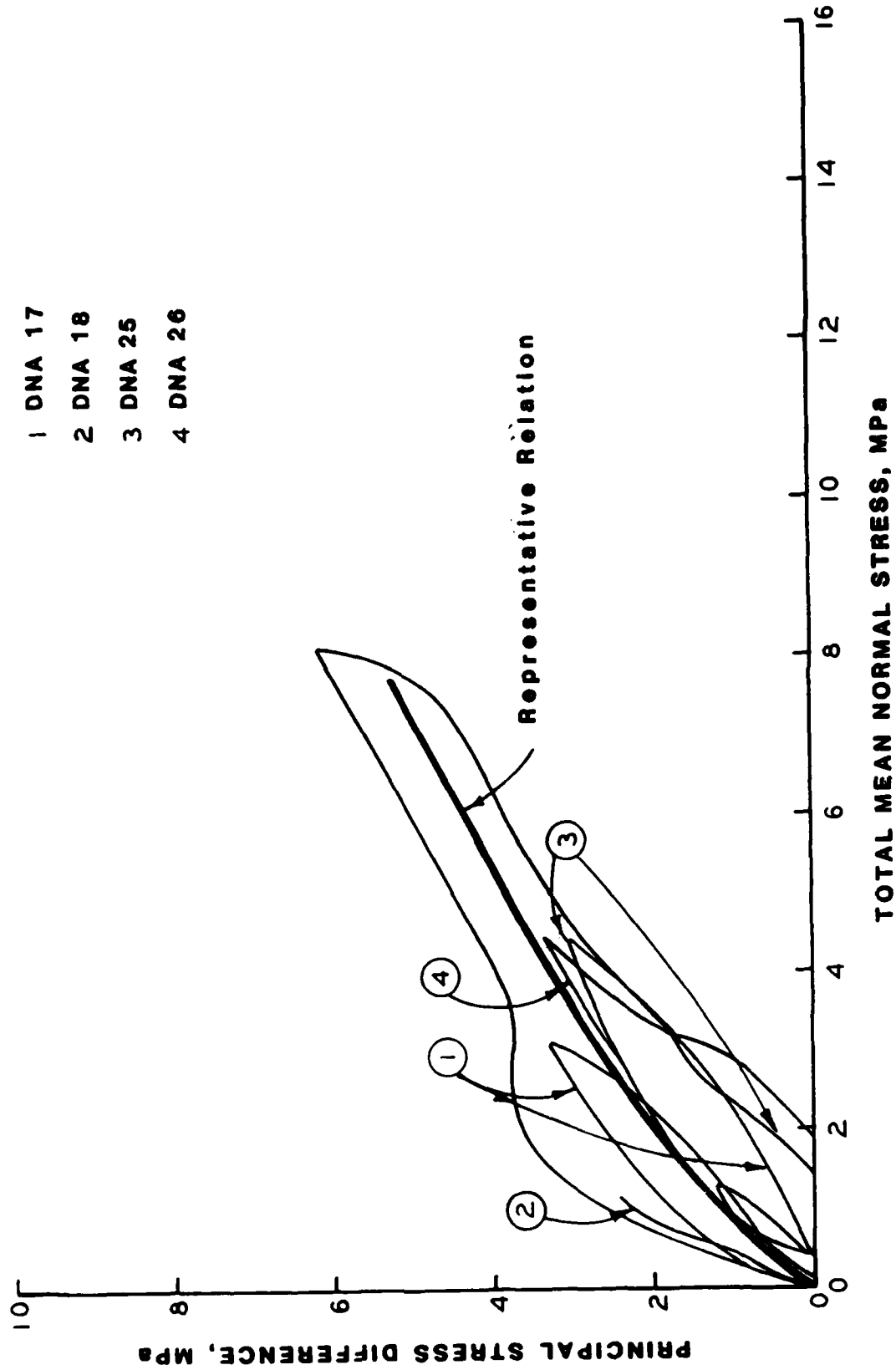
Figure 3.6 Static UX/K$_0$ test results and representative drained UX stress path relation for saturated MB sand.

28
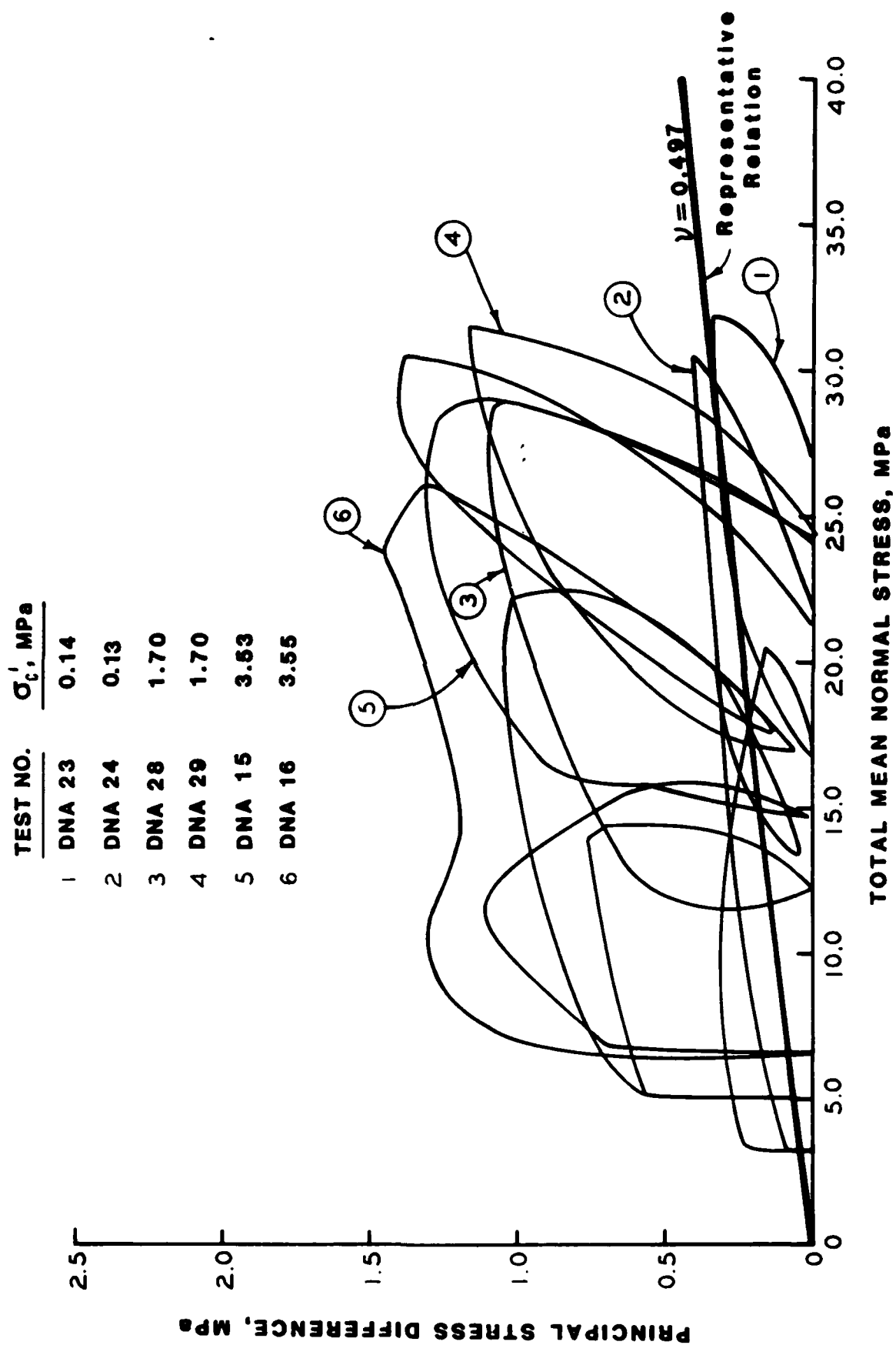
Figure 3.7 Static UX/K_O test results and representative undrained UX stress path relation for saturated MB sand.
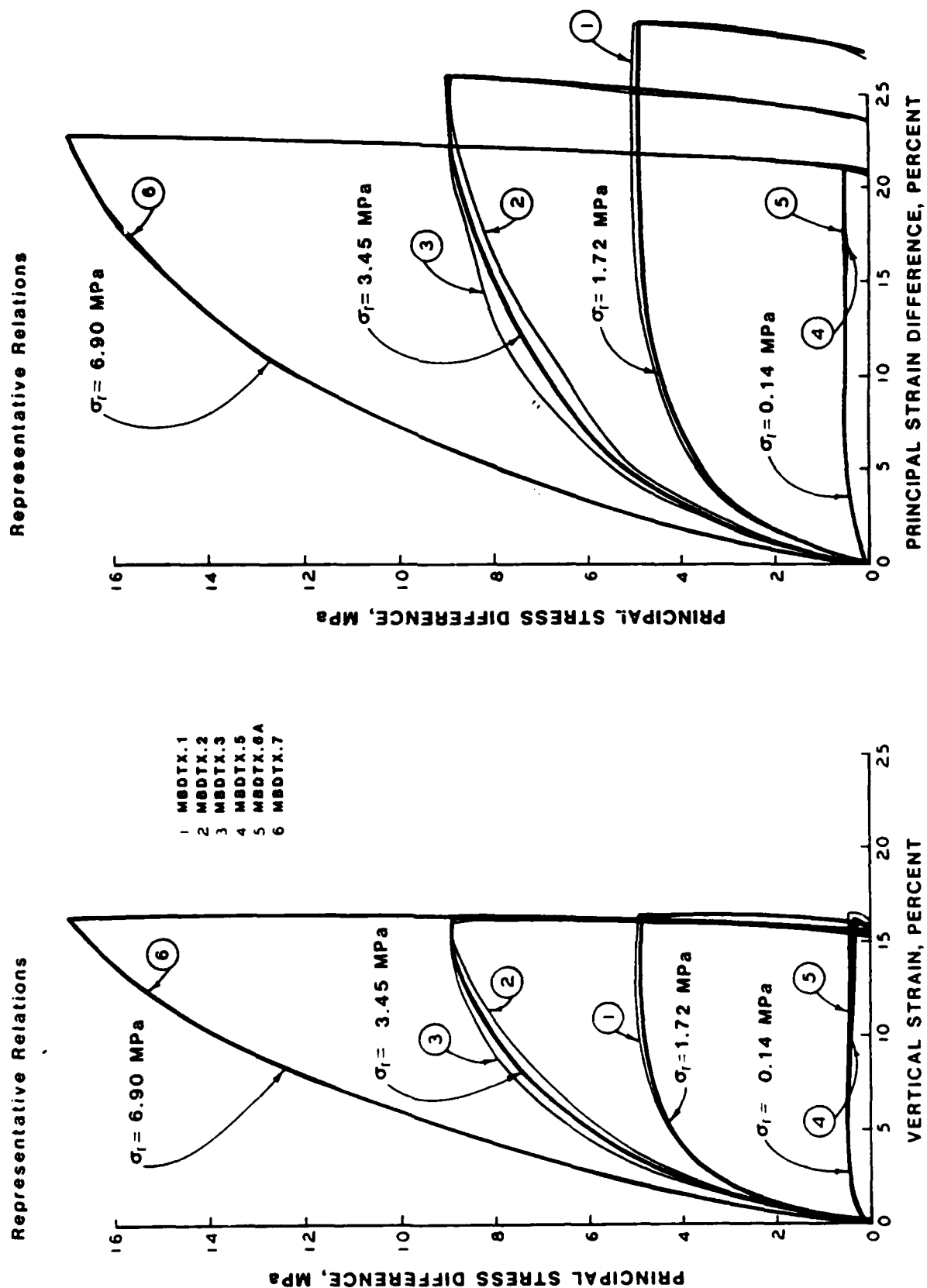
Figure 3.8 Static TXC test results and representative TXC stress-strain relation for dry MB sand.
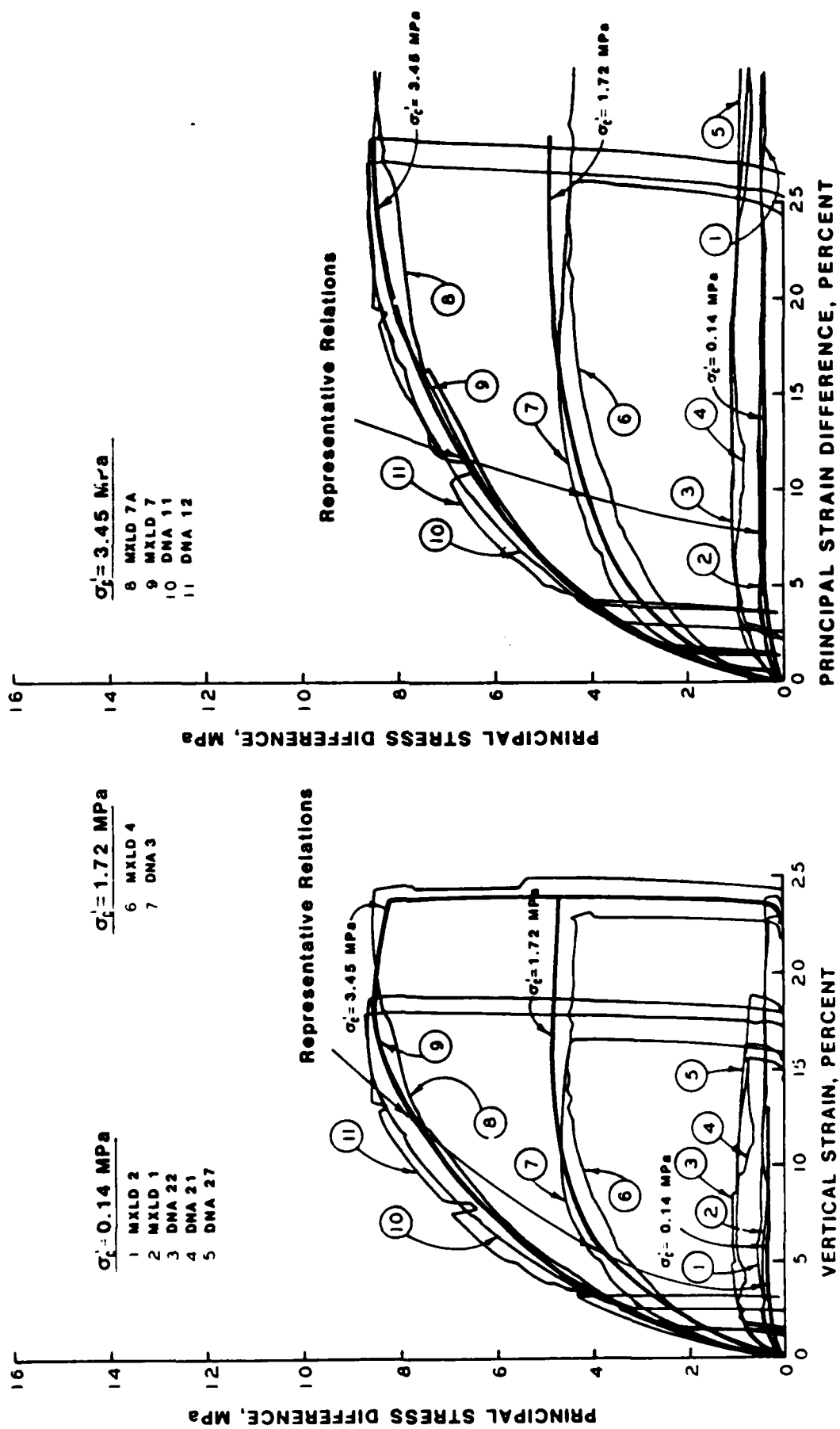
Figure 3.9 Static TXC test results and representative drained TXC stress-strain relation for saturated MB sand at effective stresses of 0.14, 1.72, and 3.45 MPa.

31
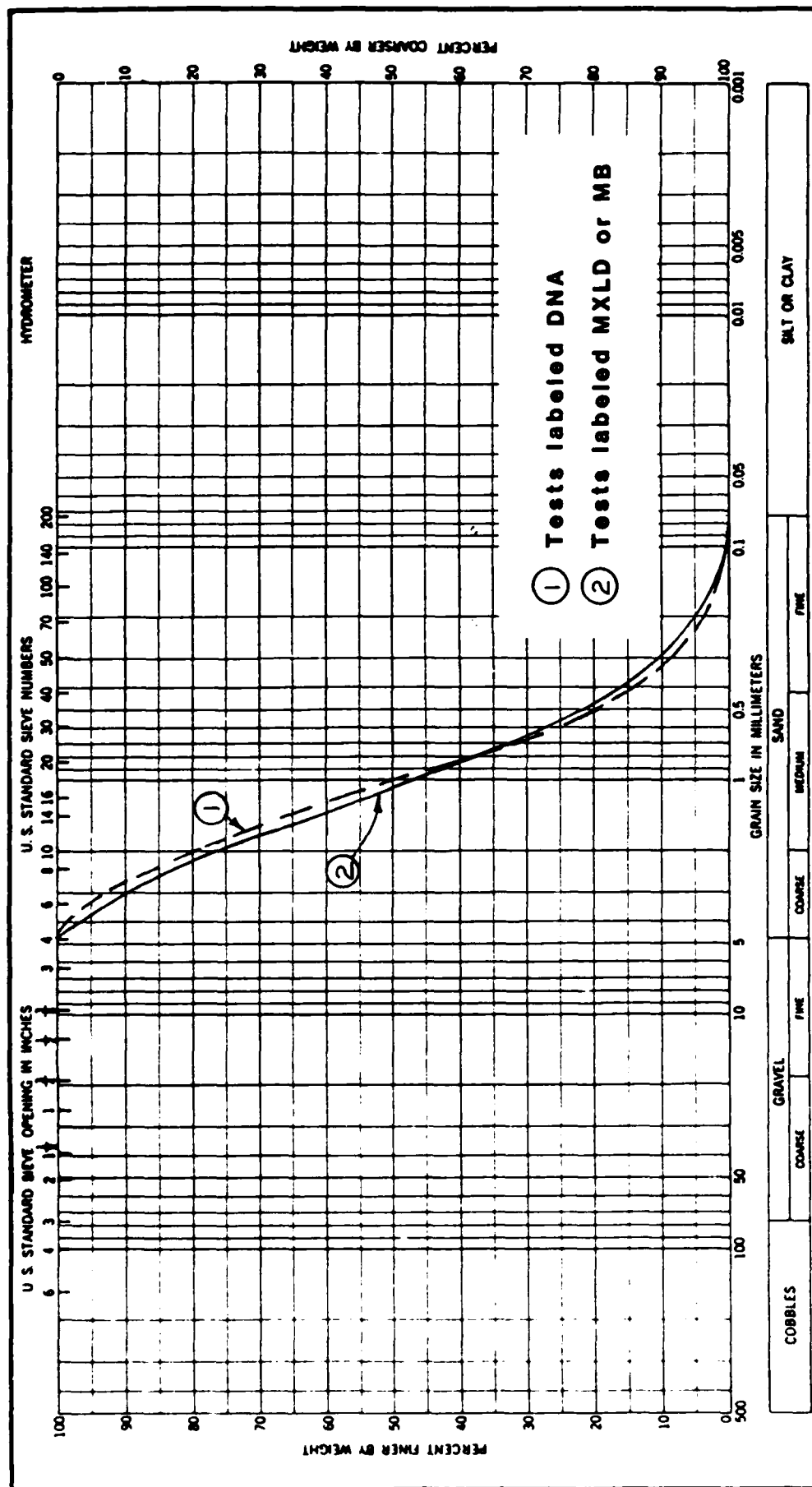
Figure 3.10 Comparison of gradation data for CD TXC tests labeled DNA, MXLD, and MB.
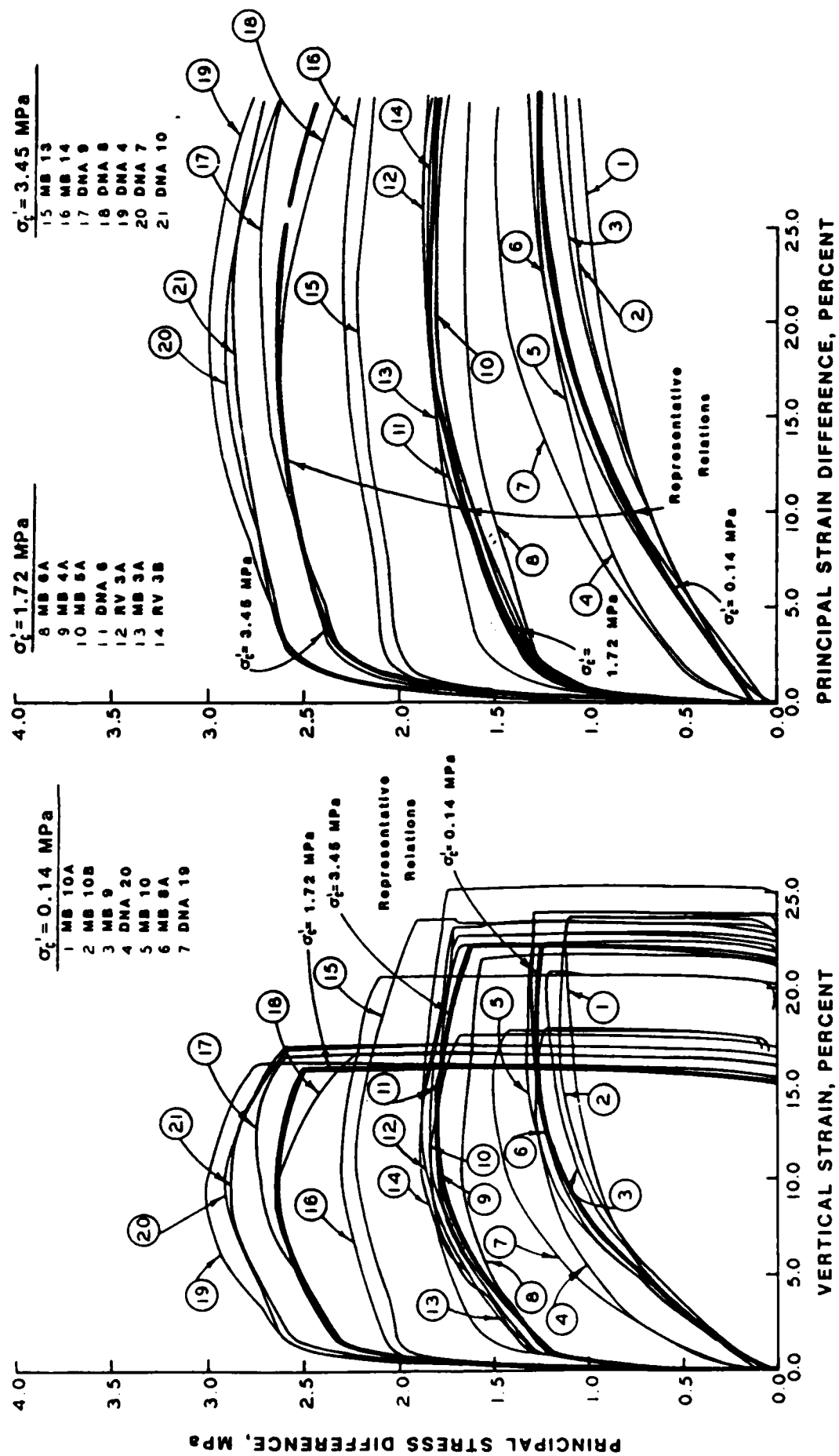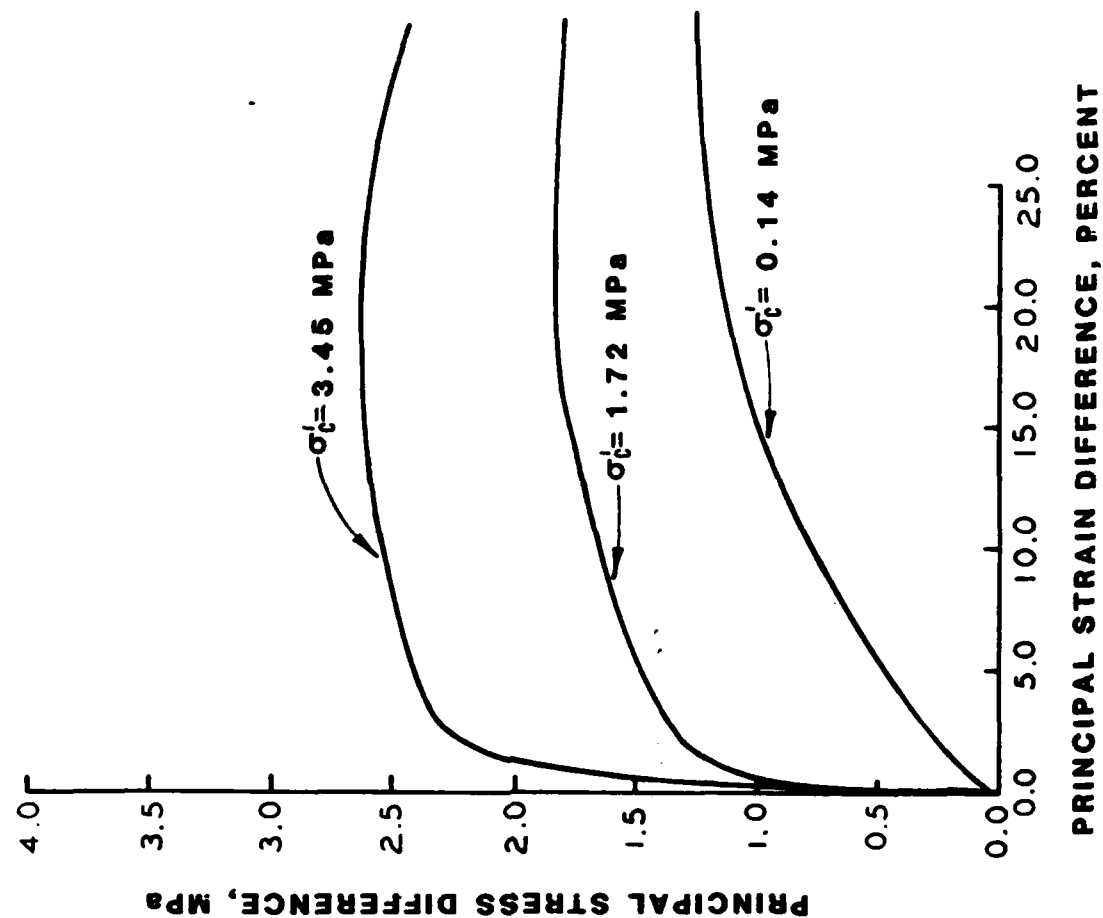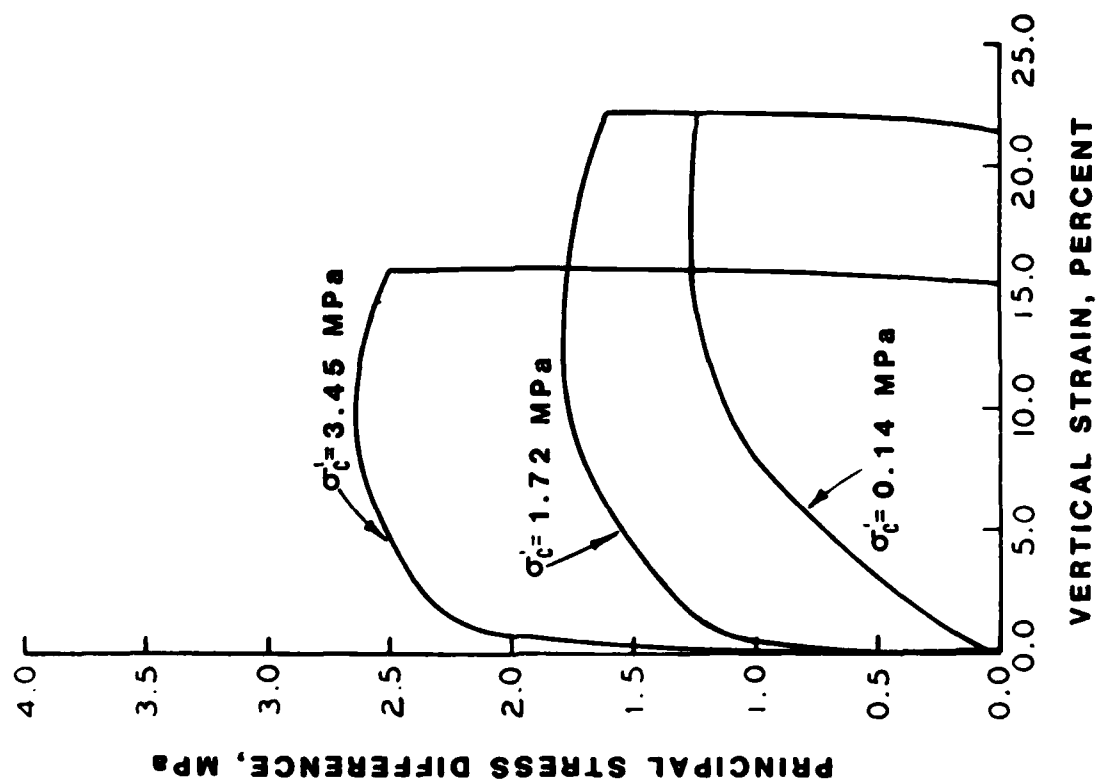
Figure 3.11 Static TXC test results and representative undrained TXC stress-strain relation for saturated MB sand at effective stresses of 0.14, 1.72, and 3.45 MPa.

33
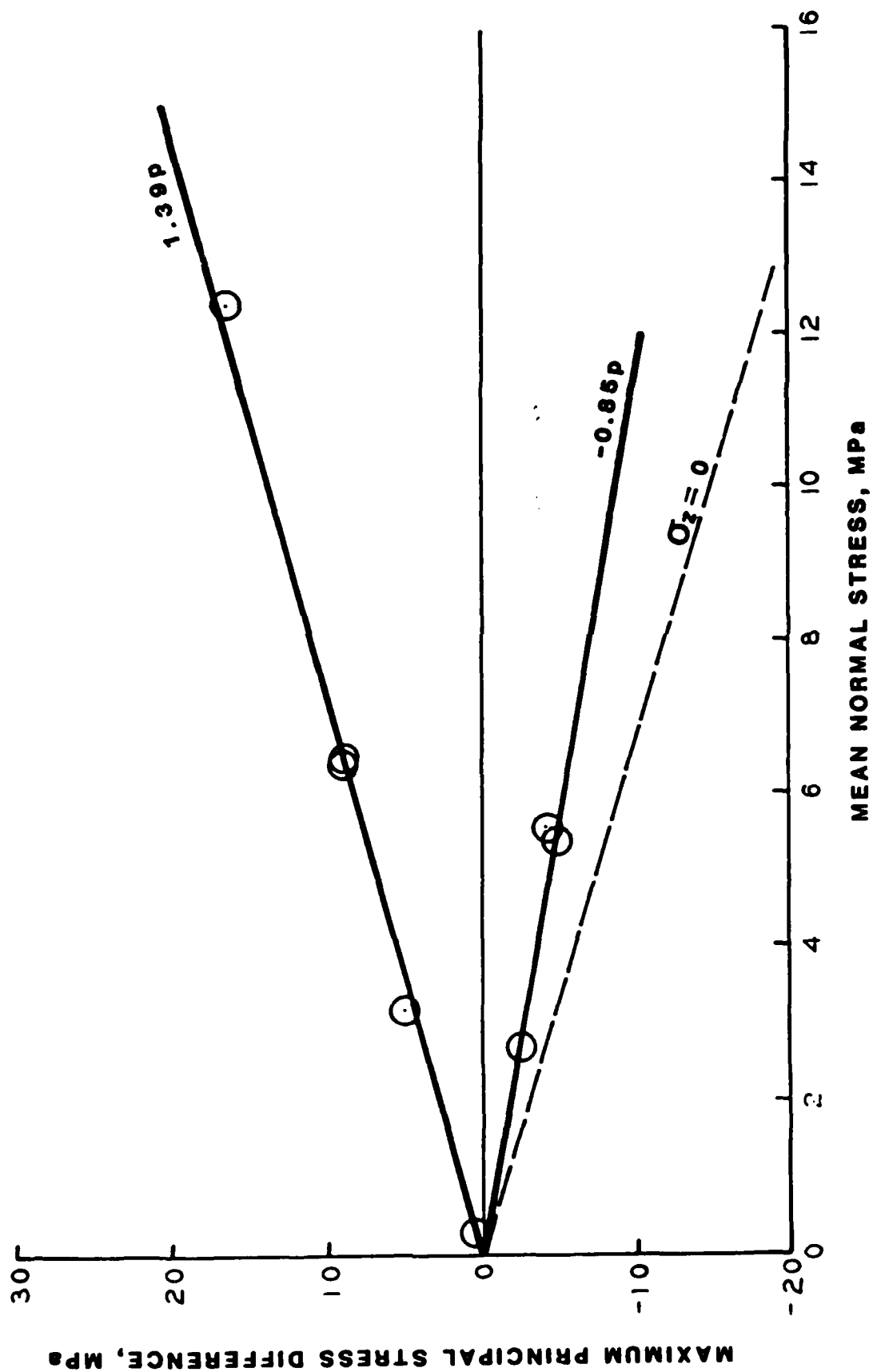
Figure 3.12 Static TXC and TXE failure points and representative TX failure relation for dry MB sand.
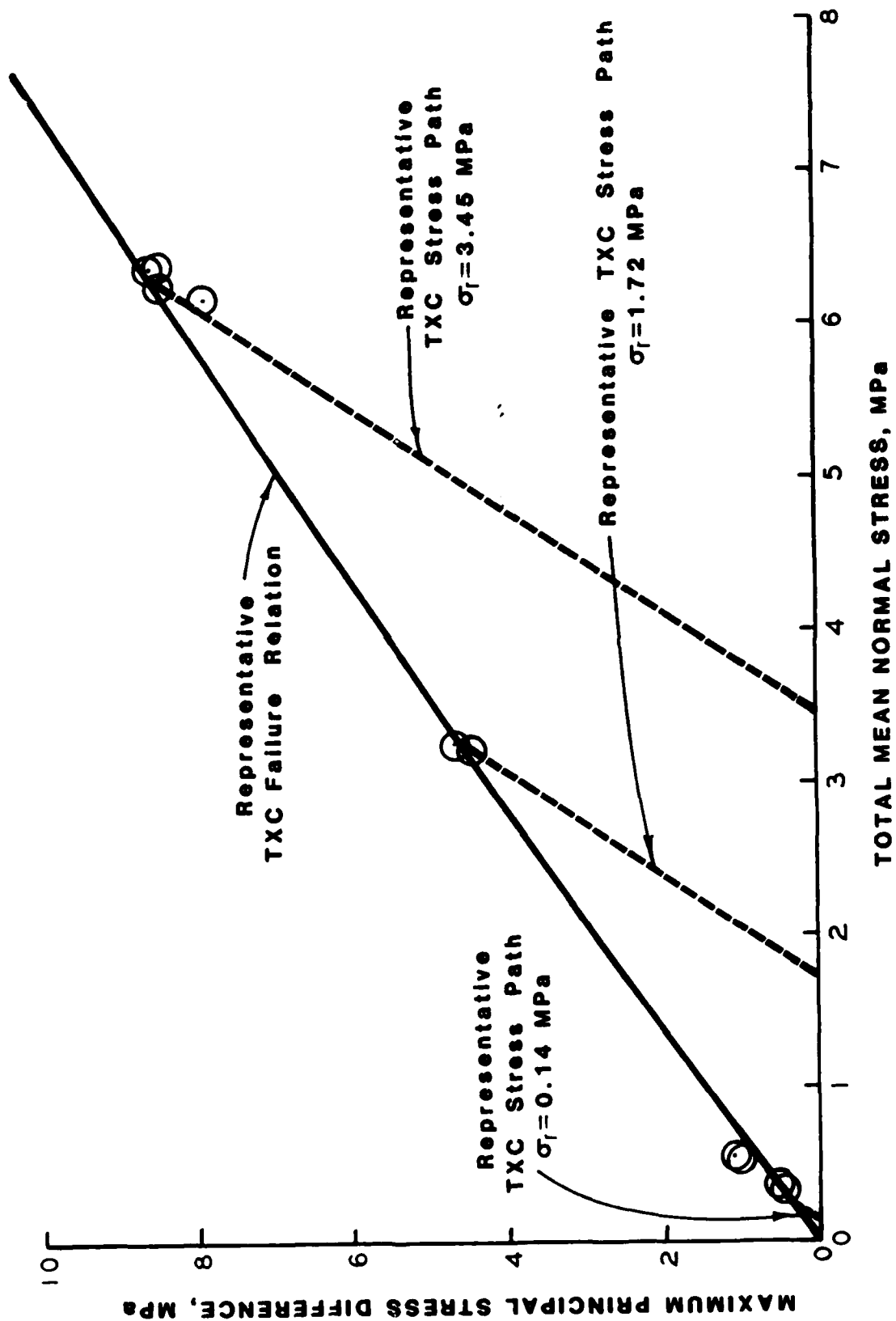
Figure 3.13 Static TXC failure points and representative drained TXC failure and TXC stress path relation for saturated MB sand.

35

Figure 3.14 Static TXC test results and representative undrained TXC failure relation and representative undrained TXC stress path relations for saturated MB sand at effective stresses of 0.14, 1.72, and 3.45 MPa.
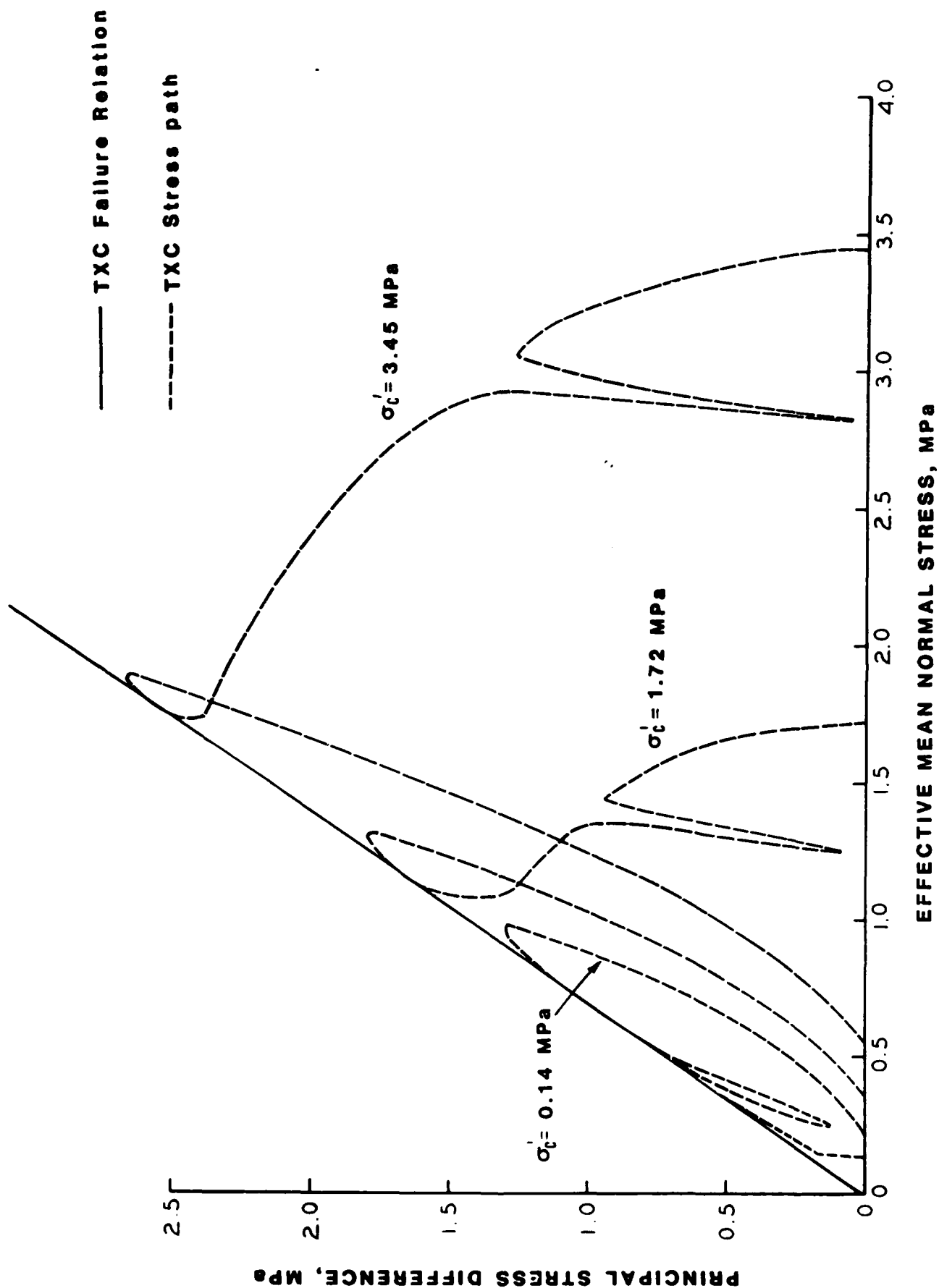
36
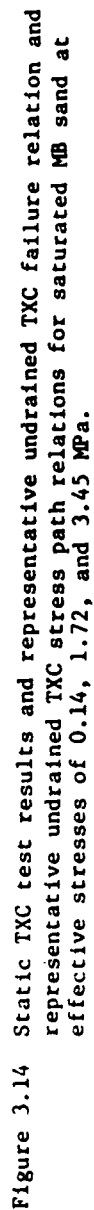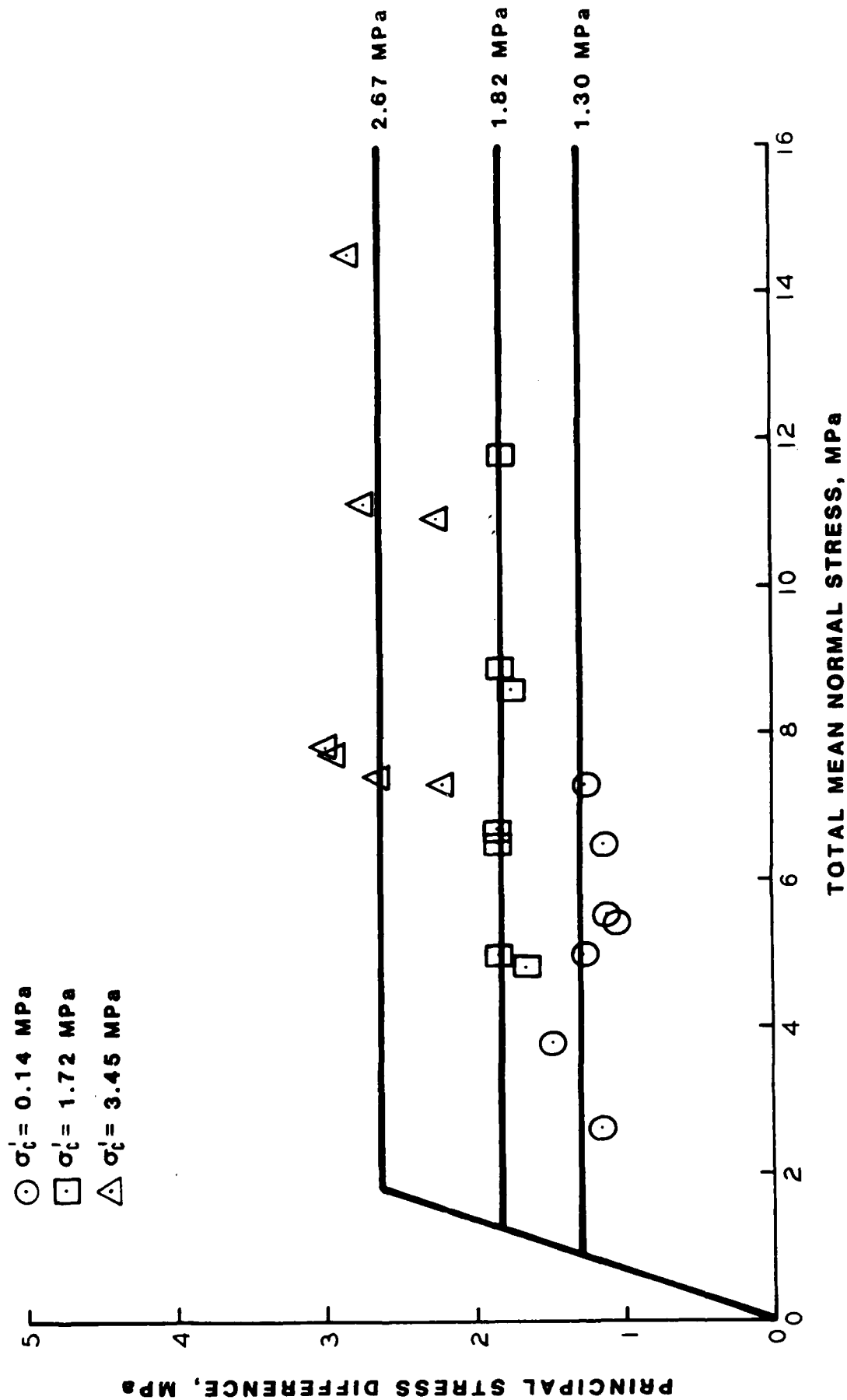
Figure 3.15 Static TXC failure points and representative undrained TXC total stress failure relation for saturated MB sand at effective stresses of 0.14, 1.72, and 3.45 MPa.
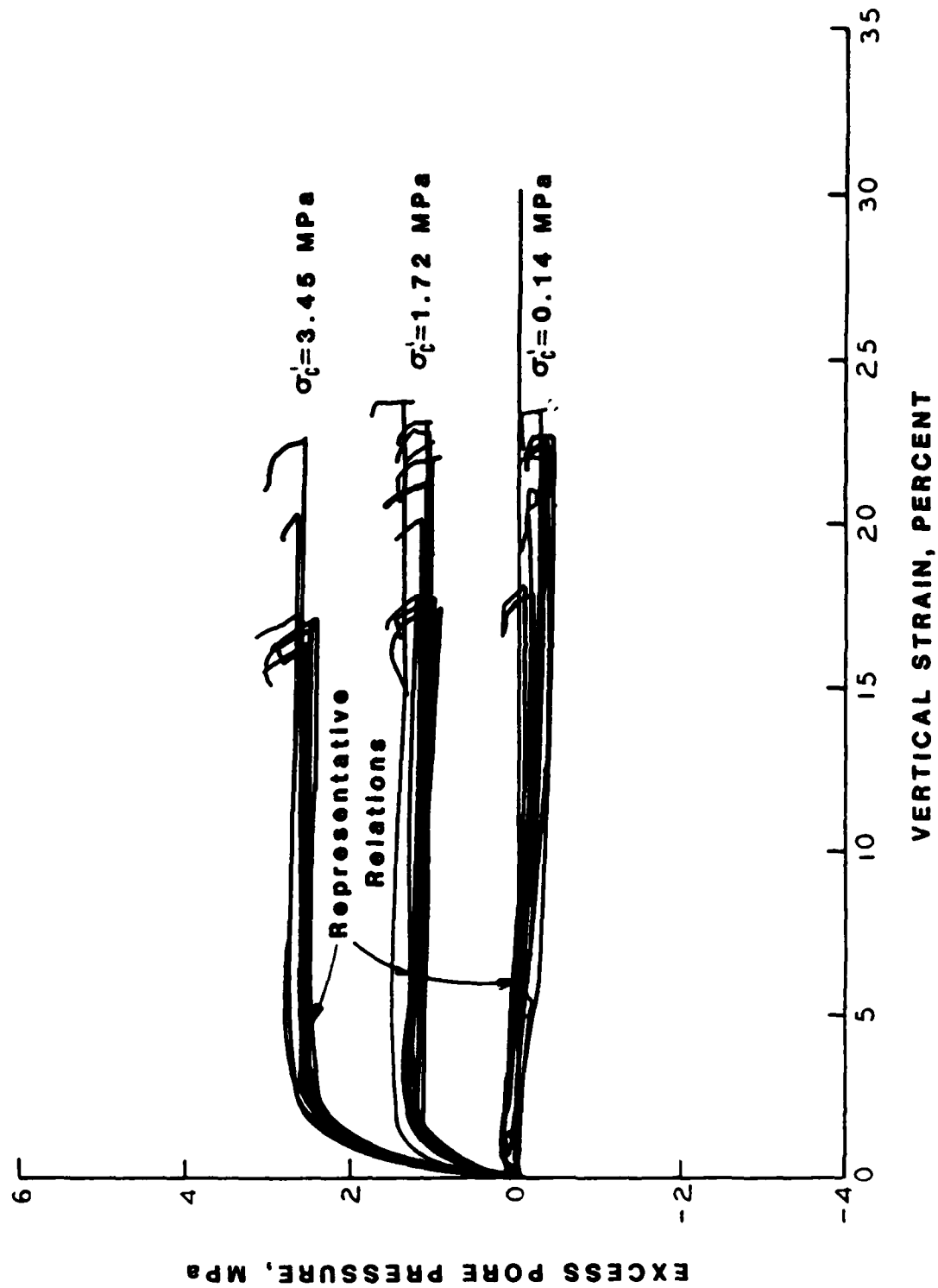
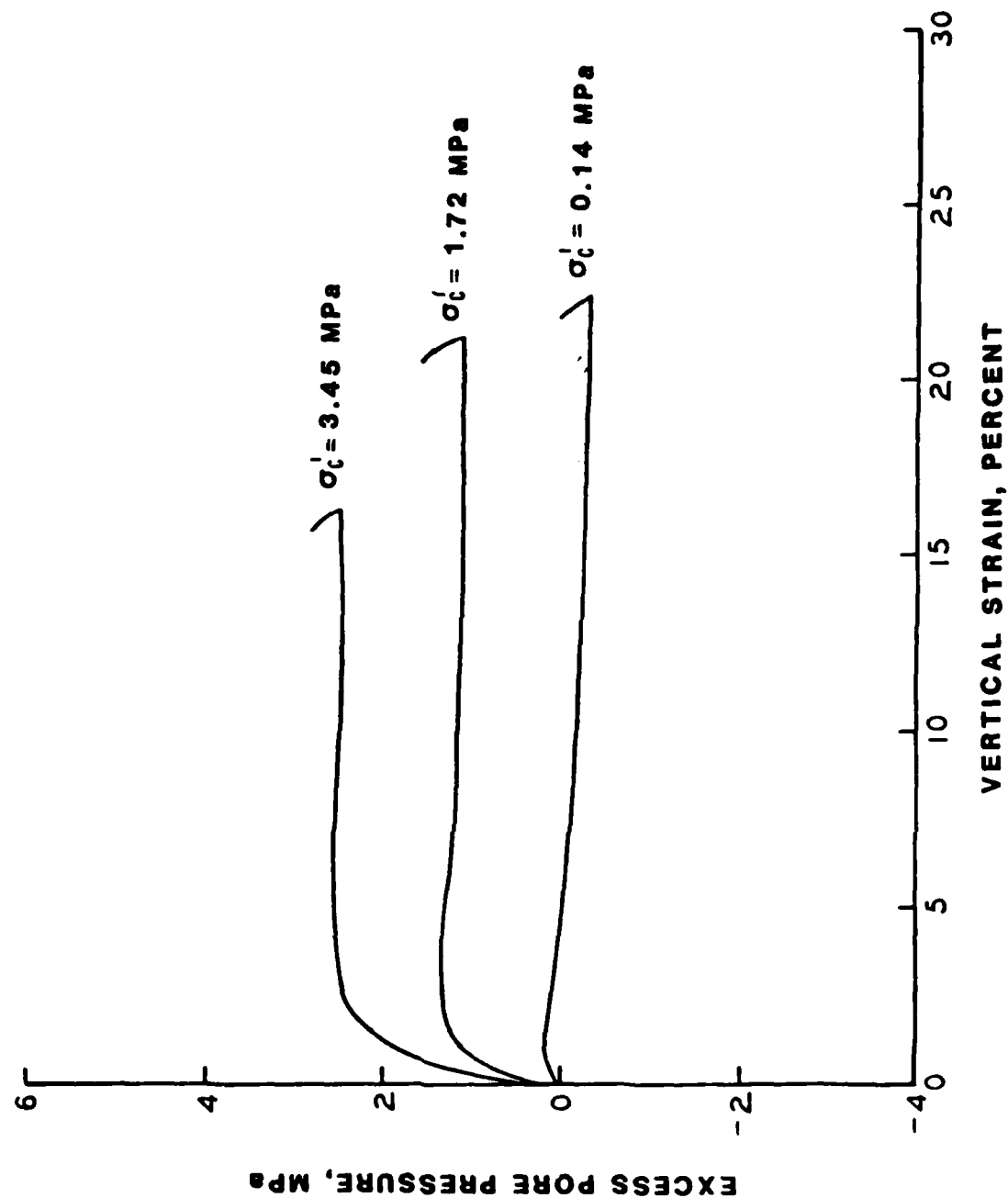Figure 3.16 Static TXC test results and representative undrained pore pressure versus vertical strain relations for saturated MB sand at effective stresses of 0.14, 1.72, and 3.45 MPa.

38
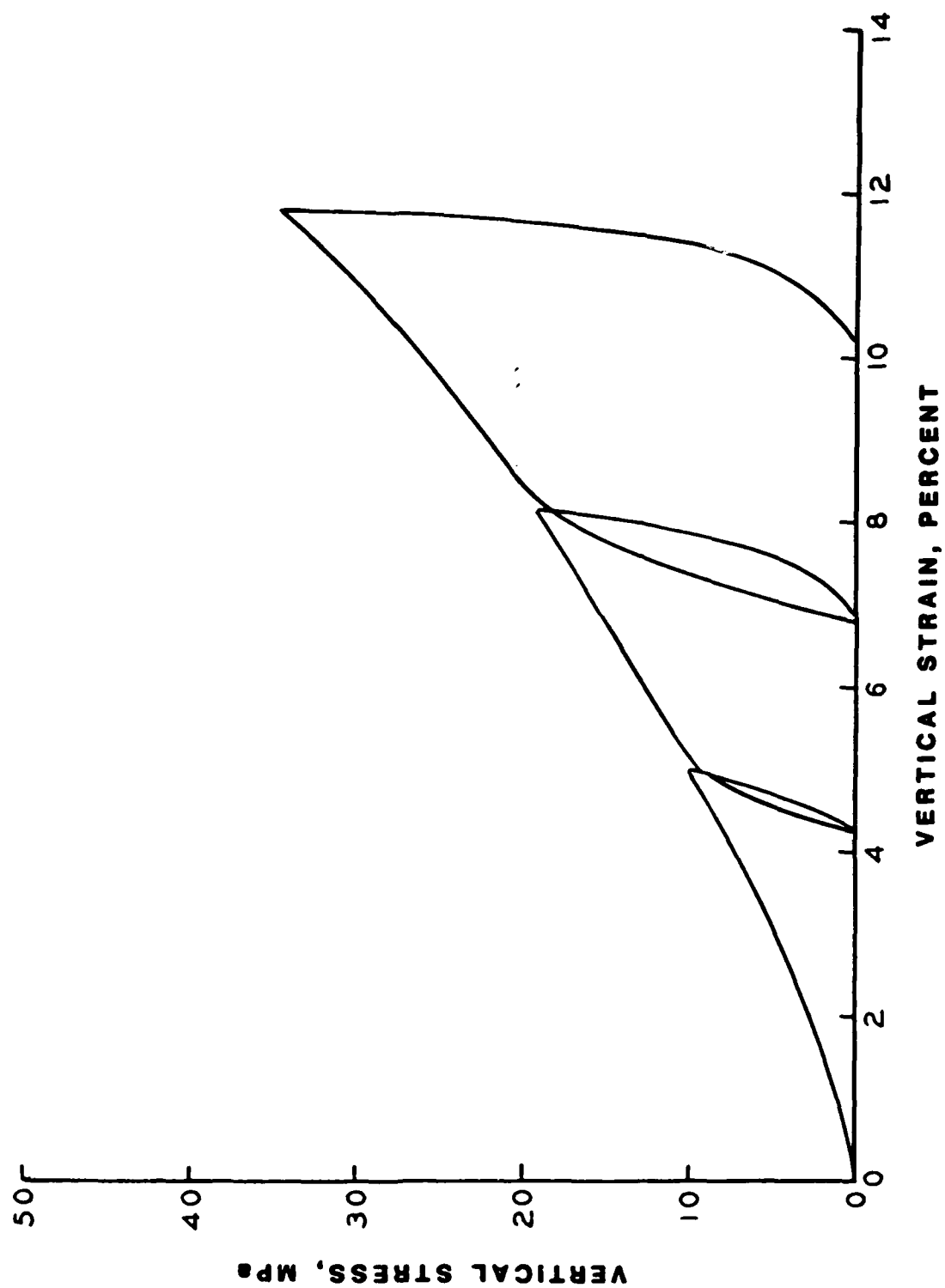
Figure 3.17 Representative UX compressibility relation for dry MB sand.
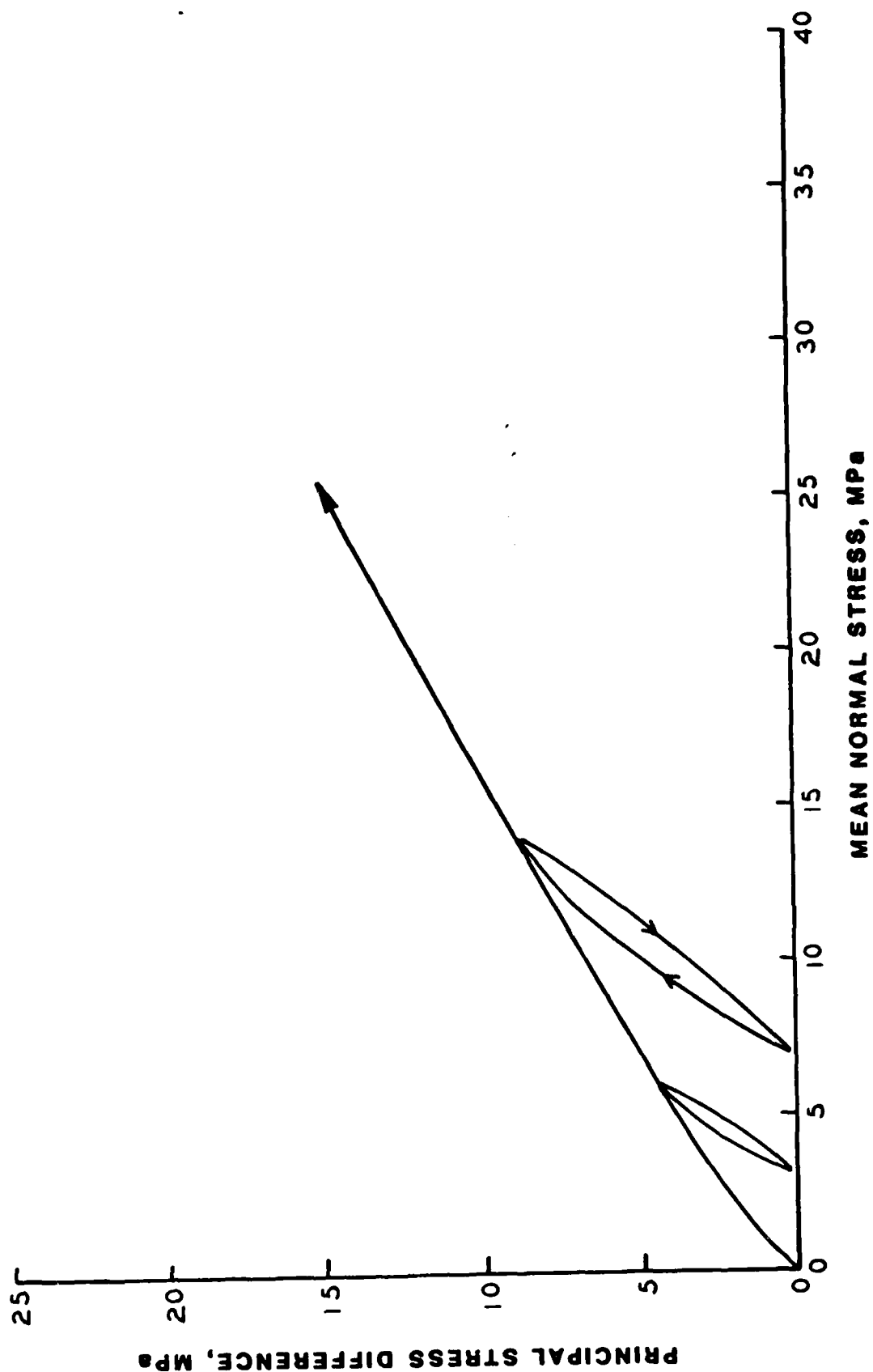
Figure 3.18 Representative UX stress path for dry MB sand.
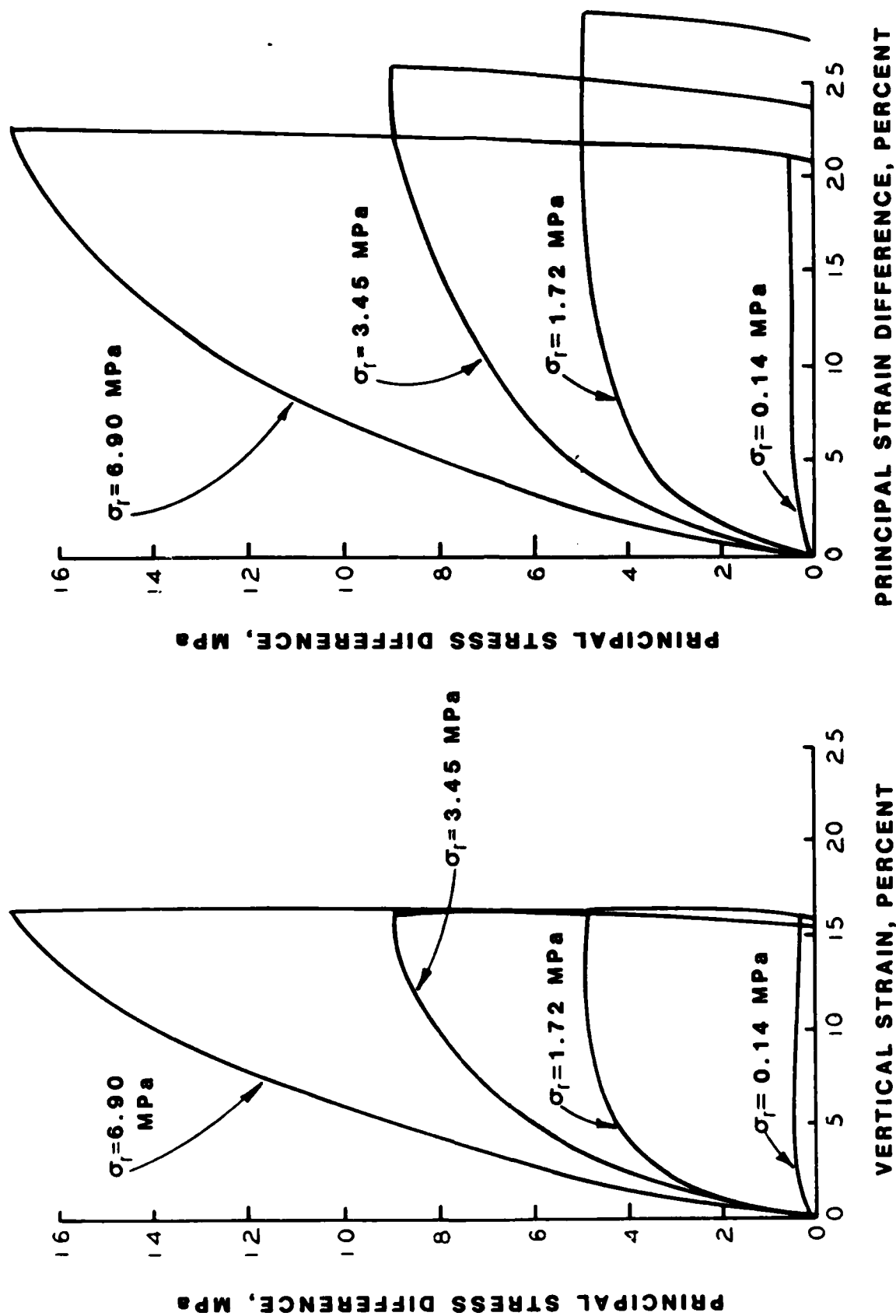
Figure 3.19 Representative TXC stress-strain relations for dry MB sand at confining stresses of 0.14, 1.72, 3.45, and 6.90 MPa.

MEAN NORMAL STRESS, MPa

PRINCIPAL STRESS DIFFERENCE, MPa

1.39p

−0.85p
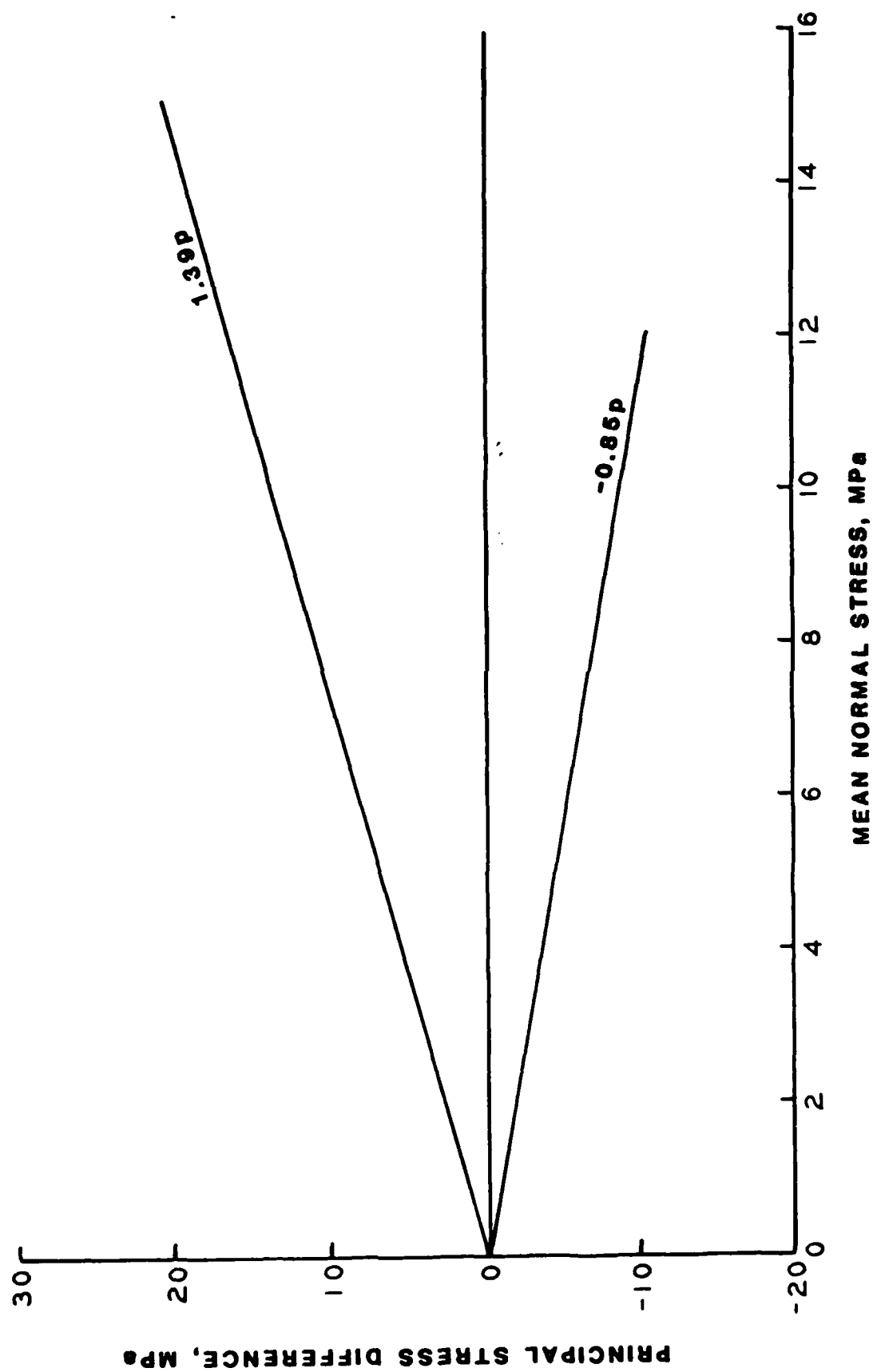
Figure 3.20 Representative TXC and TXE failure relations for dry MB sand.
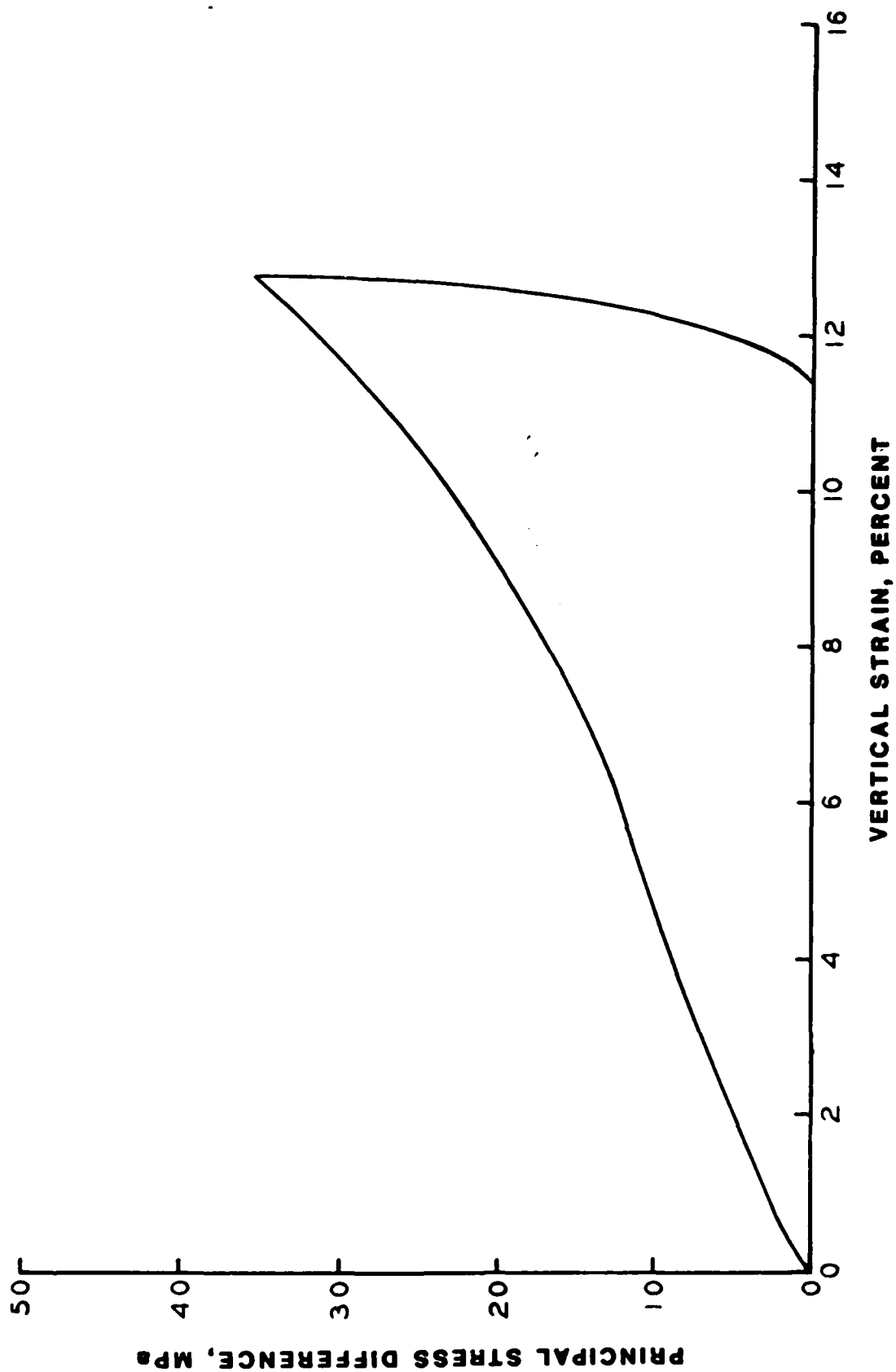
Figure 3.21 Representative drained UX compressibility relation for saturated MB sand.

43
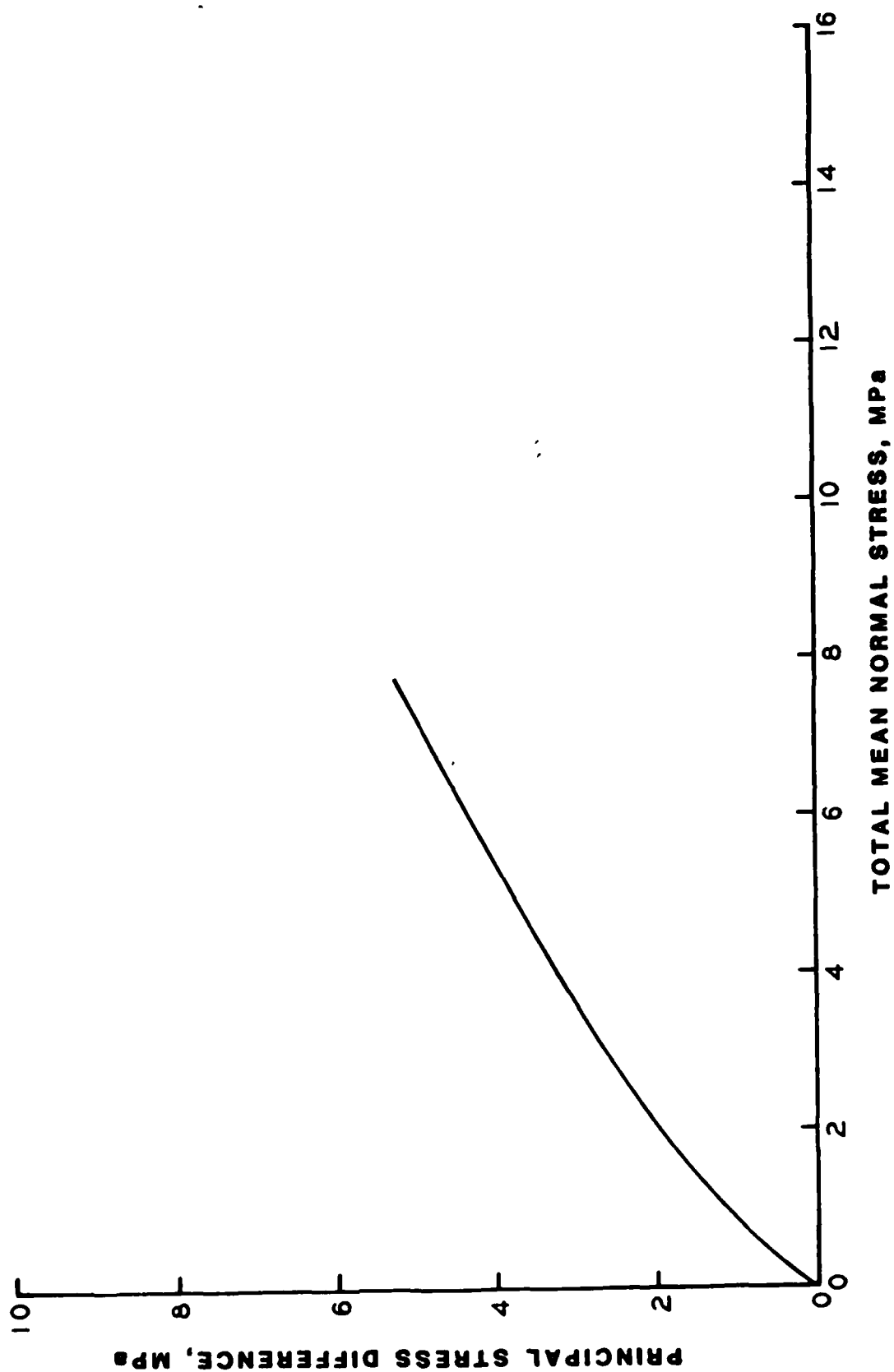
Figure 3.22 Representative drained UX stress path for saturated MB sand.

44
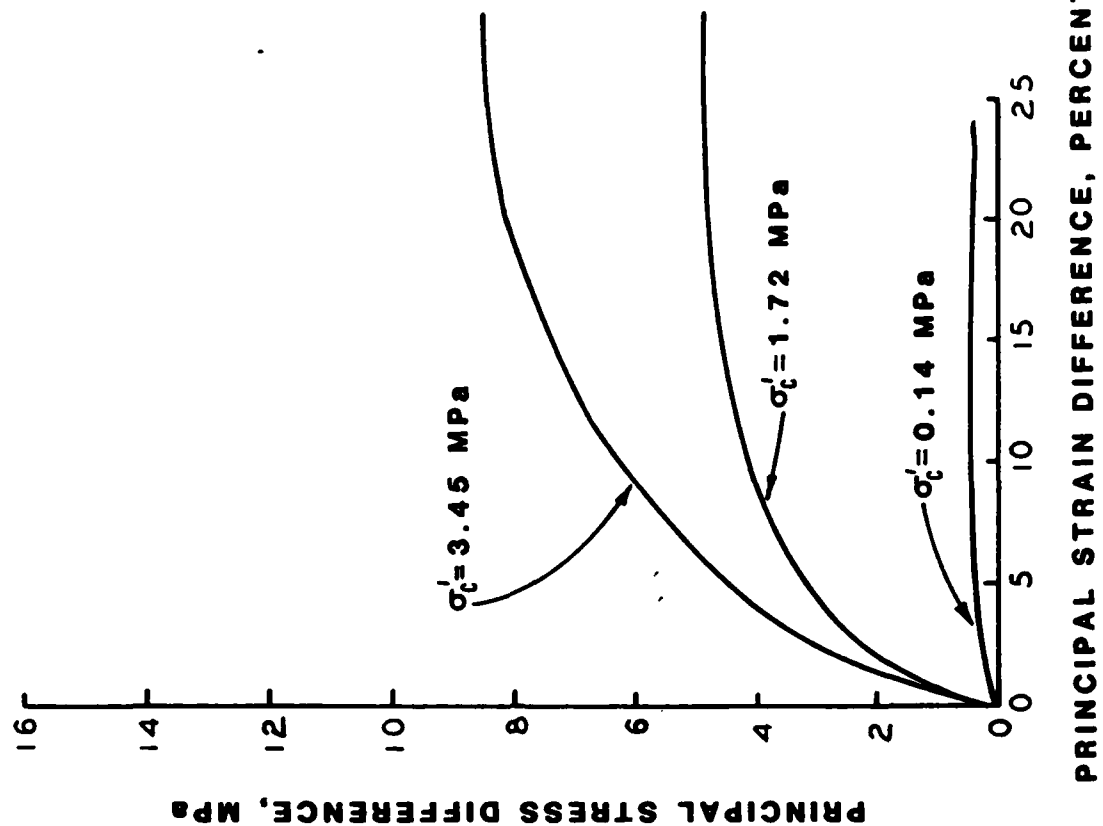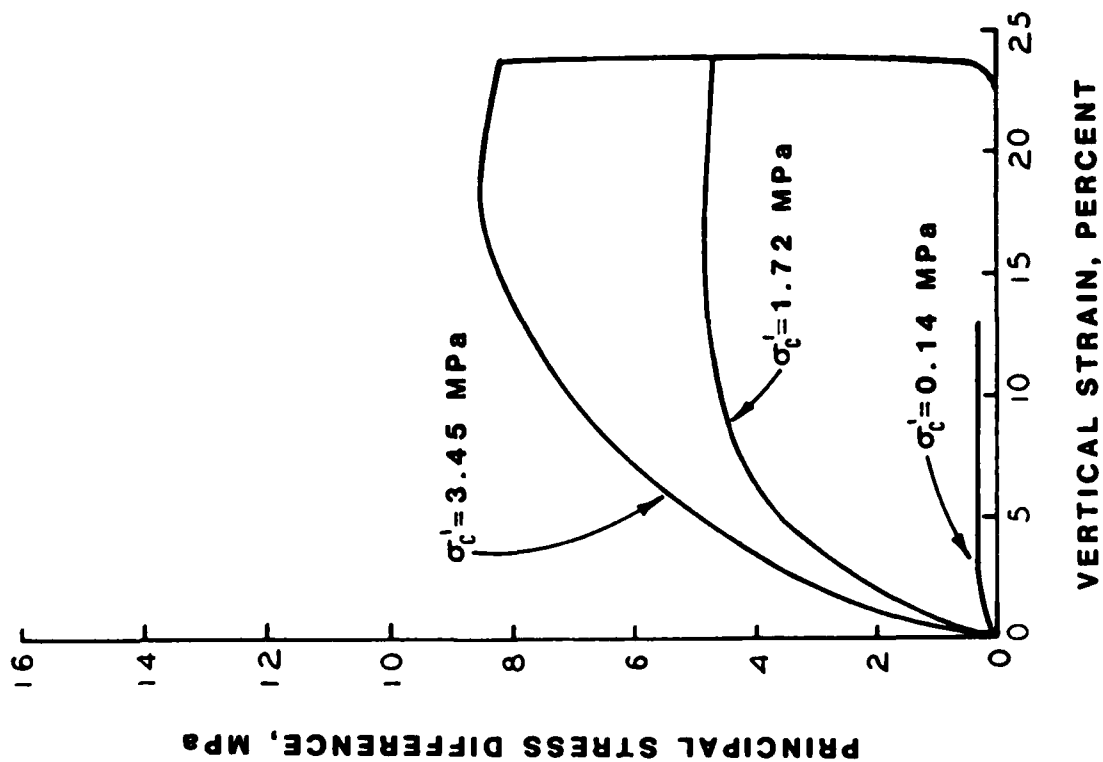
Figure 3.23 Representative drained TXC stress-strain relations for saturated MB sand at effective stresses of 0.14, 1.72, and 3.45 MPa.

45

TOTAL MEAN NORMAL STRESS, MPa

MAXIMUM PRINCIPAL STRESS DIFFERENCE, MPa
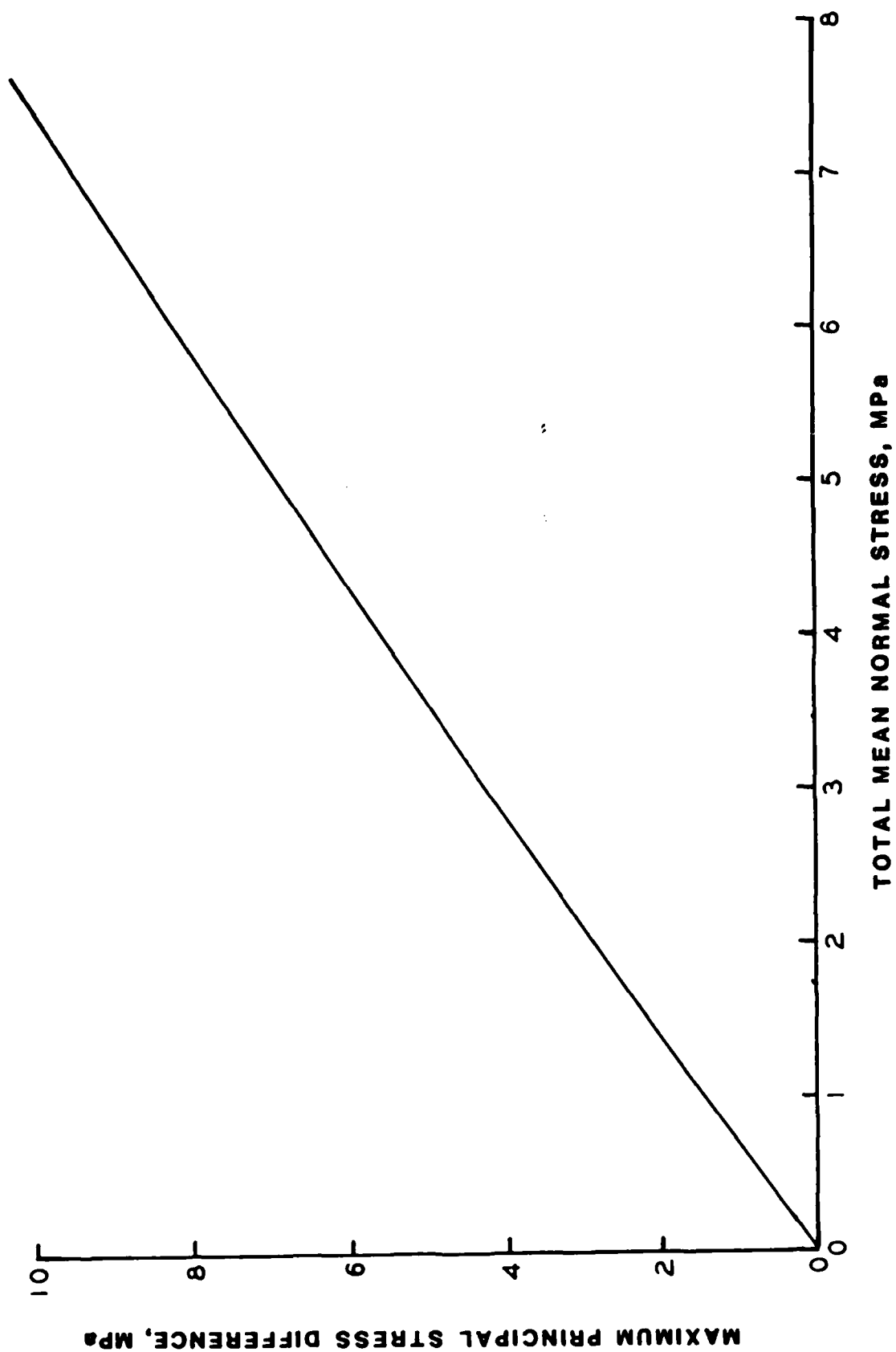
Figure 3.24 Representative drained TXC failure relation for saturated MB sand.
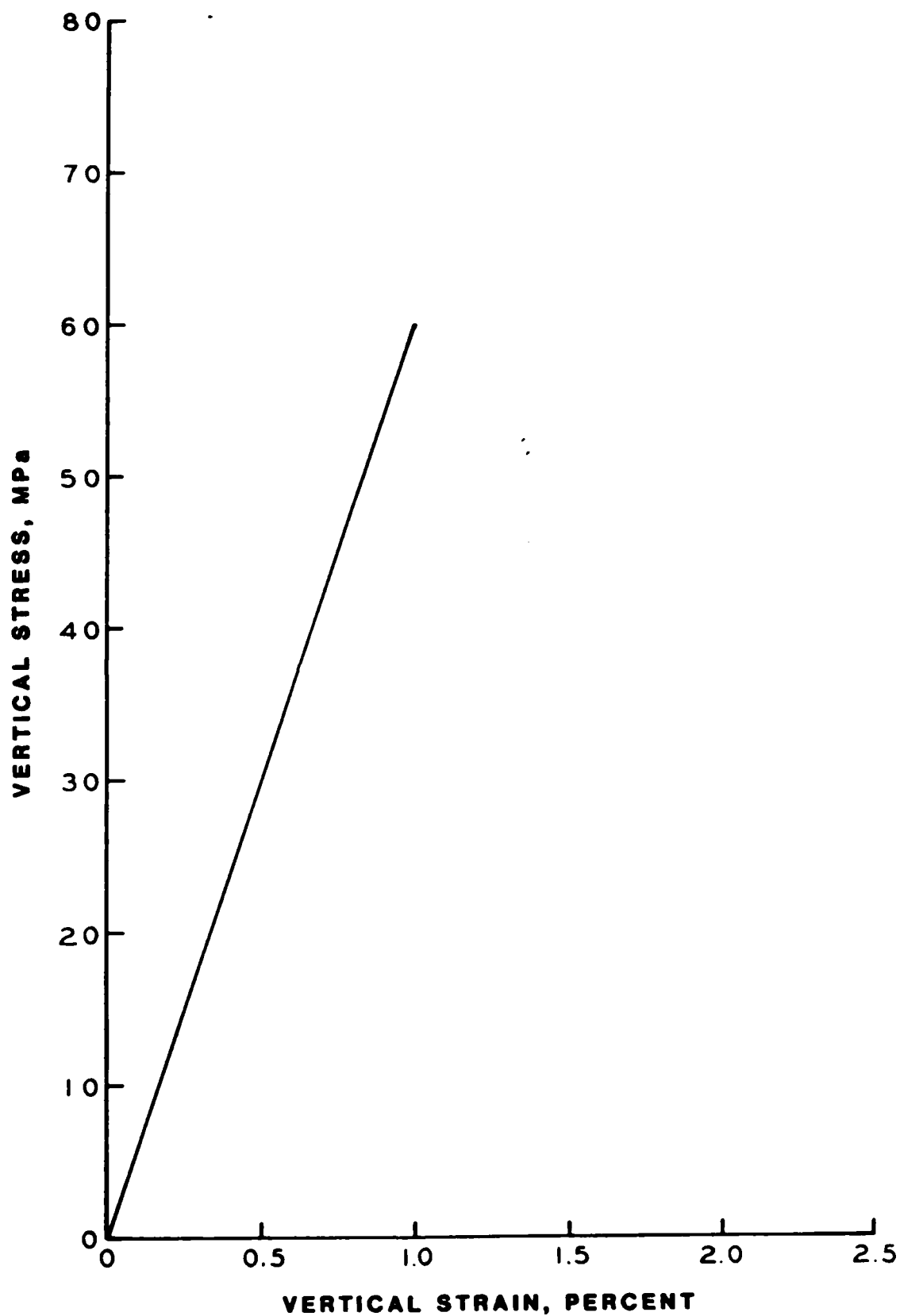
Figure 3.25 Representative undrained UX compressibility
relation for MB sand.

47
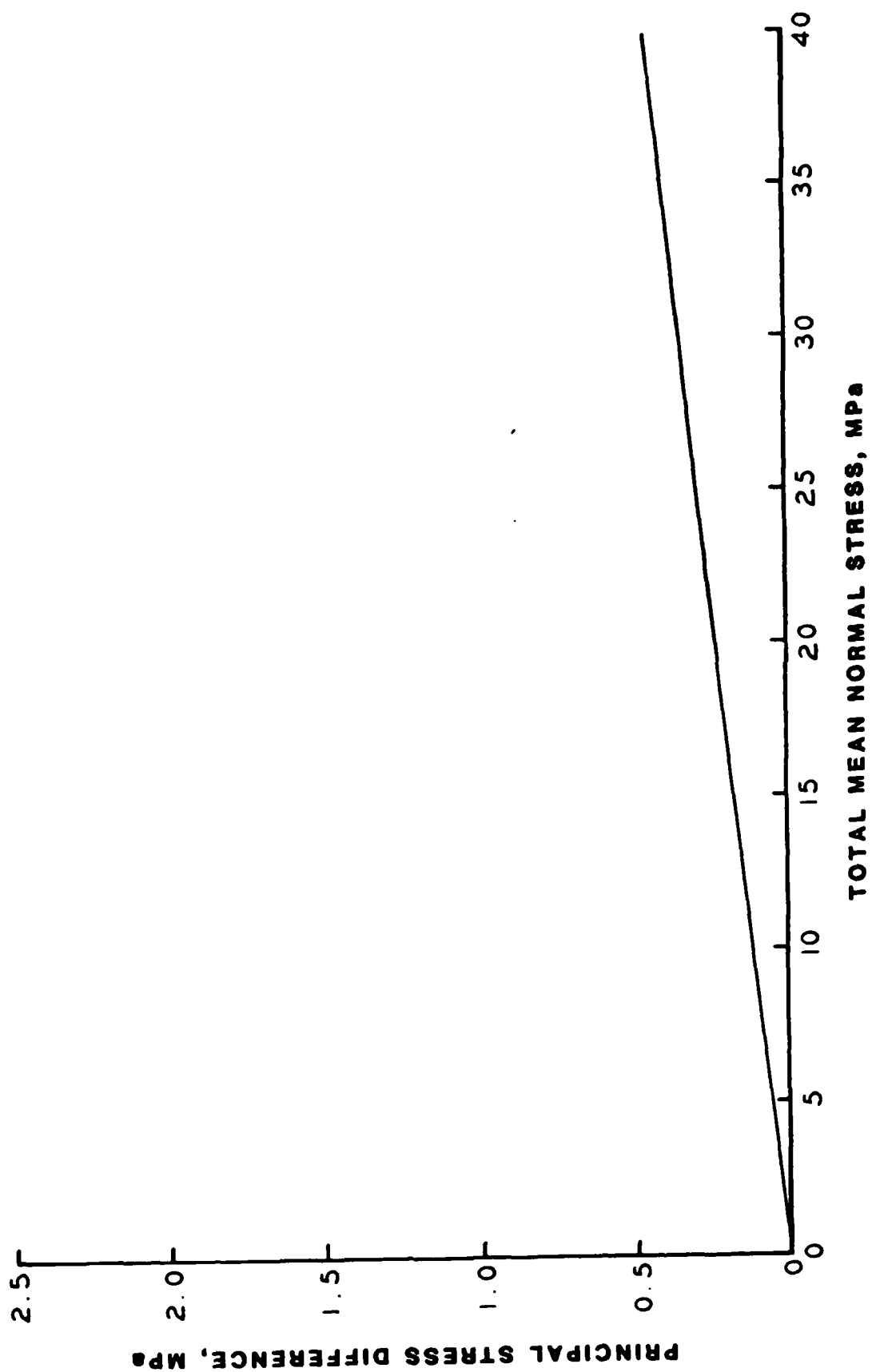
Figure 3.26 Representative undrained UX stress path for saturated MB sand.

Figure 3.27 Representative undrained TXC stress-strain relations for saturated MB sand at effective stresses of 0.14, 1.72, and 3.45 MPa.

49

Figure 3.28 Representative undrained TXC failure relation and TXC effective stress paths for saturated MB sand at effective stresses of 0.14, 1.72, and 3.45 MPa.

50
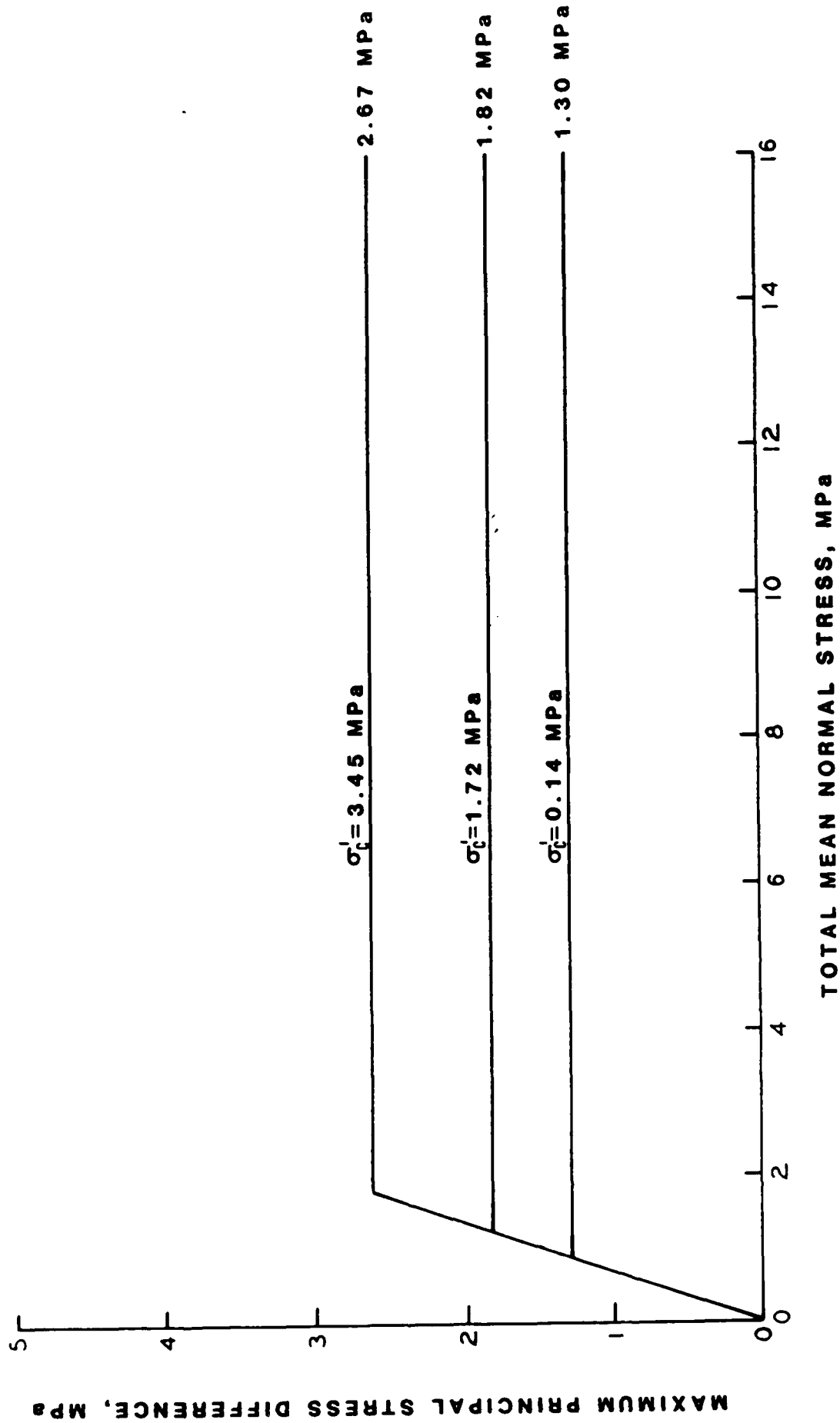
Figure 3.29 Representative undrained TXC total stress failure relation for saturated MB sand.

51

Figure 3.30 Representative undrained TXC pore pressure versus vertical strain relations for MB sand at effective stresses of 0.14, 1.72, and 3.45 MPa.

52

CHAPTER 4

COMPARISONS AND CONCLUSIONS

In the past, conclusions concerning the relationship between sands tested dry and the same material tested in a saturated condition were based on results obtained from laboratory tests at conventional stresses (< about 1 MPa). In Chapter 3, representative curves were presented for MB sand under three test conditions, i.e., UU tests on dry sand (UD), CD tests on saturated sand (DS), and CU tests on saturated sand (US). These data offer an opportunity to examine the relationships of the response of MB sand under these three conditions at higher stress levels than normally obtained in conventional testing laboratories.

4.1 UX RELATIONS

Figure 4.1 shows a comparison of the representative UX compressibility relations for each of the three initial conditions. Although the UD and DS curves are similar, they differ below 10 MPa; the UD curve has an initial positive curvature while the DS curvature is negative in that region. The US curve is highly incompressible and yields a constrained modulus of approximately 6000 MPa.

A plot of the UX stress paths for the three sets of initial conditions are shown in Figure 4.2. Unlike the compressibility relations, the UD and DS curves are identical within the stress levels shown. The US relation is extremely low and has an implied Poisson's ratio of 0.497.

4.2 TX RELATIONS

Figure 4.3 shows the representative principal stress difference versus vertical strain curves for the three effective confining stresses. The UD curves represent confining stresses of 0.14, 1.72, and 3.45 MPa; the DS and US curves represent initial effective confining stresses of 0.14, 1.72, and 3.45 MPa. In each case, the UD and DS curves agree within the scatter of the data; however, the curve shapes are slightly different. The maximum principal stress difference for the DS curves occurs at a smaller value of vertical strain than for the UD relations.

53

The relationship between the DS and US responses in Figure 4.3 is a function of the initial effective stress. Figure 4.4 shows the following representative US and DS TXC relations for the 0.14 and 1.72 MPa effective stresses: (a) excess pore pressure versus vertical strain, (b) TXC stress-strain, and (c) stress path. During the drained tests on saturated MB sand the cell pressure was kept constant and the pore water was permitted to drain during application of the TXC load. Since effective confining stress is the difference between the cell pressure and the pore pressure, the effective confining stress was also constant during application of the load in these tests, resulting in representative stress paths with a slope of 3. For the undrained tests the cell pressure was kept constant but the pore water was not allowed to drain and pore pressures were developed which resulted in changes in the initial effective confining stress and a corresponding change in behavior during TXC loading. For MB sand at an initial effective stress of 0.14 MPa, the pore pressure increases initially during undrained applica-tion of the load and then decreases to values below the initial pore pressure at vertical strains of 10 to 15 percent. The net effect is for the effective confining stress at failure in the US response to be greater than the effec-tive confining stress at failure for the DS response and therefore the corresponding US strength is greater than the DS strength. For the same material at an initial effective stress of 1.72 MPa, a large initial increase in pore pressure is followed by a small decrease at larger strains. This response results in an effective confinirg stress at failure for the US relation which is less than that for the DS response and therefore the US strength is less than the DS strength. This trend is more pronounced at the 3.45-MPa effective stress, as shown in Figure 4.3.

A summary of the total-stress failure relation for the UD and US condi-tions and a rezeroed (to the point after back-pressure saturation occurred) DS total-stress failure relation is presented in Figure 4.5. These relations overlay until the US relation reaches the von Mises limit for each effective stress. At higher stresses, the DS relation and the UD relation agree very well.

4.3 UD VERSUS DS RESPONSE

For the MB sand, the following conclusions can be made about the rela-tionship between UD and DS behavior at high stress levels: (a) the initial

54

compressibility behavior exhibits a difference at stress levels below 10 MPa, (b) the TXC principal stress difference versus vertical strain relations are slightly different with the DS relation attaining a maximum principal stress difference at a smaller vertical strain than the UD relation, and (c) the DS and UD failure relations are essentially the same within the stress levels which were investigated. These general observations are based only on the results in this study, and further research should be conducted to identify and quantify these observations in more detail.
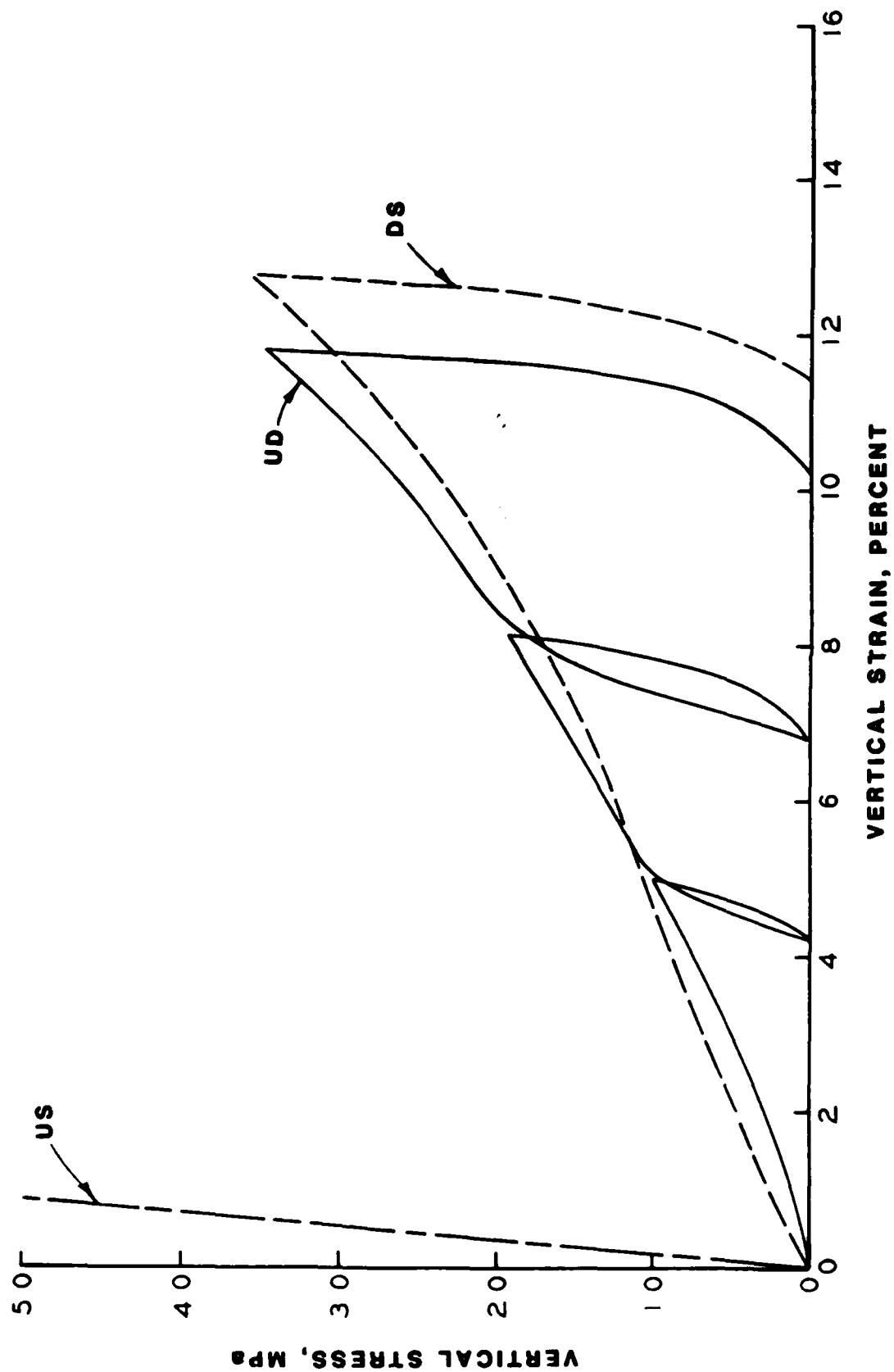
Figure 4.1 Comparison of the representative UX compressibility relation for dry MB sand with the representative drained and undrained UX compressibilities for saturated MB sand.
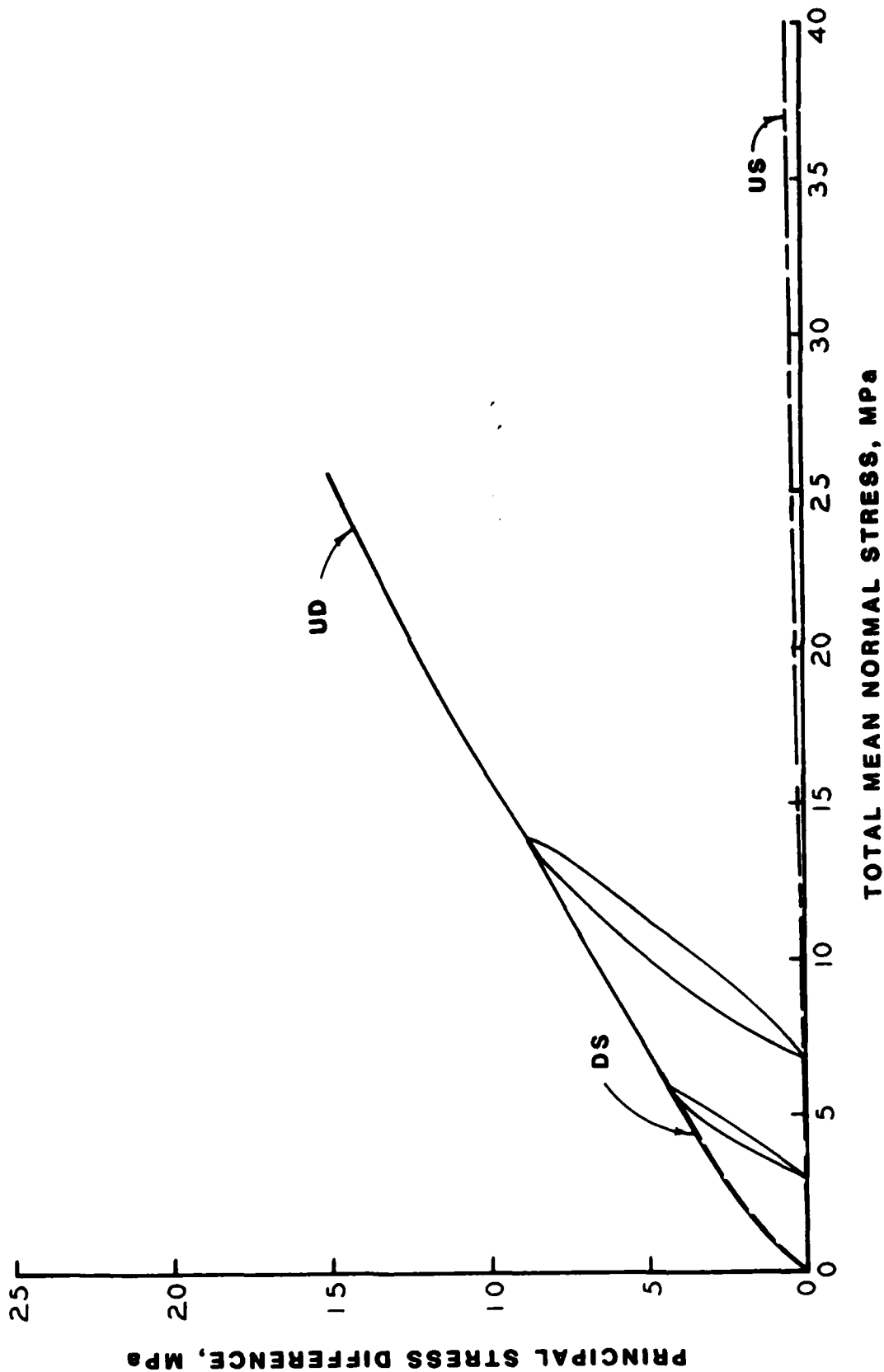
Figure 4.2 Comparison of the representative UX stress path for dry MB sand with the representative drained and undrained UX stress paths for saturated MB sand.

57
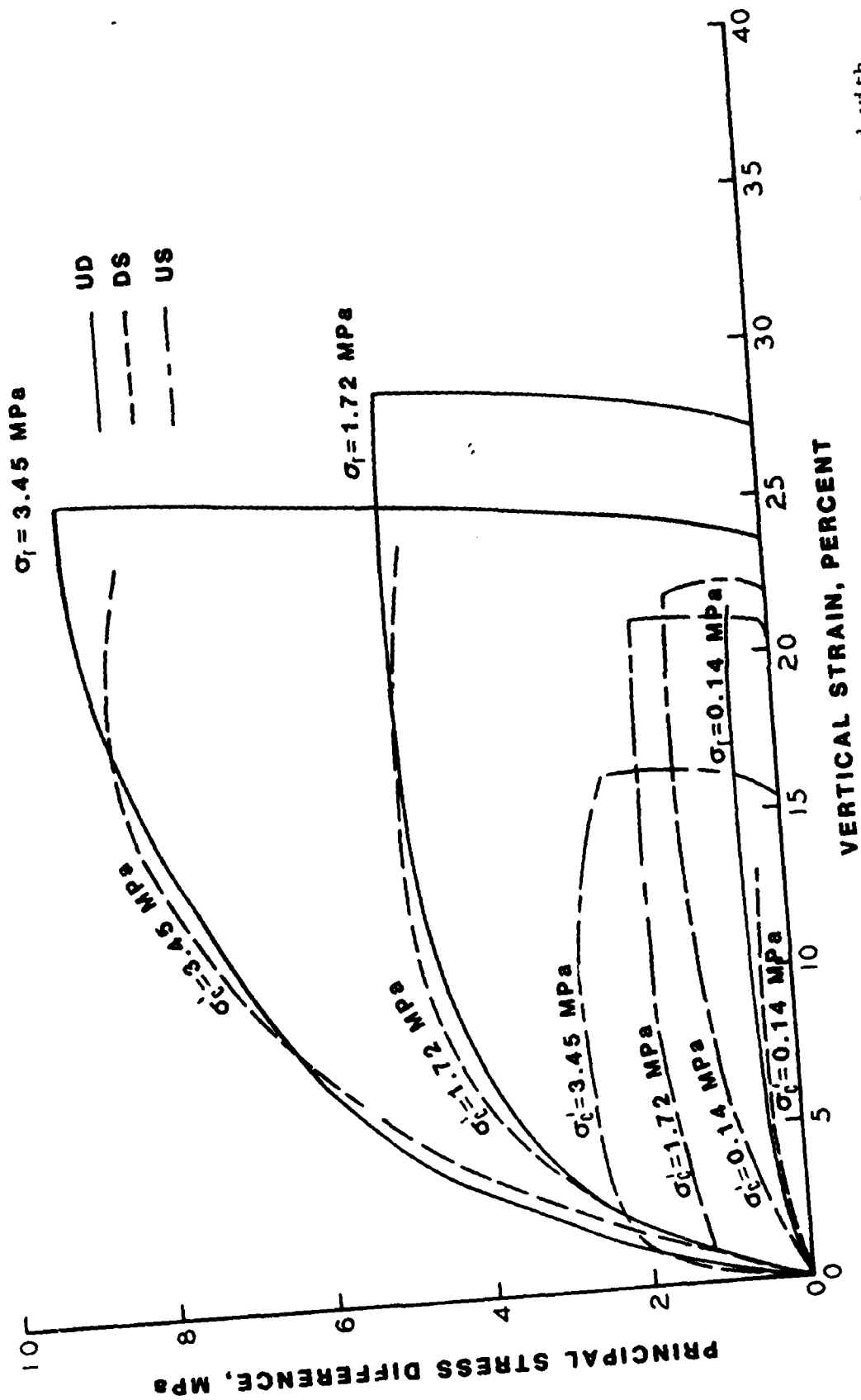
Figure 4.3 Comparison of the representative TXC stress-strain relations for dry MB sand with the representative drained and undrained TXC stress-strain relations for saturated MB sand.

58
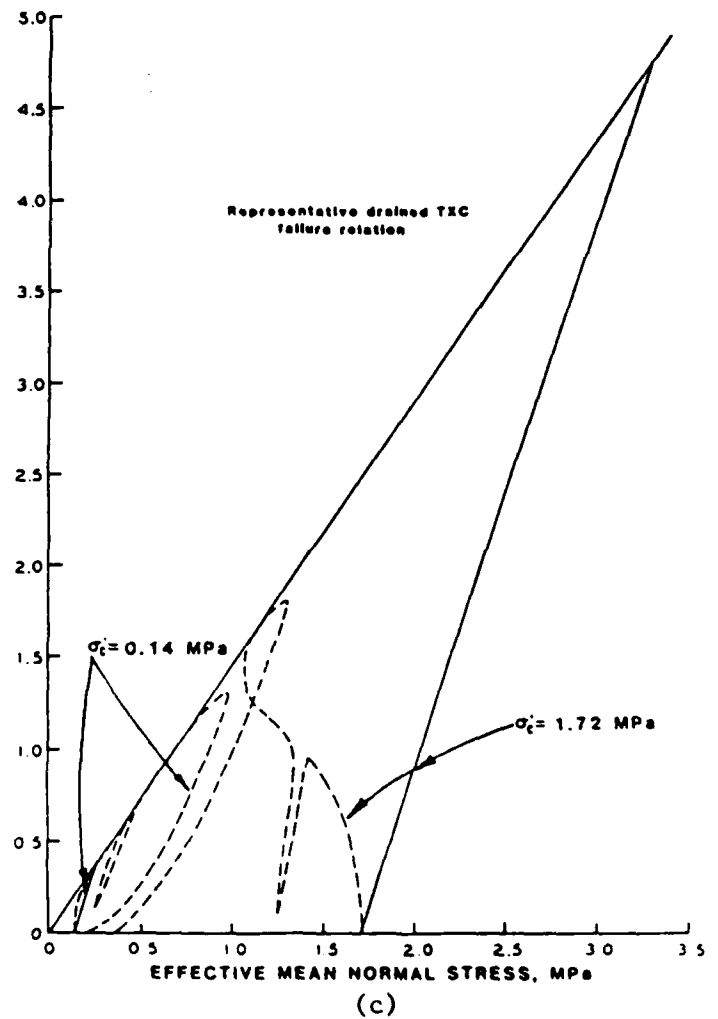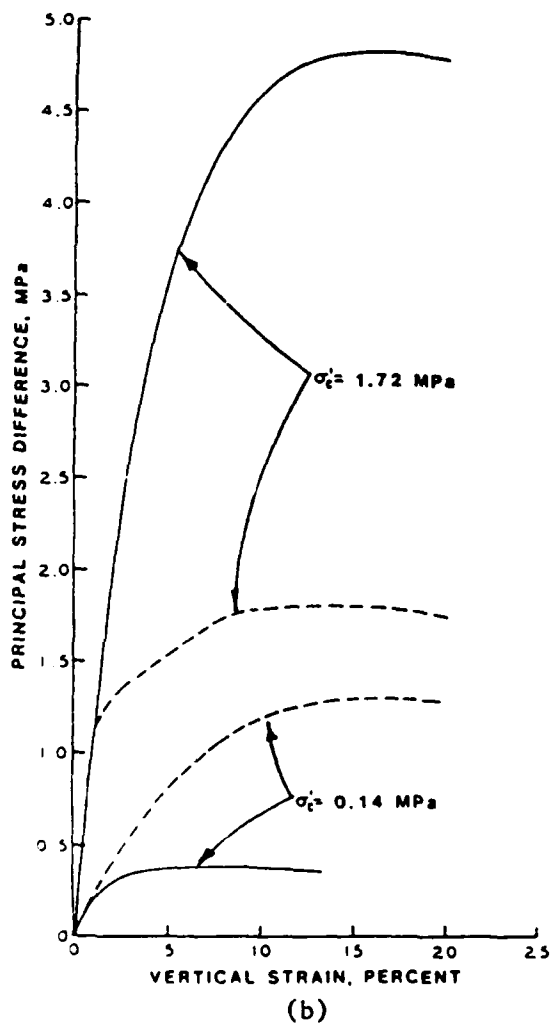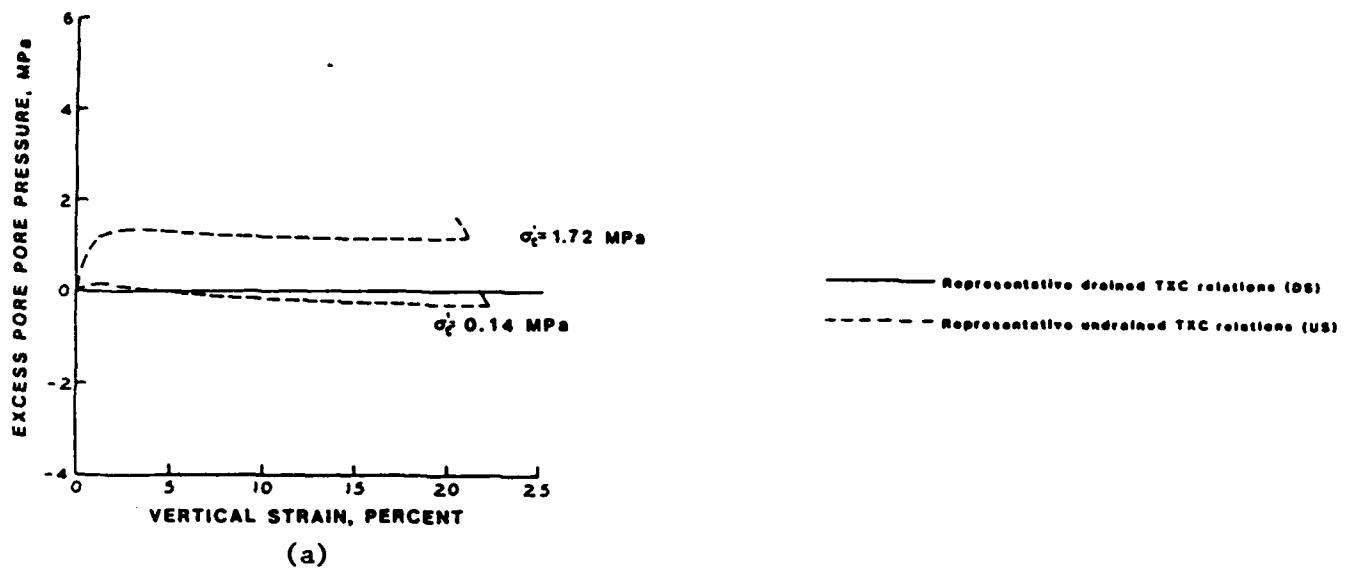
Figure 4.4 Representative drained and undrained TXC relations for saturated MB sand at effective stresses of 0.14 and 1.72 MPa.
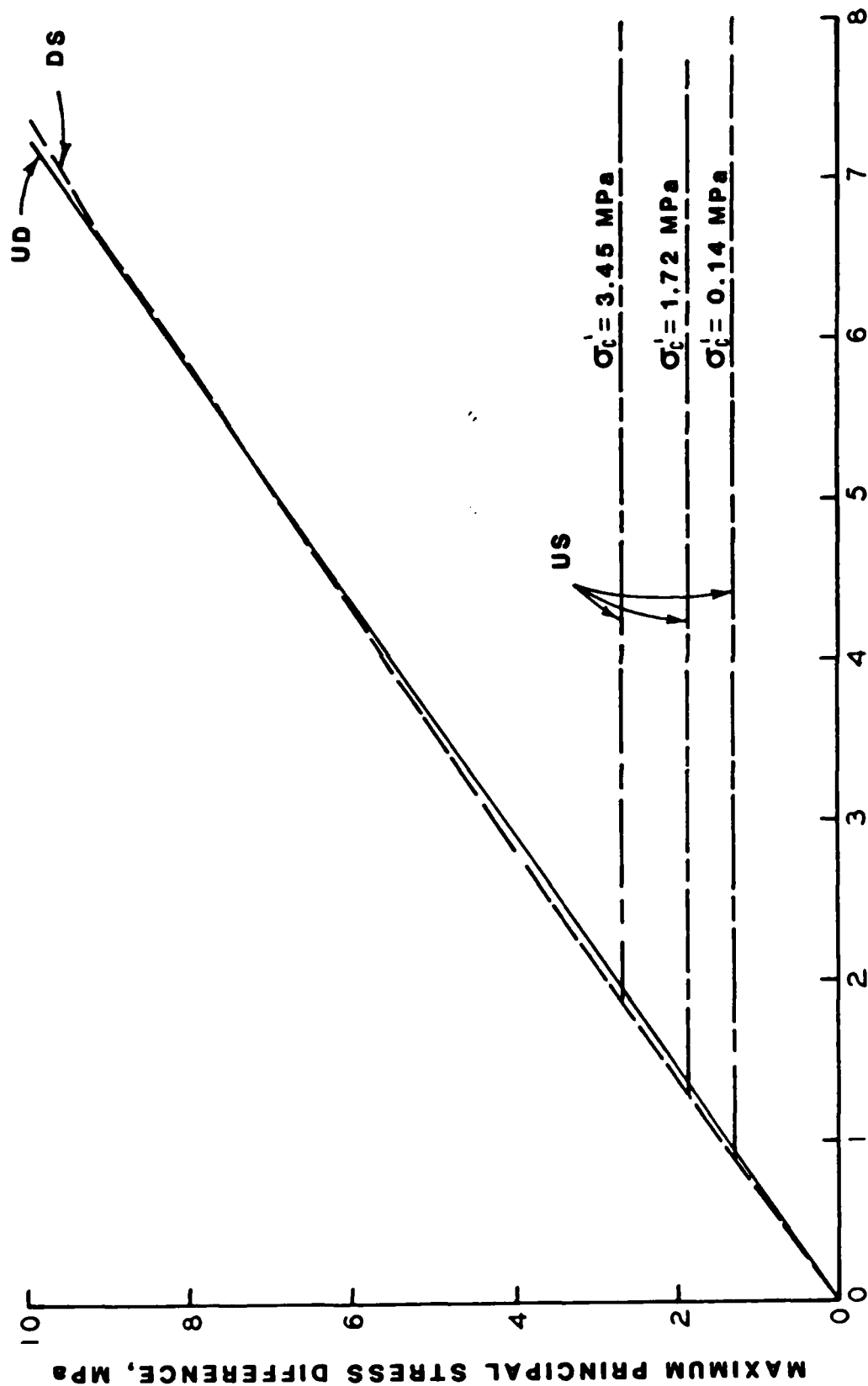
Figure 4.5 Comparison of the representative TXC failure relation for dry MB sand with the representative drained and undrained total stress TXC failure relations for saturated MB sand

REFERENCES

1. B. R. Phillips; "Mechanical Response of Dry Reid-Bedford Model Sand and Saturated Misers Bluff Sand"; January 1982; U. S. Army Engineer Waterways Experiment Station, CE, Vicksburg, MS.

2. Headquarters, Department of the Army, Office, Chief of Engineers; "Laboratory Soils Testing"; Engineering Manual No. EM-1110-2-1906, 30 November 1970 (amended 1 May 1980); Washington, DC.

3. U. S. Army Engineer Waterways Experiment Station; "The Unified Soil Classification System"; Technical Memorandum No. 3-357, April 1960 (reprinted May 1967); CE, Vicksburg, MS.

4. J. Q. Ehrgott; "Calculation of Stress and Strain from Triaxial Test Data on Undrained Soil Specimens"; Miscellaneous Paper S-71-9, May 1971; U. S. Army Engineer Waterways Experiment Station, CE, Vicksburg, MS.

5. R. O. Davis and J. J. Blake; "Synthesis of Soil Hugonoits Between 1 and 100 Kilobars"; AFWL-TR-72-83, September 1972; Air Force Weapons Laboratory, Air Force Systems Command, Kirtland Air Force Base, NM.

6. Alan W. Bishop and D. J. Henkel; The Measurement of Soil Properties in the Triaxial Tests; 1962; Edward Arnold LTD, London.
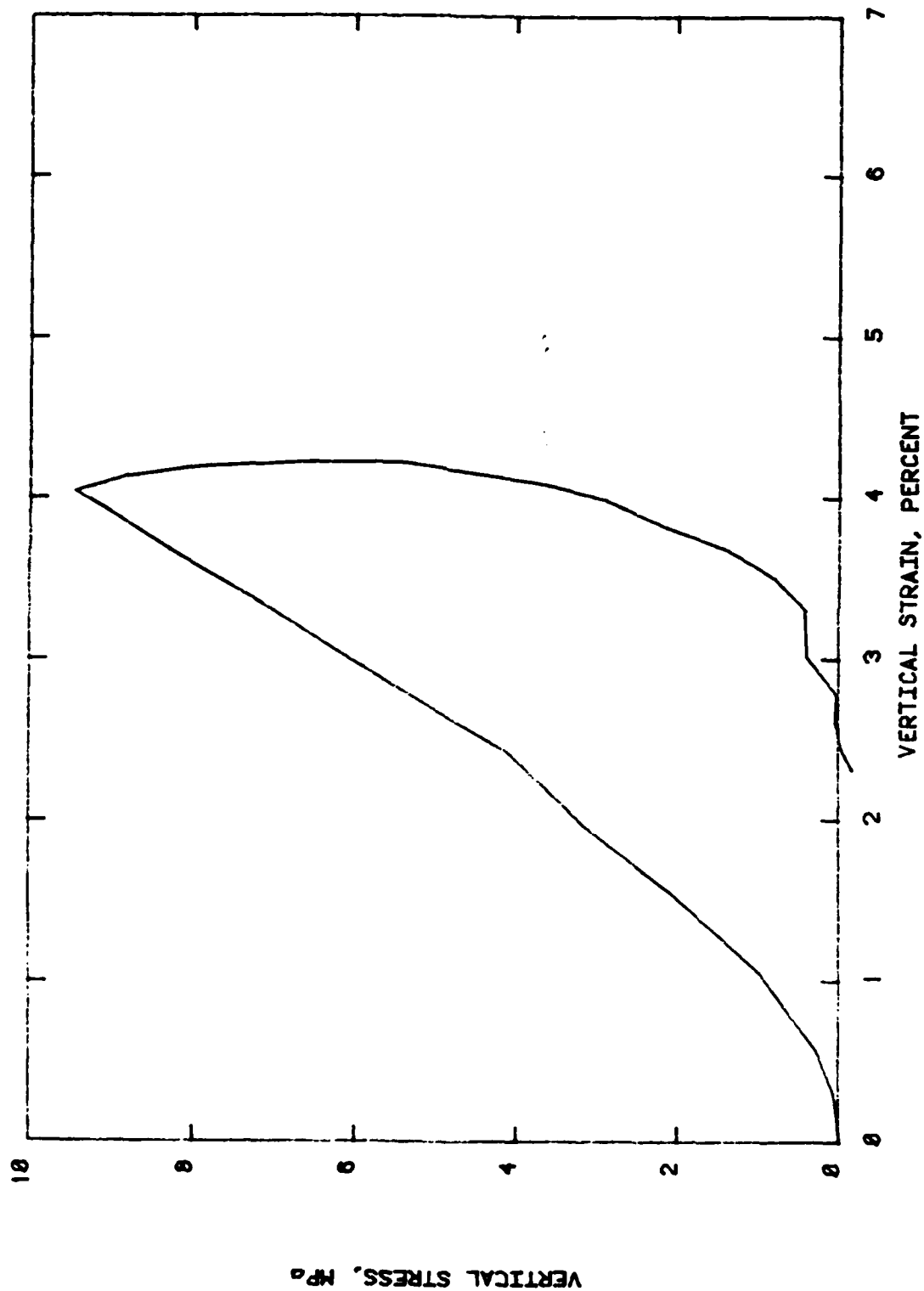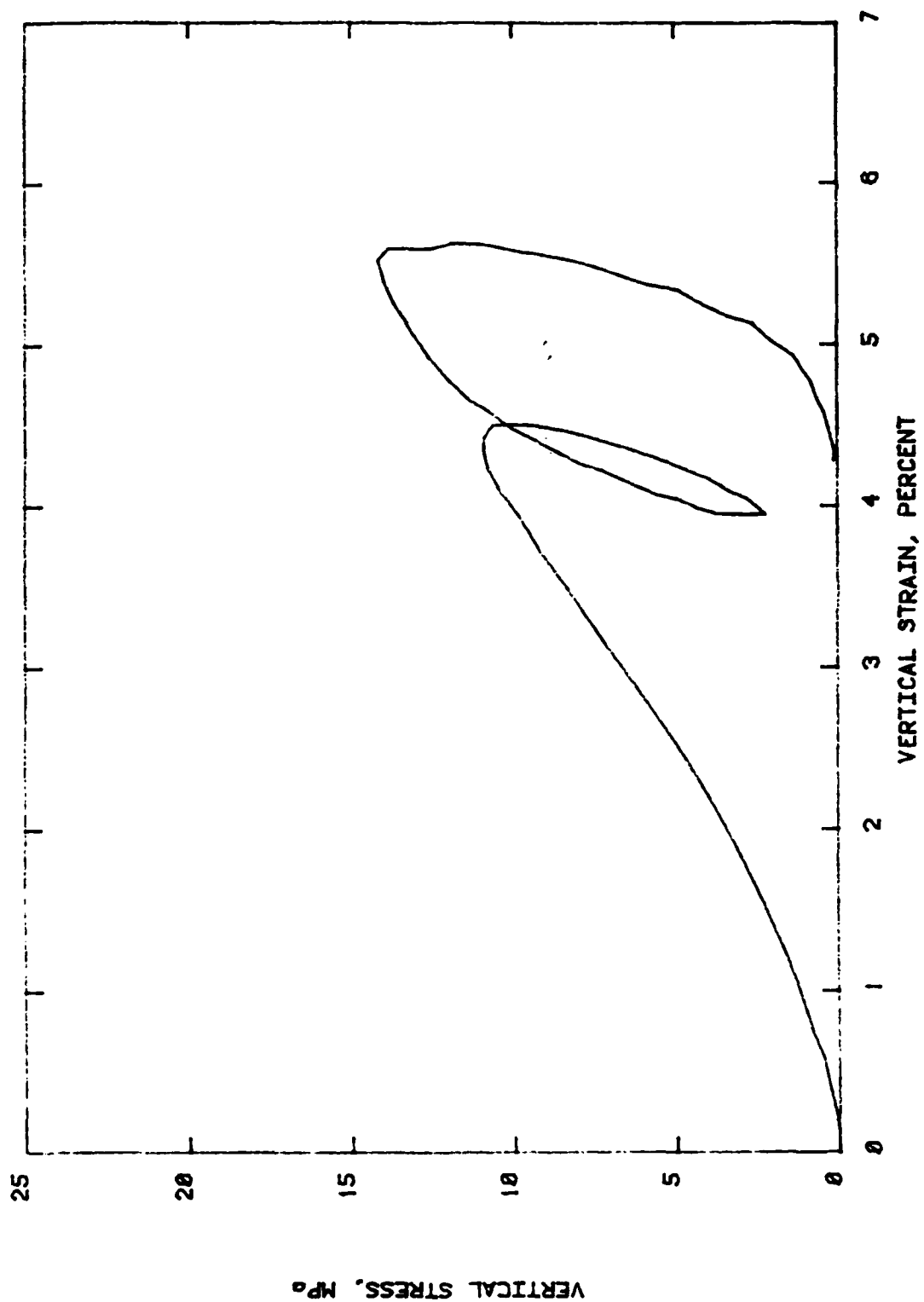
TEST NUMBER:MBDUX.1

STATIC UNIAXIAL STRAIN TEST RESULTS

VERTICAL STRAIN, PERCENT

VERTICAL STRESS, MPa

PLATE 1
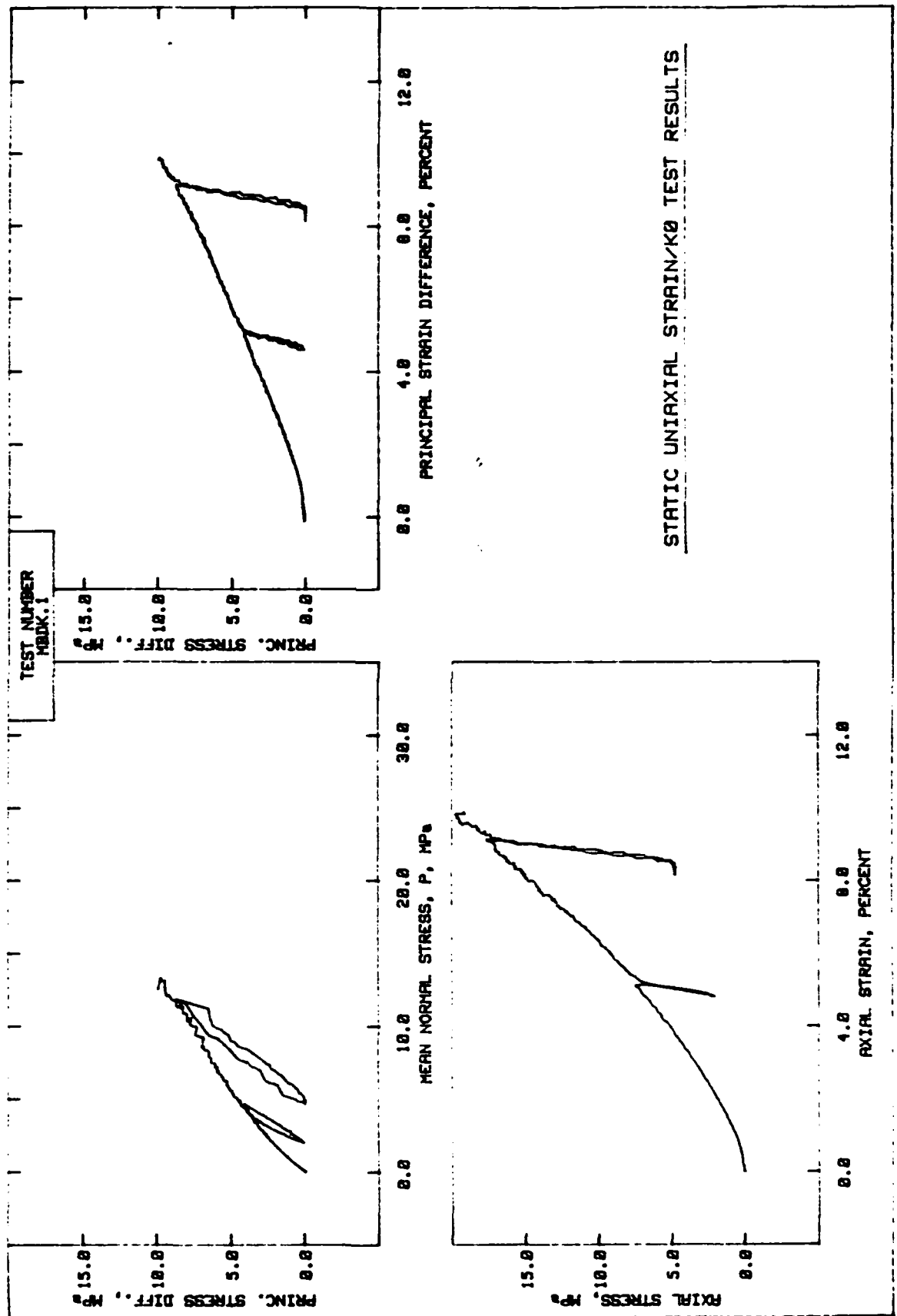
TEST NUMBER:MBDUX.1A

STATIC UNIAXIAL STRAIN TEST RESULTS

VERTICAL STRAIN, PERCENT

VERTICAL STRESS, MPa

PLATE 2

VERTICAL STRAIN, PERCENT

VERTICAL STRESS, MPa
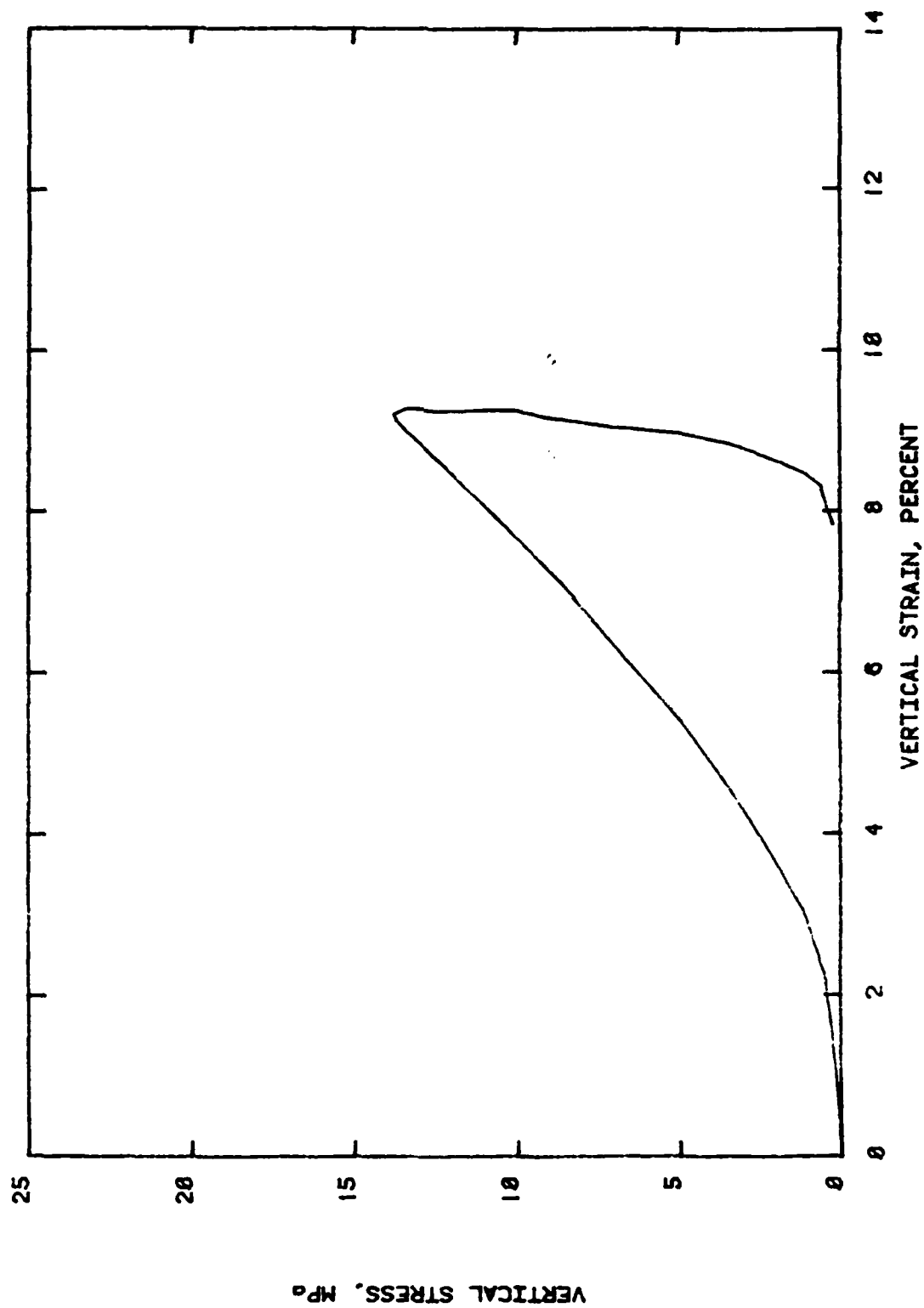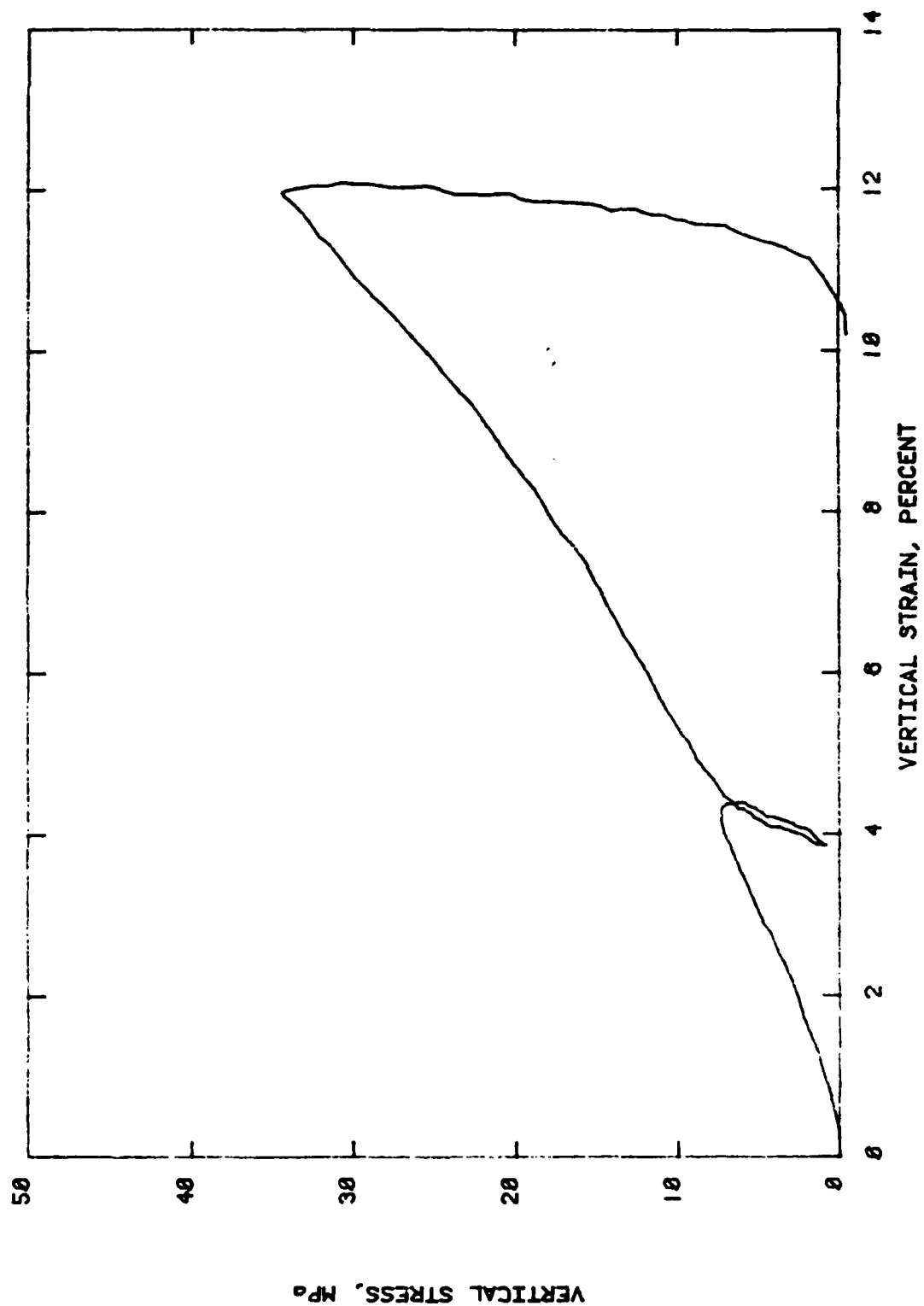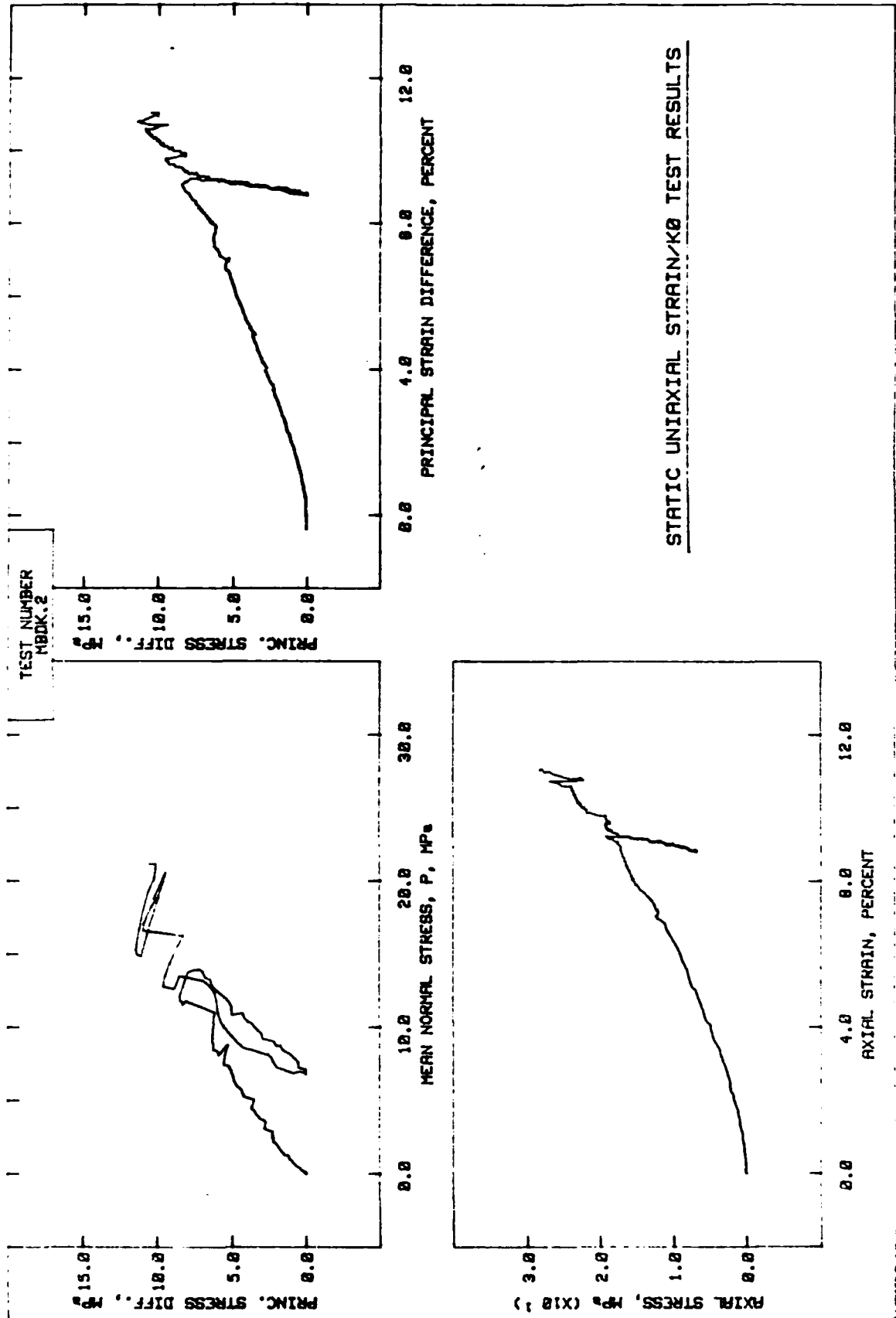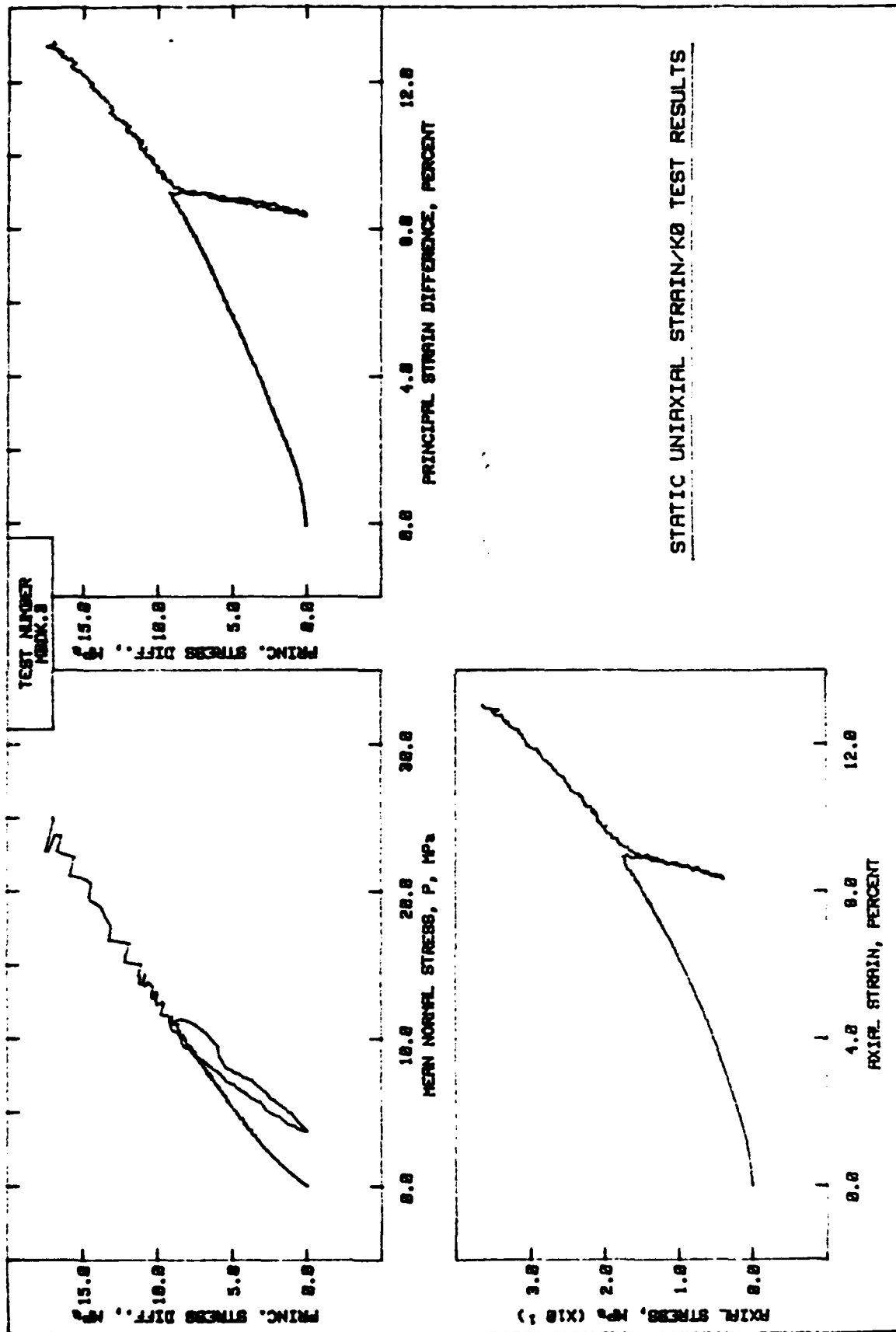
TEST NUMBER:MBDUX.2

STATIC UNIAXIAL STRAIN TEST RESULTS
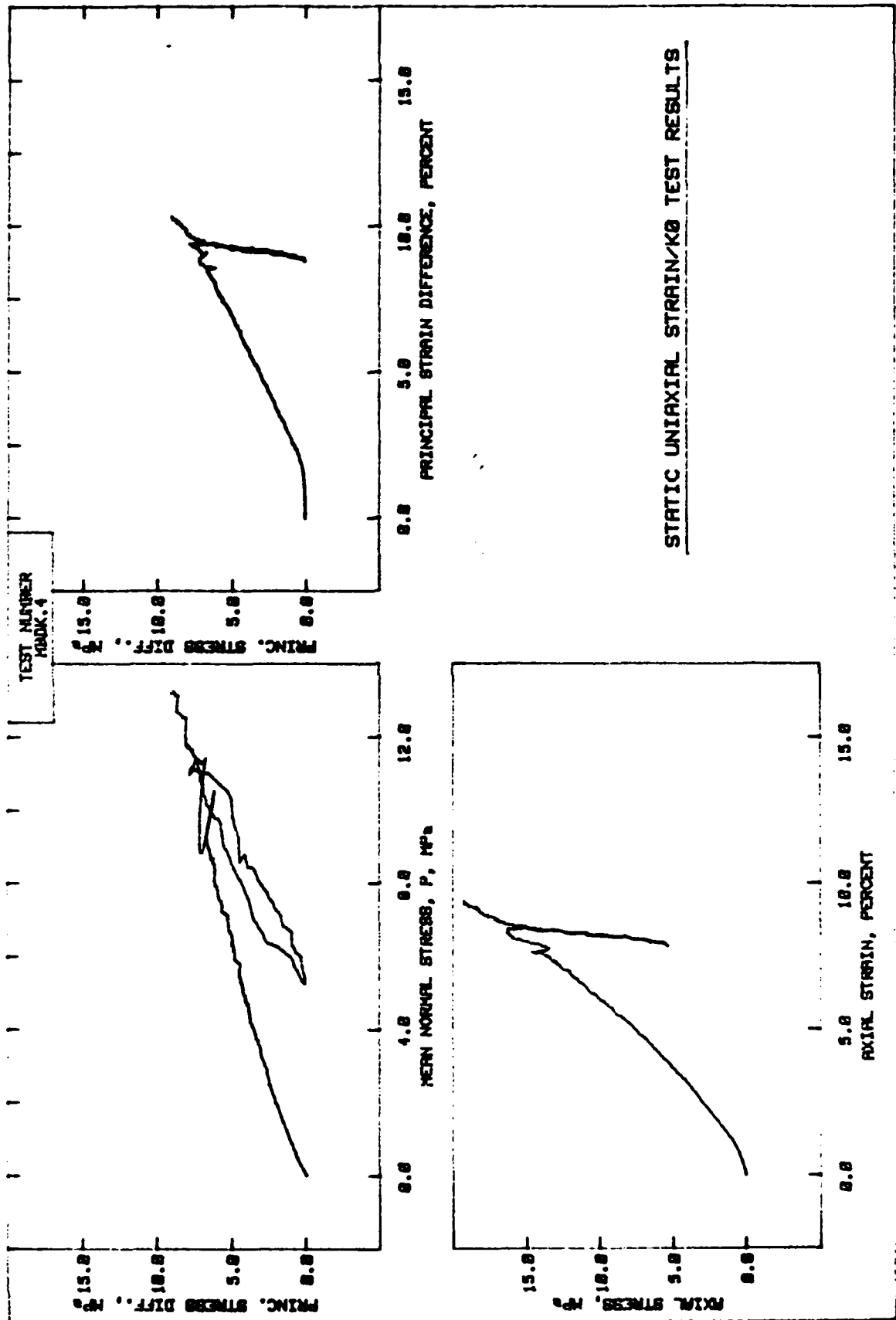
PLATE 3

VERTICAL STRAIN, PERCENT

VERTICAL STRESS, MPa
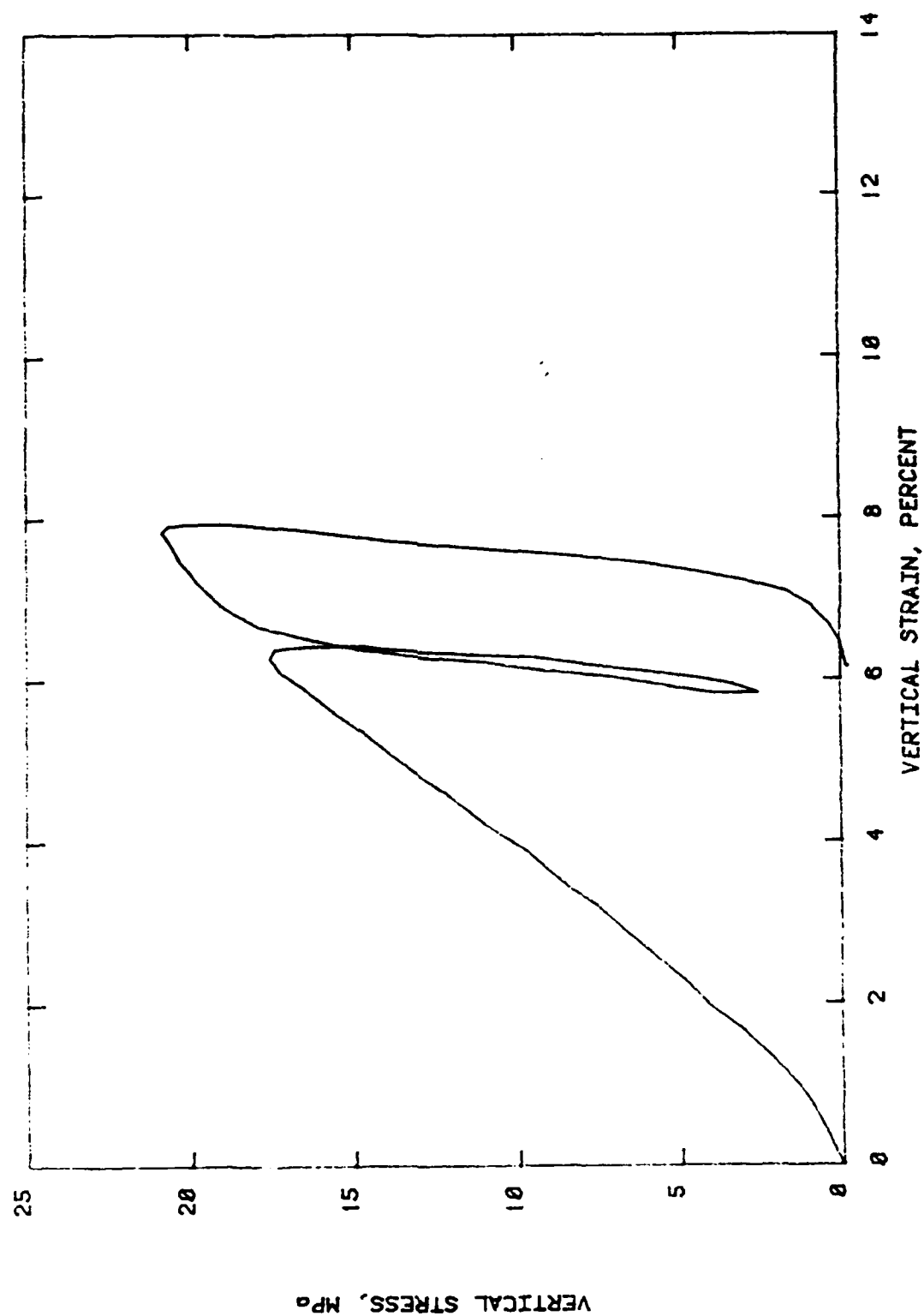
TEST NUMBER:MBDUX.2A

STATIC UNIAXIAL STRAIN TEST RESULTS

PLATE 4

VERTICAL STRESS, MPa

VERTICAL STRAIN, PERCENT

TEST NUMBER:MBDUX.3

DYNAMIC UNIAXIAL STRAIN TEST RESULTS

PLATE 5

VERTICAL STRAIN, PERCENT

VERTICAL STRESS, MPa

TEST NUMBER:MBDUX.4

DYNAMIC UNIAXIAL STRAIN TEST RESULTS

PLATE 6

VERTICAL STRAIN, PERCENT

VERTICAL STRESS, MPa
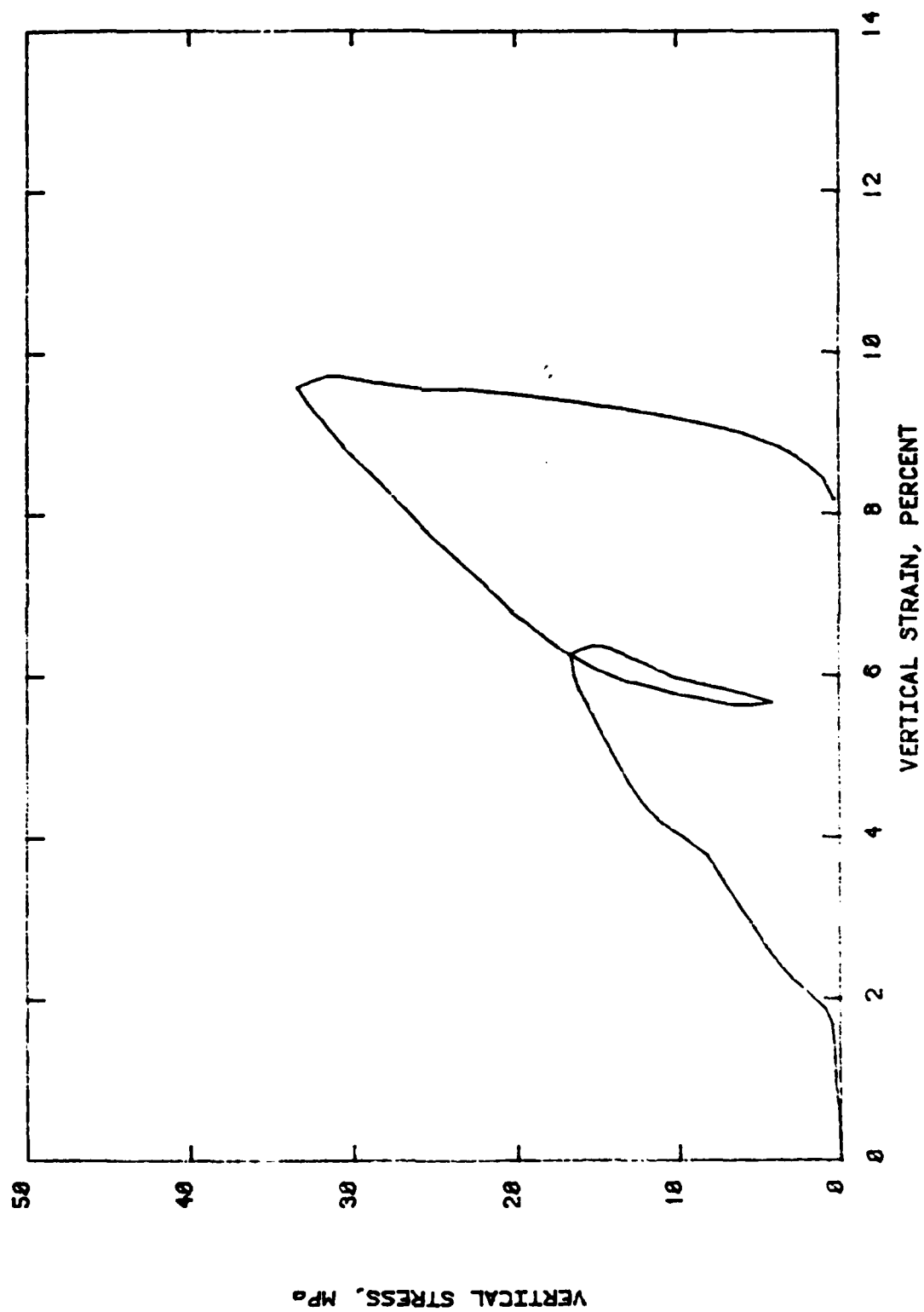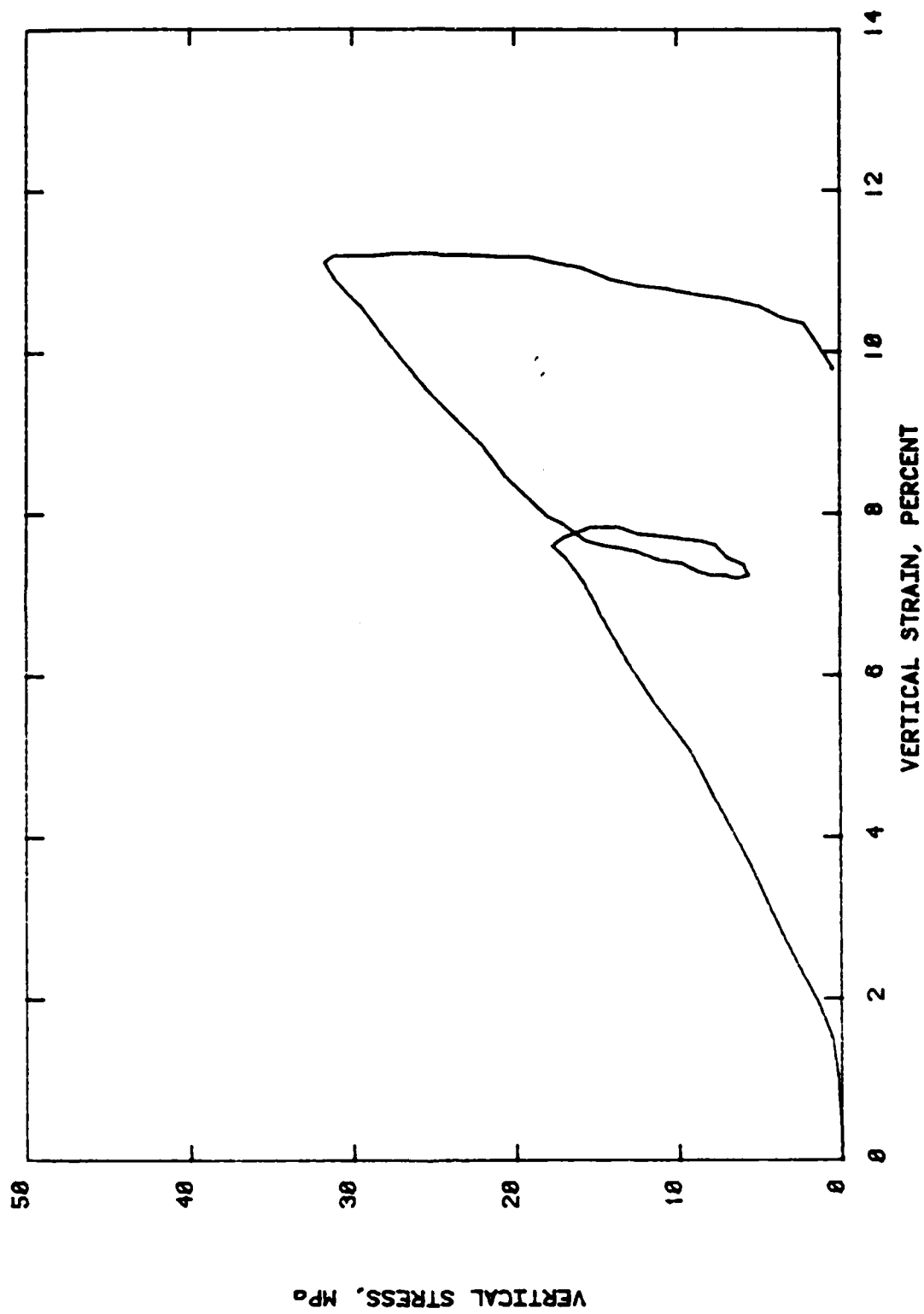
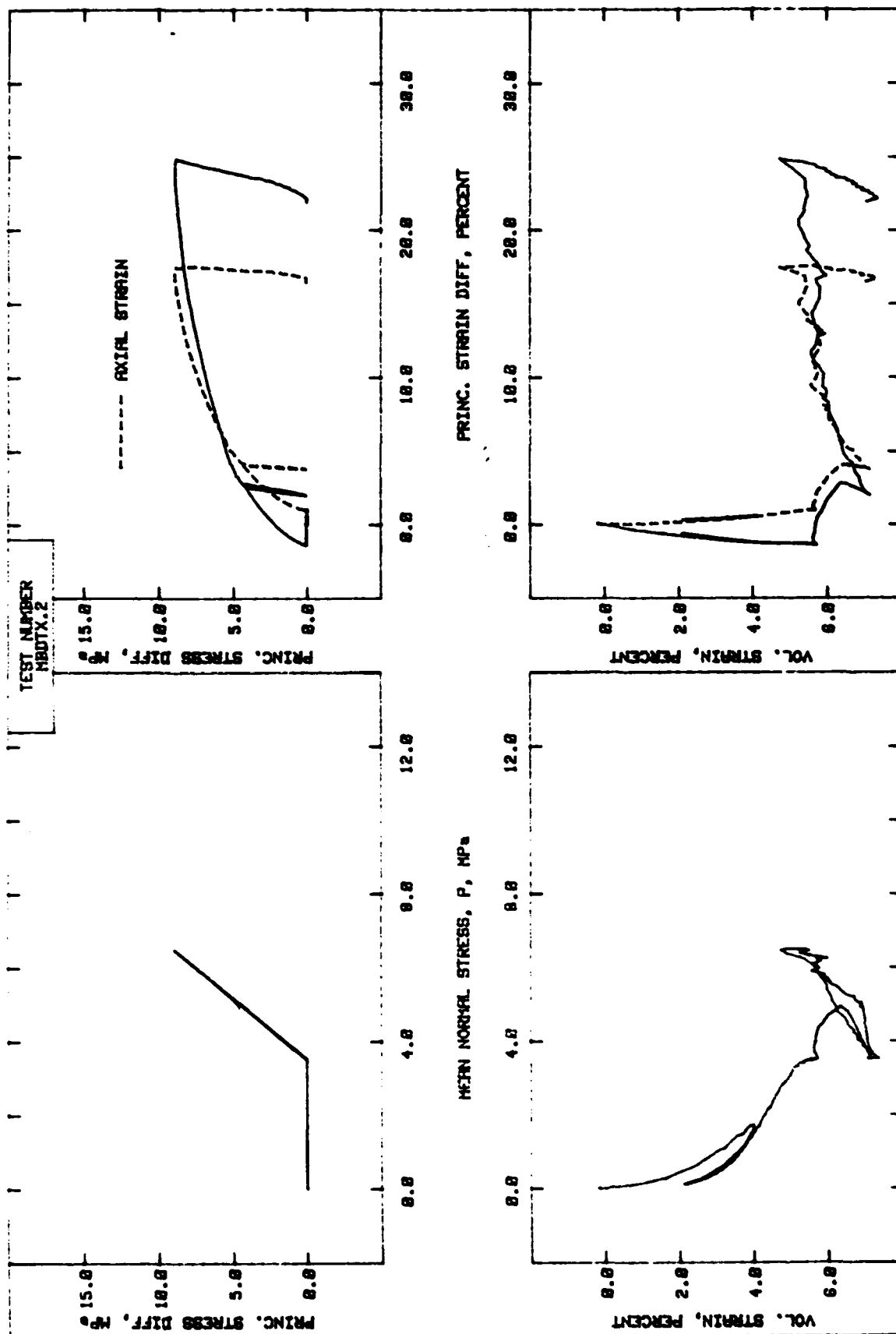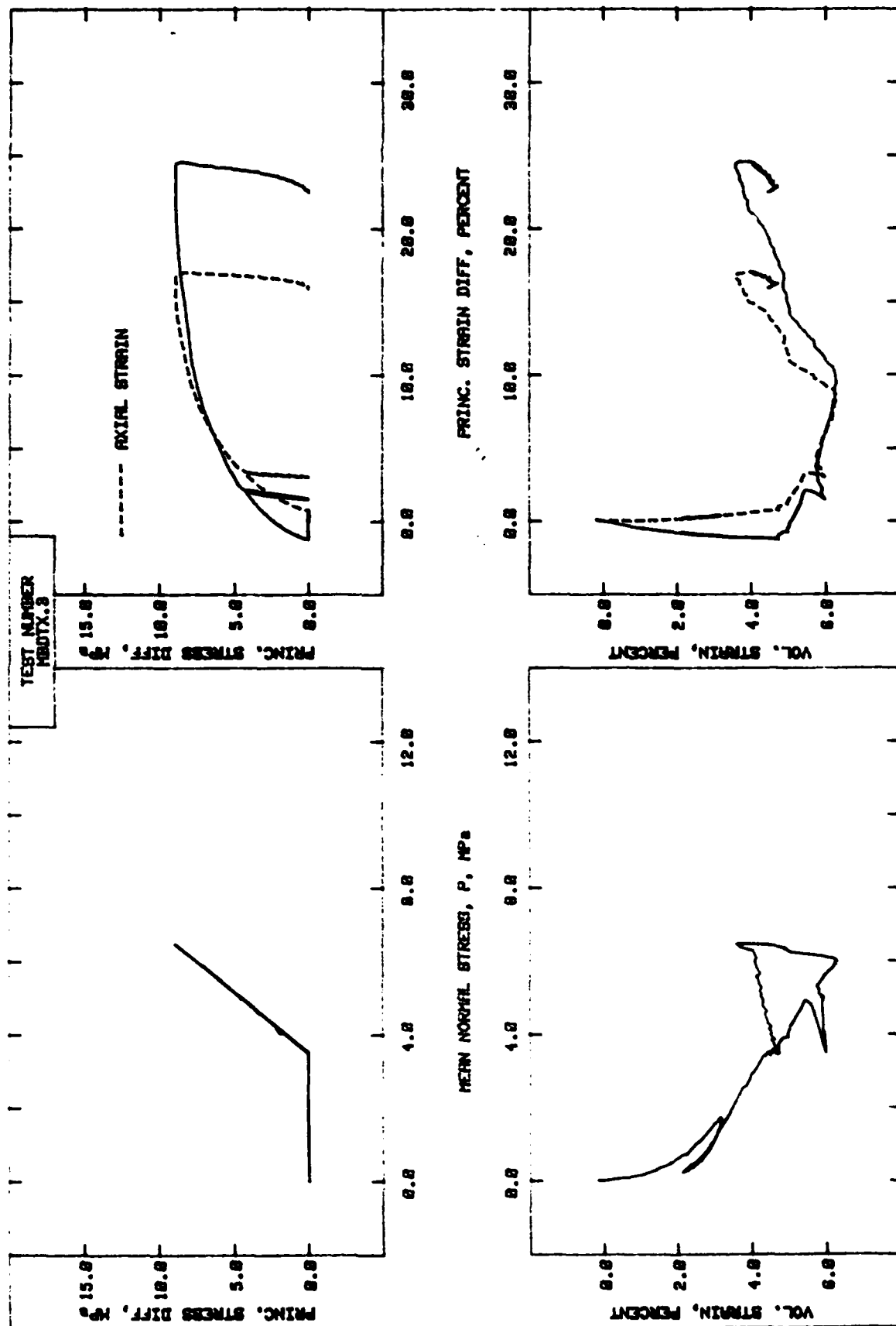TEST NUMBER:MBDUX.5

DYNAMIC UNIAXIAL STRAIN TEST RESULTS

PLATE 7

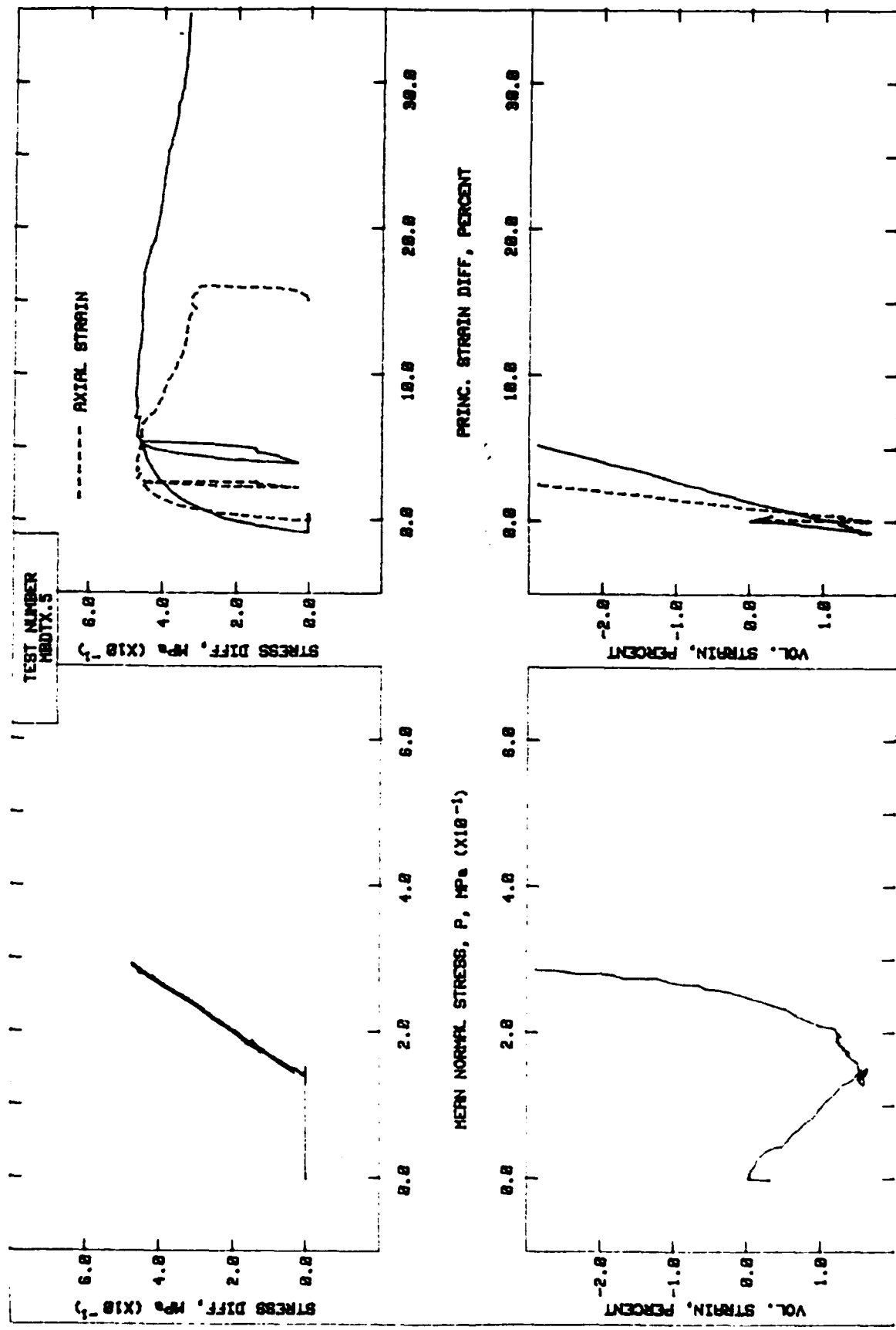STATIC UNIAXIAL STRAIN/K0 TEST RESULTS

TEST NUMBER
MBDK.1

PLATE 8

STATIC UNIAXIAL STRAIN/K0 TEST RESULTS

TEST NUMBER
MBDK.2

PLATE 9

STATIC UNIAXIAL STRAIN/K0 TEST RESULTS

PLATE 10

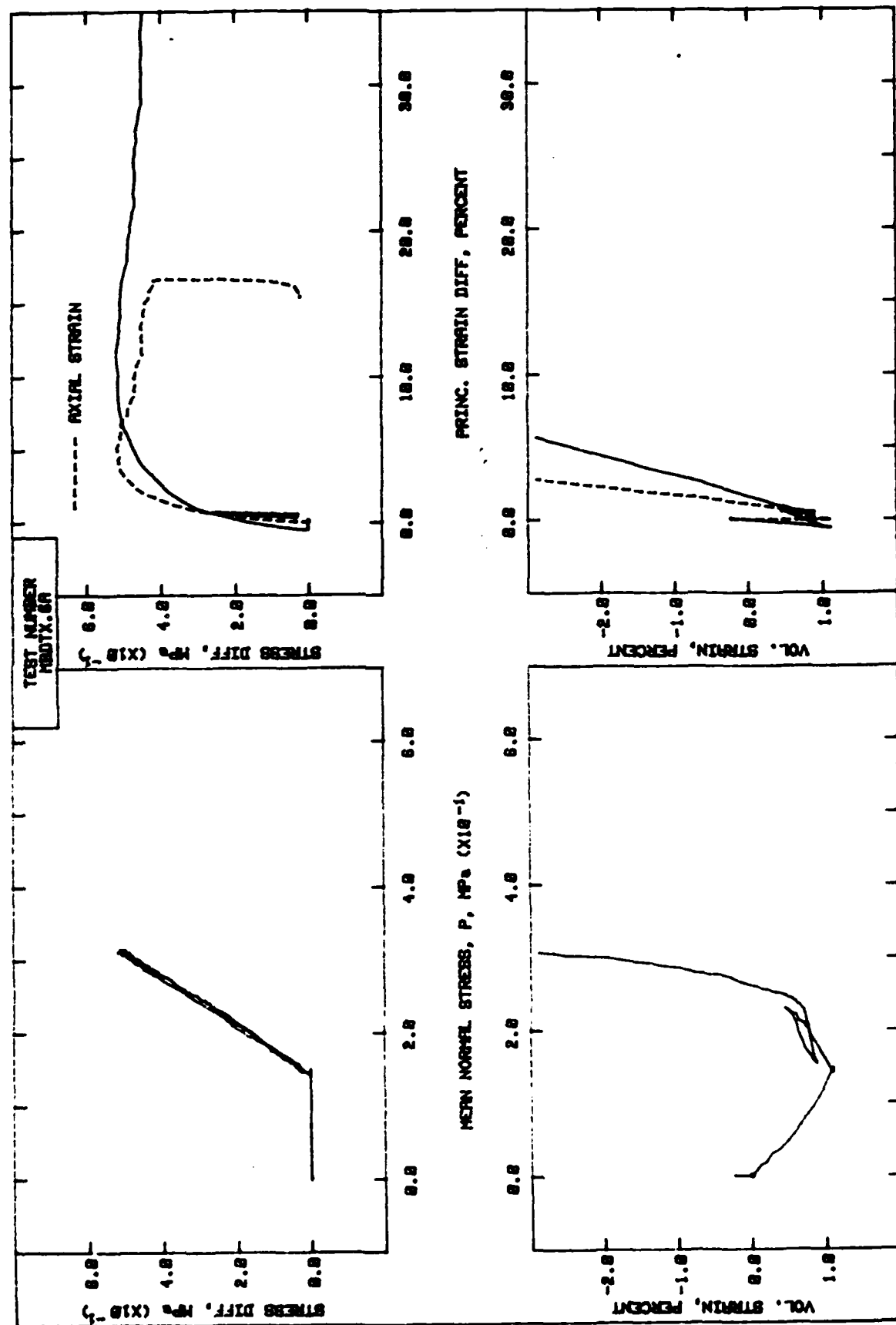STATIC UNIAXIAL STRAIN/K0 TEST RESULTS

PLATE 11

STATIC IC-TXC TEST RESULTS

PLATE 12

STATIC IC-TXC TEST RESULTS
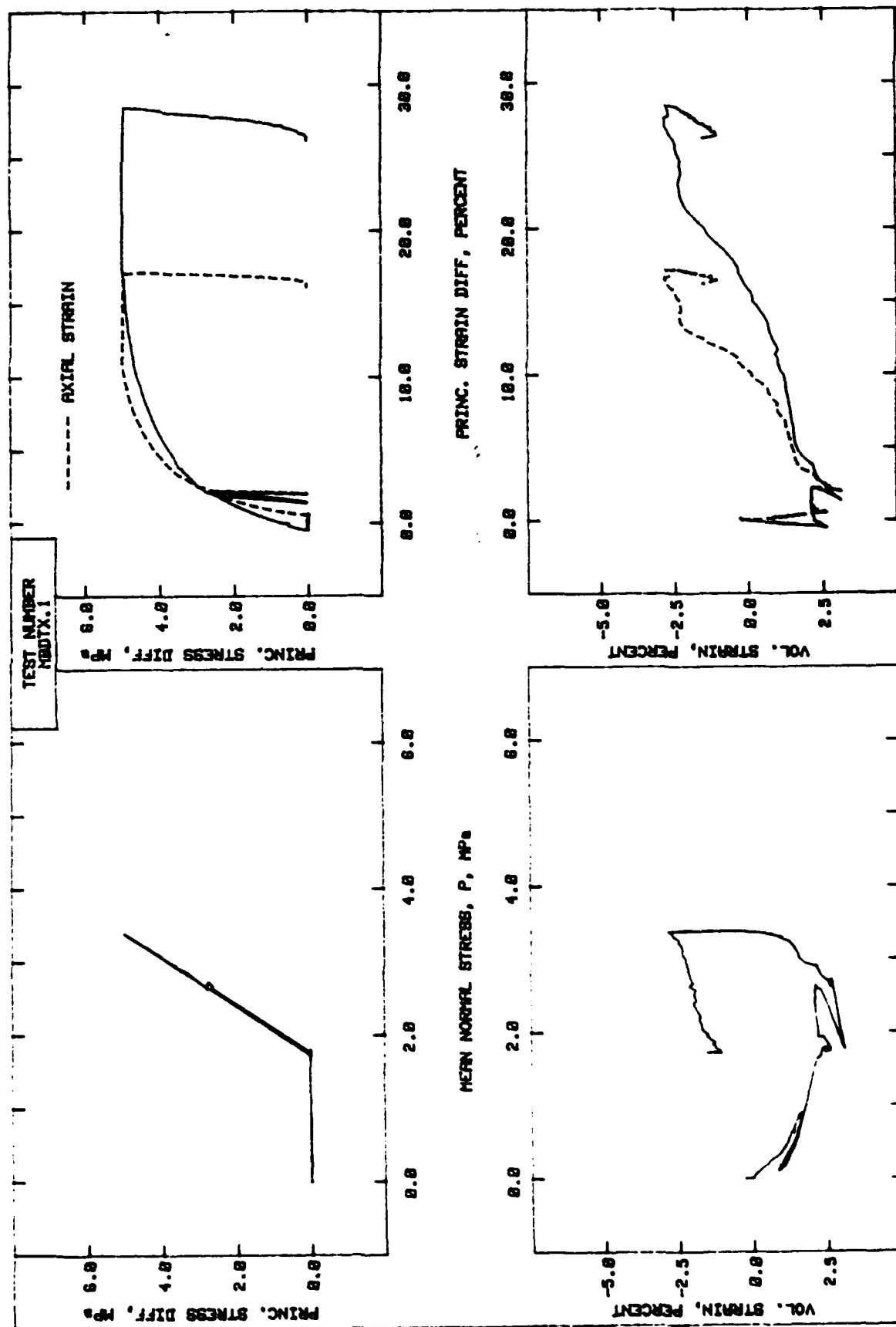
PLATE 13

STATIC IC-TXC TEST RESULTS

PLATE 14

STATIC IC-TXC TEST RESULTS

PLATE 15

STATIC IC-TXC TEST RESULTS

PLATE 16

STATIC IC-TXC TEST RESULTS

PLATE 17

STATIC IC-TXE TEST RESULTS

PLATE 18

STATIC IC-TXE TEST RESULTS

TEST NUMBER
MODE.5

------ AXIAL STRAIN

PRINC. STRESS DIFF, MPa

PRINC. STRAIN DIFF, PERCENT

MEAN NORMAL STRESS, P, MPa

VOL. STRAIN, PERCENT

PLATE 19

STATIC IC-TXE TEST RESULTS

PLATE 20

END
DTION
10— 86